Doctoral Dissertation

Anti-Blood Cancer Activities of Bioactive Compounds from Rice (*Oryza sativa* var. Koshihikari) and an Invasive Weed (*Andropogon virginicus*)

LA HOANG ANH

Graduate School for International Development and Cooperation

Hiroshima University

September 2022

Anti-Blood Cancer Activities of Bioactive Compounds from Rice (*Oryza sativa* var. Koshihikari) and an Invasive Weed (*Andropogon virginicus*)

D190581

LA HOANG ANH

A Dissertation Submitted to

the Graduate School for International Development and Cooperation

of Hiroshima University in Partial Fulfillment

of the Requirements for the Degree of

Doctor of Agriculture

September 2022

We hereby recommend that the dissertation by Mr. LA HOANG ANH entitled "Anti-Blood Cancer Activities of Bioactive Compounds from Rice (*Oryza sativa* var. Koshihikari) and an Invasive Weed (*Andropogon virginicus*)" be accepted in partial fulfillment of the requirements for the degree of DOCTOR OF AGRICULTURE.

Committee on Final Examination:

TRAN Dang Xuan, Associate Professor
Chairperson

HOSAKA Tetsuro, Associate Professor

LEE Han Soo, Professor

ICHIHASHI Masaru, Professor

TAKAMI Akiyoshi, Professor
Aichi Medical University School of Medicine

Date: August 4th, 2022

Approved:

ICHIHASHI Masaru, Professor
Dean

Date: Sep. 2, 2022

Graduate School for International Development and Cooperation
Hiroshima University

ACKNOWLEDGMENTS

First and foremost, I would like to convey my heartfelt appreciation and gratitude to my main academic supervisor, Associate Professor TRAN DANG XUAN for his outstanding support and guidance. Throughout my doctoral course, his zeal and diligence have always inspired and motivated me. He has taught me a wide range of abilities in both academics and sciences. He enlightened me from the most fundamental concept to accomplish major results. He assisted me in overcoming obstacles to attain my objectives. Furthermore, he has always stimulated and supported me in both study and life. It is my honor to be his doctoral student, and I am forever grateful for an excellent pattern of a successful researcher like him.

I would like to send my special gratitude to my sub-supervisors Professor LEE HAN SOO and Associate Professor HOSAKA TETSURO for their valuable recommendations and suggestions during my program. These valuable comments help me complete my study more significantly and comprehensively. I would like to extend my sincere appreciations to Professor ICHIHASHI MASARU for the constructive comments and questions which improve my doctoral dissertation.

I would like to compliment my deep thanks and appreciation to Assistant Professor NGUYEN VAN QUAN for his instructions and encouragements in my experiments and academic writing since the beginning of my doctoral course. I am immensely thankful for his unfailing aid, which not only strengthened my academic performance but also assisted me in balancing with other aspects of my life.

I would like to acknowledge Professor AKIYOSHI TAKAMI, Division Chief of Department of Internal Medicine, Division of Hematology, Aichi Medical University for permitting me to research at the Division of Hematology in term of collaboration project between the Laboratory of Plant Physiology and Biochemistry, Hiroshima University and

the Laboratory of Hematology, Aichi Medical University. My distinctive gratefulness also goes to him for his kind instructions and supports during my study.

I would like to specially thank Mr. VU QUANG LAM, a doctoral student at Aichi Medical University for his enthusiastic supports through my experiments in the Laboratory of Hematology, Aichi Medical University. I would like to express gratitude to Ms. TOMOKO AMIMOTO, a technician of Natural Science Center for Basic Research and Development (N-BARD), Hiroshima University for her significant expert advice, analytical insights, and decent training programs. I am grateful for the support and collaboration of all members of the Xuan lab who are not only kind partners but also great friends. I gratefully acknowledge the Japanese Government–Monbukagakusho (MEXT) Scholarship for funding my studies at Hiroshima University. I would like to send great thanks to all staffs at Graduate School for International Development and Cooperation (IDEC) for their unwavering supports and readiness to help me whenever I need. Finally, I am incredibly thankful, especially my parents and my brother, who have always been a pillar and an everlasting source of fuel for me to achieve my current goals.

SUMMARY

1. Background

Blood cancer (1.2 million cases per year) has been a serious human disease during a long history with a high mortality rate (58%). Therefore, this study was conducted to investigate promising candidates from plants for inhibiting blood cancer. Among plant sources, *Adropogon virginicus* is an invasive weed that distributes globally, threatening agriculture and economics in many countries. Thus, research on pharmaceutical properties may lead to further strategies to take advantage of this serious invasive weed that was once thought to be of no use. On the other hand, rice (*Oryza sativa*) is an important food crop in the world, which has been recently being received increasing attention for the research on medicinal purposes. In rice, momilactones are high valuable diterpene lactones exhibiting multiple biological benefits. Based on these reasons, we aimed (1) to explore potential phytochemicals and pharmaceutical properties of the invasive weed *A. virginicus* with focus on antioxidant, anti-skin aging, anti-diabetic, and anti-blood cancer properties and (2) to determine the potentials of momilactones isolated from rice (*O. sativa* var. Koshihikari) for preventing blood cancer.

2. Structure of dissertation

Chapter 1. General introduction

Chapter 2. Pharmaceutical properties of an invasive weed *Andropogon virginicus*

Chapter 3. Cytotoxic activities of momilactones against leukemia, lymphoma, and multiple myeloma cell lines

Chapter 4. Cytotoxic mechanism of momilactones against acute promyelocytic leukemia and multiple myeloma cell lines

Chapter 5. Effects of *in vitro* digestion on anti-blood cancer properties of momilactones

Chapter 6. General discussion

3. Materials and methods

Materials

A. virginicus' aerial plant parts were extracted by Soxhlet extraction method, followed by liquid-liquid phase extraction to obtain total crude (T-Anvi), hexane (H-Anvi), ethyl acetate, (E-Anvi), butanol (B-Anvi), and water (H-Anvi) extracts.

Momilactones were isolated and purified from the laboratory of Plant Physiology and Biochemistry, Hiroshima University, Japan (Quan et al., 2019b).

Biological activity

Antioxidant activities of samples were determined via antiradical (DPPH and ABTS), reducing power, β-carotene bleaching assays (Quan et al., 2019).

Enzymatic assays including tyrosinase and α-amylase inhibitory effects of *A. virginicus*' extracts were evaluated following the method presented by Quan et al. (2019).

Anticancer assays consisting of MTT, annexin V apoptosis, cell cycle, and western blotting were conducted to screen the anticancer properties of momilactones. The corresponding cell lines for blood cancer were included leukemia (HL60, Meg-01, and K562), lymphoma (Mino), and myeloma (KMS-11 and U266). Besides, a non-cancerous cell line namely MeT-5A was used in this study.

In vitro digestion model

The effects of *in vitro* digestion on the bioaccessibility and cytotoxic activities of momilactones against blood cancer cell lines were investigated following the method described by Un et al. (2022).

Phytochemical analysis

The chemical analyses were conducted applying spectrophotometer, gas chromatography-mass spectrometry (GC-MS), and liquid chromatography-electrospray ionization-tandem mass spectrometry (LC-ESI-MS/MS) methods.

4. Results and discussion

In Chapter 2, we indicate that the invasive weed *A. virginicus* may be a promising source of antioxidants, anti-α-amylase, and anti-tyrosinase abilities, and cytotoxicity against chronic myeloid leukemia cell lines. Besides, *A. virginicus* aerial parts are rich in flavonoids, palmitic acid, phytol, and γ-sitosterol, which may play a vital role in the biological activities of the respective extracts.

From Chapter 3, we highlight that MB and MAB can inhibit various blood cancer cell lines including leukemia, lymphoma, and multiple myeloma by inducing cell apoptosis. Notably, the cytotoxicity of MB and MAB is close to the well-known drugs of Doxorubicin in inhibiting Meg-01 and K562. Meanwhile these compounds are stronger than the widely applied medicines of Doxorubicin and Ibrutinib in suppressing HL-60 and U266, respectively. Whereas these compounds display an insignificant effect on non-cancerous cells.

In Chapter 4, MB and MAB at 5 μM promote acute promyelocytic leukemia (HL-60) and multiple myeloma (U266) cell apoptosis by activating the phosphorylation of p-38 in the mitogen-activated protein kinase (MAPK) pathway and regulating the relevant proteins (BCL-2 and caspase-3) in the mitochondrial pathway. Besides, these compounds may induce G2 phase arrest in HL-60 cell cycle through the activation of p-38 and disruption of CDK1 and cyclin B1 complex. Meanwhile MB and MAB show insignificant effects on cell apoptosis and cell cycle of non-cancerous cell line MeT-5A.

For Chapter 5, the finding shows that the bioaccessibility and cytotoxicity of momilactones significantly reduce through the digestive stages including oral, gastric, and intestinal phases.

A general discussion is presented in Chapter 6. Particularly, this is the first study to highlight that *A. virginicus* may be a promising source of antioxidant, anti-diabetic, anti-skin

aging, and anti-blood cancer agents. In addition, momilactones isolated from rice (*O. sativa* var. Koshihikari) husks can inhibit blood cancer cell lines by regulating the proteins related to apoptosis and cell cycle pathways. However, the cytotoxic activities of momilactones may be significantly decreased during digestion. Therefore, forthcoming studies should be conducted to improve the bioaccessibility of momilactones, followed by *in vivo* and clinical tests to confirm their capacity to develop novel anti-blood cancer drugs. In another aspect, the combination of momilactones from rice and isolated components from *A. virginicus* may be a potential approach for developing blood cancer treatments, especially for patients complicated with other health problems such as oxidative stress and chronic disorders.

ABBREVIATIONS

ABTS: 2,2′-azinobis-(3-ethylbenzothiazoline-6-sulfonic acid)

APL: acute promyelocytic leukemia

ATCC: American Type Culture Collection

B-Anvi: butanol extract from *Andropogon virginicus*

BHT: butylated hydroxytoluene

CML: chronic myeloid leukemia

DPPH: 2,2-diphenyl-1-picrylhydrazyl

DW: dry weight

E- Anvi: ethyl acetate extract from *Andropogon virginicus*

GAE: gallic acid equivalent

GC-MS: gas chromatography-mass spectrometry (GC-MS)

H-Anvi: hexane extract from *Andropogon virginicus*

KI: Kovats index

LC-ESI-MS/MS: liquid chromatography-electrospray ionization-tandem mass spectrometry

LPI: lipid peroxidation inhibition

LRI: linear retention index

MA: momilactone A

MAB: the mixture of momilactones A and B (1:1, w/w)

MB: momilactone B

MCL: mantle cell lymphoma

MM: multiple myeloma

MS: mass spectra

RE: relative expression

RE: rutin equivalent

T-Anvi: total crude extract from *Andropogon virginicus*

TFC: total flavonoid content

TPC: total phenolic content

UPLC-ESI-MS: ultra-performance liquid chromatography-electrospray ionization-mass spectrometry

W-Anvi: water extract from *Andropogon virginicus*

LIST OF CONTENTS

ACKNOWLEDGMENTS ..... **I**

SUMMARY ..... **III**

ABBREVIATIONS ..... **VII**

LIST OF CONTENTS ..... **IX**

LIST OF TABLES ..... **XIV**

LIST OF FIGURES ..... **XVI**

CHAPTER 1: GENERAL INTRODUCTION **1**

1.1. Blood cancer **1**

1.2. Anticancer potentials of natural compounds from plants **3**

1.3. Rice **4**

1.3.1. Rice and rice by-products 4

1.3.2. Momilactones 5

1.3.3. Biological activities of momilactones 8

1.4. *Andropogon virginicus* **10**

1.4.1. Morphology 11

1.4.2. Distribution 11

1.5. Main objectives **11**

CHAPTER 2: PHARMACEUTICAL PROPERTIES OF AN INVASIVE WEED *ANDROPOGON VIRGINICUS* **13**

2.1. Introduction **13**

2.2. Materials and methods **15**

2.2.1. Materials 15

2.2.2. Sample preparation and extraction 16

2.2.3. Total phenolic (TPC) and flavonoid (TFC) contents 16

2.2.4. Antioxidant activity 17
2.2.5. Enzymatic inhibitory assays 18
2.2.6. Cytotoxic activity against K562 and Meg-01 cell lines 19
2.2.7. Identification of phytochemical component 20
2.2.8. Data analysis 21
2.3. Results 22
2.3.1. Yield and total phenolics (TPC) and flavonoids (TFC) of *A. virginicus* extracts . 22
2.3.2. Antioxidant activity of extracts from *A. virginicus* 22
2.3.3. Tyrosinase and α-amylase inhibitory activities of *A. virginicus* extracts 25
2.3.4. Cytotoxic activity of extracts from *A. virginicus* against K562 and Meg-01 cell lines 26
2.3.5. Correlations between total phenolics (TPC) and flavonoids (TFC) and biological properties of *A. virginicus* extracts. 27
2.3.6. GC-MS results 28
2.3.7. HPLC-ESI-MS/MS results 29
2. 4. Discussion 32
2.5. Conclusions 38
CHAPTER 3: CYTOTOXIC ACTIVITIES OF MOMILACTONES AGAINST LEUKEMIA, LYMPHOMA, AND MULTIPLE MYELOMA CELL LINES 39
3.1. Introduction 39
3.2. Materials and methods 40
3.2.1. Materials 40
3.2.2. Cell viability (MTT) assay 41
3.2.3. Cell apoptosis (annexin V) assay 42
3.3. Results 42

3.3.1. Effects of momilactones A (MA) and B (MB) and their mixture (MAB) on cell viability of blood cancer cell lines 42
3.3.2. Apoptosis-inducing activities of momilactones against blood cancer cell lines ... 45
3.4. Discussion 51
3.5. Conclusions 54
CHAPTER 4: CYTOTOXIC MECHANISM OF MOMILACTONES A AND B AGAINST ACUTE PROMYELOCYTIC LEUKEMIA AND MULTIPLE MYELOMA CELL LINES 55
4.1. Introduction 55
4.2. Materials and methods 57
4.2.1. Materials 57
4.2.2. Cell viability (MTT) assay 57
4.2.3. Cell apoptosis (annexin V) assay 58
4.2.4. Cell cycle assay 59
4.2.5. Western blotting assay 59
4.2.6. Statistical analysis 60
4.3. Results 60
4.3.1. Effects of momilactones on cell viability of non-cancerous (MeT-5A), acute promyelocytic leukemia (HL-60), and multiple myeloma (U266) cell lines 60
4.3.2. Apoptosis-inducing activities of momilactones against non-cancerous (MeT-5A), acute promyelocytic leukemia (HL-60), and multiple myeloma (U266) cell lines 63
4.3.3. Effects of momilactones on inducing cell cycle arrest of non-cancerous (MeT-5A), acute promyelocytic leukemia (HL-60), and multiple myeloma (U266) cell lines 66

4.3.4. Effects of momilactones on expressions of proteins related to apoptosis induction and cell cycle arrest of acute promyelocytic leukemia (HL-60), and multiple myeloma (U266) cell lines 68

4.4. Discussion 71

4.5. Conclusions 77

CHAPTER 5: EFFECTS OF *IN VITRO* DIGESTION ON ANTI-BLOOD CANCER PROPERTIES OF MOMILACTONES 78

5.1. Introduction 78

5.2. Materials and methods 79

5.2.1. Materials 79

5.2.2. *In vitro* digestion model 80

5.2.3. Cell viability (MTT) assay 82

5.2.4. Quantification of momilactones 83

5.3. Results 84

5.3.1. Effects of *in vitro* digestion on cytotoxic activity of momilactones against acute promyelocytic leukemia (HL-60) cell line 84

5.3.2. Effects of *in vitro* digestion on cytotoxic activity of momilactones against chronic myeloid leukemia (Meg-01) cell line 85

5.3.3. Effects of *in vitro* digestion on cytotoxic activity of momilactones against mantle cell lymphoma (Mino) cell line 86

5.3.4. Effects of *in vitro* digestion on cytotoxic activity of momilactones against multiple myeloma (U266) cell line 87

5.3.5. Bioaccessibility of momilactones during *in vitro* digestion 88

5.3.6. Correlation coefficients between quantities of momilactones and their cytotoxic activities during *in vitro* digestion 90

5.4. Discussion 91

CHAPTER 6: GENERAL DISCUSSION 94

6.1. Key findings 94

6.2. Comparison between cytotoxic activities of isolated components from rice (*O. sativa* var. Koshihikari) and the invasive weed (*A. virginicus)* 97

6.3. Exploitation of products from rice (*O. sativa*) and the invasive weed (*A. virginicus*) for developing blood cancer treatments 98

SUPPLEMENTARY DATA 101

REFERENCES 119

LIST OF TABLES

Table 1. Extraction yield and total phenolic (TPC) and flavonoid (TFC) contents..... 22

Table 2. Tyrosinase and α-amylase inhibitory activities of *A. virginicus* extracts..... 25

Table 3. Pearson's correlation coefficients between total phenolic and flavonoid contents and biological activities of *A. virginicus* extracts..... 28

Table 4. Dominant phytochemicals in H-Anvi extract from *A. vigirnicus* identified by GC-MS 29

Table 5. Phytocompounds in E-Anvi extract from *A. virginicus* detected by HPLC-ESI-MS/MS..... 31

Table 6. Cytotoxic activities of momilactones A and B against non-cancerous (MeT-5A), chronic myeloid leukemia (Meg-01 and K562), acute promyelocytic leukemia (HL-60), mantle cell lymphoma (Mino), and multiple myeloma (U266 and KMS-11) cell lines 43

Table 7. Cytotoxic activities (IC_{50}) of momilactones A and B against MeT-5A, HL-60, and U266 cell lines (Obtained results from Chapter 3)..... 62

Table 8. List of blood cancer cell lines..... 79

Table 9. Components of artificial digestion juices (Un et al., 2022)..... 80

Table 10. Effect of *in vitro* digestion on cytotoxic activity against HL-60 cell line of momilactones (IC_{50}, μM)..... 85

Table 11. Effect of *in vitro* digestion on cytotoxic activity against Meg-01 cell line of momilactones (IC_{50}, μM)..... 86

Table 12. Effect of *in vitro* digestion on cytotoxic activity against Mino cell line of momilactones (IC_{50}, μM)..... 87

Table 13. Effect of *in vitro* digestion on cytotoxic activity against U266 cell line of momilactones (IC_{50}, μM)..... 88

Table 14. Variation percentages of momilactones under digestion..... 89

Table 15. Correlation coefficients between quantities of momilactones and their cytotoxicity during digestion 90

Table 16. Key findings 95

Table 17. Cytotoxic activities of isolated components from broomsedge bluestem and rice (Achieved results from Chapters 2 and 3) 97

LIST OF FIGURES

Figure 1. Number of worldwide cancer new cases and mortality rate in 2020 (GLOBOCAN, 2020) 1

Figure 2. Number of worldwide blood cancer new cases and mortality rate in 2020 (Sung et al., 2021) 2

Figure 3. Anti-blood cancer substances derived from natural plants (Xie et al., 2016; Zadeh et al., 2022; Espinoza et al., 2017) 3

Figure 4. Structures of momilactones A (MA) and B (MB) 6

Figure 5. Momilactones isolated and purified from the laboratory of Plant Physiology and Biochemistry, Hiroshima University, Japan (Quan et al., 2019) 7

Figure 6. Anticancer potentials of diterpene lactones (Kumar et al., 2004; Ji et al., 2007) 8

Figure 7. *Andropogon virginicus* in Higashi-Hiroshima Campus, Hiroshima University . 11

Figure 8. Anti-radical activities (ABTS and DPPH assays) of *A. virginicus* extracts. Different letters (a,b,c,d) enclosed with columns (same colors) express significant differences at $p < 0.05$ (one-way ANOVA). DPPH, 2,2-diphenyl-1-picrylhydrazyl; ABTS, 2,2′-azinobis-(3-ethylbenzothiazoline-6-sulfonic acid); T-Anvi, total crude extract; H-Anvi, hexane extract; E-Anvi, ethyl acetate extract; B-Anvi, butanol extract; W-Anvi, water extract; BHT, butylated hydroxytoluene. 23

Figure 9. Inhibition on lipid peroxidation of *A. virginicus* extracts. Different letters (a,b,c,d) enclosed with columns indicate significant differences at $p < 0.05$ (one-way ANOVA). LPI, lipid peroxidation inhibition; T-Anvi, total crude extract; H-Anvi, hexane extract; E-Anvi, ethyl acetate extract; B-Anvi, butanol extract; W-Anvi, water extract; BHT, butylated hydroxytoluene. 24

Figure 10. Potassium ferricyanide reducing power of *A. virginicus* extracts. T-Anvi, total crude extract; H-Anvi, hexane extract; E-Anvi, ethyl acetate extract; B-Anvi, butanol extract; W-Anvi, water extract; BHT, butylated hydroxytoluene. 25

Figure 11. Dose-response curves of *A. virginicus* extracts for cytotoxicity against (a) K562 and (b) Meg-01 cell lines. T-Anvi, total crude extract; H-Anvi, hexane extract; E-Anvi, ethyl acetate extract; B-Anvi, butanol extract; W-Anvi, water extract. 27

Figure 12. GC-MS chromatogram of H-Anvi extract 29

Figure 13. HPLC chromatogram of E-Anvi extract 30

Figure 14. Dose-responding curves of momilactones A and B for cytotoxic activities against non-cancerous (MeT-5A), chronic myeloid leukemia (Meg-01 and K562), acute promyelocytic leukemia (HL-60), mantle cell lymphoma (Mino), and multiple myeloma (U266 and KMS-11) cell lines. MA, momilactone A; MB, momilactone B; MAB, the mixture of momilactones A and B (1:1, w/w). 45

Figure 15. Apoptosis-inducing effects of momilactone B (MB) and the mixture of momilactone A and B (MAB) (1:1, w/w) at 5 μM against non-cancerous MeT-5A cell line after 24 h and 48 h. 46

Figure 16. Apoptosis-inducing effects of momilactone B (MB) and the mixture of momilactone A and B (MAB) (1:1, w/w) at 5 μM against chronic myeloid leukemia (CML) (a) Meg-01 and (b) K562 cell lines after 24 h and 48 h. 47

Figure 17. Apoptosis-inducing effects of momilactone B (MB) and the mixture of momilactone A and B (MAB) (1:1, w/w) at 5 μM against acute promyelocytic leukemia (APL) HL-60 cell line after 24 h and 48 h. 48

Figure 18. Apoptosis-inducing effects of momilactone B (MB) and the mixture of momilactone A and B (MAB) (1:1, w/w) at 5 μM against mantle cell lymphoma (MCL) Mino cell line after 24 h and 48 h. 49

Figure 19. Apoptosis-inducing effects of momilactone B (MB) and the mixture of momilactone A and B (MAB) (1:1, w/w) at 5 μM against multiple myeloma (MM) (a) U266 and (b) KMS-11 cell lines after 24 h and 48 h. 50

Figure 20. Effects of momilactones A (MA) and B (MB) and their mixture (MAB) (1:1, w/w) on cell viability of non-cancerous (MeT-5A), acute promyelocytic leukemia (HL-60), and multiple myeloma (U266) cell lines after 48 h. Data are expressed as mean ± standard deviation (SD). Statistical significance was determined by *t*-test. $^{*}p < 0.05$ versus control (0 μM); $^{**}p < 0.01$ versus control (0 μM); $^{***}p < 0.001$ versus control (0 μM); ns, not significant versus control. 61

Figure 21. Apoptosis-inducing effects of momilactone B (MB) and the mixture of momilactone A and B (MAB) (1:1, w/w) at 5 μM against **(a)** non-cancerous MeT-5A, **(b)** acute promyelocytic leukemia (APL) HL-60, and **(c)** multiple myeloma (MM) U266 cell lines after 24 h and 48 h. Statistical significance was determined by *t*-test. $^{*}p < 0.05$ versus control; $^{**}p < 0.01$ versus control; ns, not significant versus control. 65

Figure 22. Effects of momilactone B (MB) and the mixture of momilactone A and B (MAB) (1:1, w/w) at 5 μM on the cell cycle of **(a)** non-cancerous (MeT-5A), **(b)** acute promyelocytic leukemia (HL-60), and **(c)** multiple myeloma (U266) cell lines after 24 h and 48 h. Statistical significance was determined by *t*-test. $^{*}p < 0.05$ versus control; $^{**}p < 0.01$ versus control; $^{***}p < 0.01$ versus control; $^{\wedge\wedge}p < 0.01$ versus MAB-24 h; $^{\#\#}p < 0.01$ versus MB-48 h; ns, not significant versus control. 67

Figure 23. Effects of momilactone B (MB) and the mixture of momilactones A and B (MAB) (1:1, w/w) on the expressions of proteins related to apoptosis induction and cell cycle arrest of **(a)** acute promyelocytic leukemia (APL) HL-60, and **(b)** multiple myeloma (MM) U266 cell lines after 24 h and 48 h. Statistical significance was determined by *t*-test. $^{*}p < 0.05$ versus control; $^{**}p < 0.01$ versus control; $^{***}p < 0.001$ versus control; $^{\dagger}p < 0.05$ versus

MB-24 h; $^{\dagger\dagger}p < 0.01$ versus MB-24 h; $^{\dagger\dagger\dagger}p < 0.01$ versus MB-24 h; $^{\wedge}p < 0.05$ versus MAB-24 h; $^{\wedge\wedge}p < 0.01$ versus MAB-24 h; $^{\wedge\wedge\wedge}p < 0.001$ versus MAB-24 h; $^{\#}p < 0.05$ versus MB-48 h; $^{\#\#}p < 0.01$ versus MB-48 h. 69

Figure 24. Cytotoxic mechanism of momilactones against acute promyelocytic leukemia (HL-60) and multiple myeloma (U266) cell lines. 75

Figure 25. Procedure for *in vitro* simulated digestive model 82

Figure 26. Bioaccessibility of momilactones under digestion. MA, momilactone A; MB, momilactone B; MAB, the mixture of momilactones A and B (1:1, w/w). 89

Figure 27. Potential approach for exploiting natural compounds from rice (*O. sativa*) and the invasive weed (*A. virginicus*) for therapeutic purposes..... 99

SUPPLEMENTARY DATA

Figure S1. Standard curves of gallic acid and rutin. 101

Figure S2. Antiradical activity of *A. virginicus* extracts via 2,2′-azinobis-(3-ethylbenzothiazoline-6-sulfonic acid) (ABTS) assay. T-Anvi, total crude extract; H-Anvi, hexane extract; E-Anvi, ethyl acetate extract; B-Anvi, butanol extract; W-Anvi, water extract. 101

Figure S3. Antiradical activity of *A. virginicus* extracts via 2,2-diphenyl-1-picrylhydrazyl (DPPH) assay. T-Anvi, total crude extract; H-Anvi, hexane extract; E-Anvi, ethyl acetate extract; B-Anvi, butanol extract; W-Anvi, water extract. 102

Figure S4. Inhibition on lipid peroxidation of *A. virginicus* extracts. T-Anvi, total crude extract; H-Anvi, hexane extract; E-Anvi, ethyl acetate extract; B-Anvi, butanol extract; W-Anvi, water extract. 103

Figure S5. Tyrosinase inhibitory activities of *A. virginicus* extracts. T-Anvi, total crude extract; H-Anvi, hexane extract; E-Anvi, ethyl acetate extract; B-Anvi, butanol extract. 104

Figure S6. α-Amylase inhibitory activities of *A. virginicus* extracts. T-Anvi, total crude extract; H-Anvi, hexane extract. 104

Figure S7. Standard curve of palmitic acid 104

Figure S8. GC chromatogram of n-alkane mixture (C13–C30) 104

Figure S9. Mass spectra (MS) of palmitic acid found in hexane extracts (H-Anvi) from *A. virginnicus* analyzed by gas chromatography-mass spectrometry (GC-MS). 105

Figure S10. Effects of momilactones A (MA) and B (MB) on cell viability of tested blood cancer cell lines via MTT assay. 105

Figure S11. Effects of Bortezomib on cell viability of multiple myeloma (U266) cell lines after 48 h. $^{**}p < 0.01$ versus control (0 nM); $^{***}p < 0.001$ versus control (0 nM). 105

Figure S12. Standard curves of momilactones A and B. 106

Figure S13. (a) Extracted ion chromatograms (EIC) and **(b)** mass spectra (MS) of the standards of momilactones A (MA) and B (MB) by ultra-performance liquid chromatography-electrospray ionization-mass spectrometry (UPLC-ESI-MS)..... 107

Figure S14. (a) Extracted ion chromatograms (EIC) and **(b)** mass spectra (MS) of momilactone A (MA) in oral digested sample by ultra-performance liquid chromatography-electrospray ionization-mass spectrometry (UPLC-ESI-MS). 108

Figure S15. (a) Extracted ion chromatograms (EIC) and **(b)** mass spectra (MS) of momilactone A (MA) in gastric digested sample by ultra-performance liquid chromatography-electrospray ionization-mass spectrometry (UPLC-ESI-MS)..... 109

Figure S16. (a) Extracted ion chromatograms (EIC) and **(b)** mass spectra (MS) of momilactone A (MA) in intestinal digested sample by ultra-performance liquid chromatography-electrospray ionization-mass spectrometry (UPLC-ESI-MS)..... 110

Figure S17. (a) Extracted ion chromatograms (EIC) and **(b)** mass spectra (MS) of momilactone B (MB) in oral digested sample by ultra-performance liquid chromatography-electrospray ionization-mass spectrometry (UPLC-ESI-MS). 111

Figure S18. (a) Extracted ion chromatograms (EIC) and **(b)** mass spectra (MS) of momilactone B (MB) in gastric digested sample by ultra-performance liquid chromatography-electrospray ionization-mass spectrometry (UPLC-ESI-MS)..... 112

Figure S19. (a) Extracted ion chromatograms (EIC) and **(b)** mass spectra (MS) of momilactone B (MB) in intestinal digested sample by ultra-performance liquid chromatography-electrospray ionization-mass spectrometry (UPLC-ESI-MS)..... 113

Figure S20. (a) Extracted ion chromatograms (EIC) and **(b)** mass spectra (MS) of momilactone A (MA) and B (MB) in oral digested sample by ultra-performance liquid chromatography-electrospray ionization-mass spectrometry (UPLC-ESI-MS)..... 115

Figure S21. (a) Extracted ion chromatograms (EIC) and **(b)** mass spectra (MS) of momilactone A (MA) and B (MB) in gastric digested sample by ultra-performance liquid chromatography-electrospray ionization-mass spectrometry (UPLC-ESI-MS)..... 117

Figure S22. (a) Extracted ion chromatograms (EIC) and **(b)** mass spectra (MS) of momilactone A (MA) and B (MB) in intestinal digested sample by ultra-performance liquid chromatography-electrospray ionization-mass spectrometry (UPLC-ESI-MS)..... 118

CHAPTER 1: GENERAL INTRODUCTION

1.1. Blood cancer

In human, cancer has been a serious human disease during a long history. In 2020, the incidence of worldwide cancers was reported 19 million new cases with approximately 50% of mortality rate (Figure 1) (GLOBOCAN, 2020). Among cancer types, blood cancers, also known as hematological cancers, achieved in 1.24 million new cases, and caused nearly 60% of deaths in 2020 (Sung et al., 2021). Blood cancer initiates in the bone marrow, where normal blood cells are produced. Of which, cancer-associated mutation can cause abnormal proliferation of immature or mature of blood cells and disruption of their function. Consequently, many human health problems occur including fever, chills, persistent fatigue, weakness, loss of appetite, nausea, unexpected weight loss, night sweats, bone/joint pain, abdominal discomfort, headaches, shortness of breath, frequent infections, itchy skin/skin rash, swollen lymph nodes in the neck/underarms/groin (CTCA, 2020).

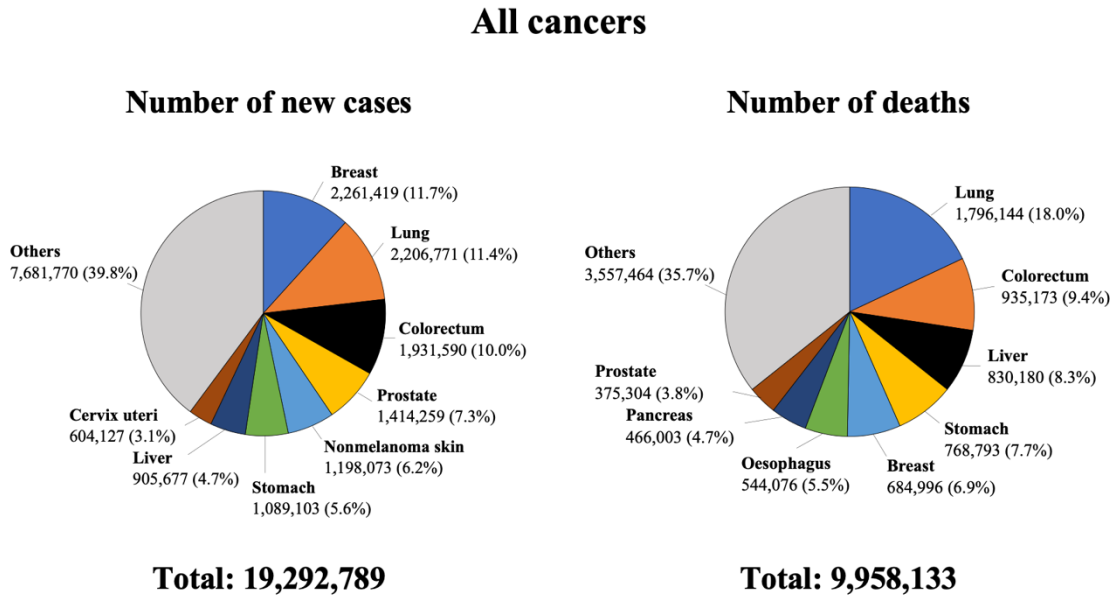

Figure 1. Number of worldwide cancer new cases and mortality rate in 2020 (GLOBOCAN, 2020)

There are three main types of blood cancers including leukemia, lymphoma, and multiple myeloma (Figure 2). In which, leukemia patients suffer from the uncontrolled

proliferation of mature or immature white blood cells with loss of function and obstruct the production of red blood cells and platelets. Leukemia comprises four major sub-groups based on the affected white blood cell types and whether it is acute (acute myeloid leukemia and acute myeloid leukemia) or chronic (chronic lymphocytic leukemia and chronic myeloid leukemia) condition (GLOBOCAN, 2020). In 2020, leukemia is the second most common blood cancer with 474,519 new cases with 66% of deaths (Figure 2) (Sung et al., 2021). On the other hand, lymphoma is the most common blood cancer that comprises 2 main types of non-Hodgkin lymphoma and Hodgkin lymphoma. Non-Hodgkin lymphoma develops from lymphocytes in the lymphatic system. While Hodgkin lymphoma is characterized by the presence of an abnormal lymphocyte namely Reed-Sternberg cell. Lymphoma was reported 544,352 new cases with mortality rate of 48% in 2020 (Figure 2) (Sung et al., 2021). Another major blood cancer type is multiple myeloma, which initiates in the plasma cells. Multiple myeloma accounted for 176,404 new cases and 66% of deaths in 2020 (Figure 2) (Sung et al., 2021).

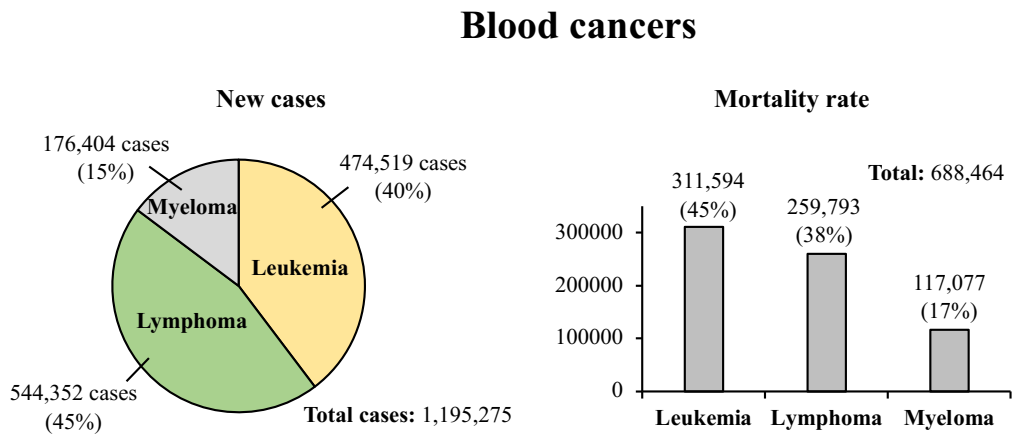

Figure 2. Number of worldwide blood cancer new cases and mortality rate in 2020 (Sung et al., 2021)

In the context that blood cancer becoming serious and complicated problems over the years, effective approaches are urgently needed to generate effective treatments for this cancer. In this study, we focus on the exploitation of natural based products from plants with

concern about their biomass availability which can contribute to the development of chemotherapy against blood cancer.

1.2. Anticancer potentials of natural compounds from plants

Recent trends in developing various herbal medicines have been to exploit benefits from plants, which are extremely abundant and well-distributed all over the world (Xu et al., 2017). Numerous compounds derived from plants exhibited antitumor properties (Zadeh et al., 2022; Espinoza et al., 2017; Kim et al., 2007; Xie et al., 2016; Zhao et al., 2018). In which, some phytocompounds showed their potential in suppressing blood cancer cells. For example, genistein found in *Leguminosae* suppressed the proliferation of human multiple myeloma cells through the downregulation of nuclear factor-κB and upregulation of microRNA-29b (Xie et al., 2016) (Figure 3). Besides, genistein impeded the proliferation and promoted cell apoptosis of human leukemia (MOLT-4) cells by inhibiting anti-apoptotic proteins (Zadeh et al., 2022) (Figure 3). Gnetin C is another anti-cancer substance derived from melinjo (*Gnetum gnemon* L. seeds) and grapes (*Vitis vinifera*) (Figure 3). This compound exhibited simultaneous inhibition on the mTOR and MAPK pathways, leading to apoptosis enhancement in acute myeloid leukemia (Espinoza et al., 2017).

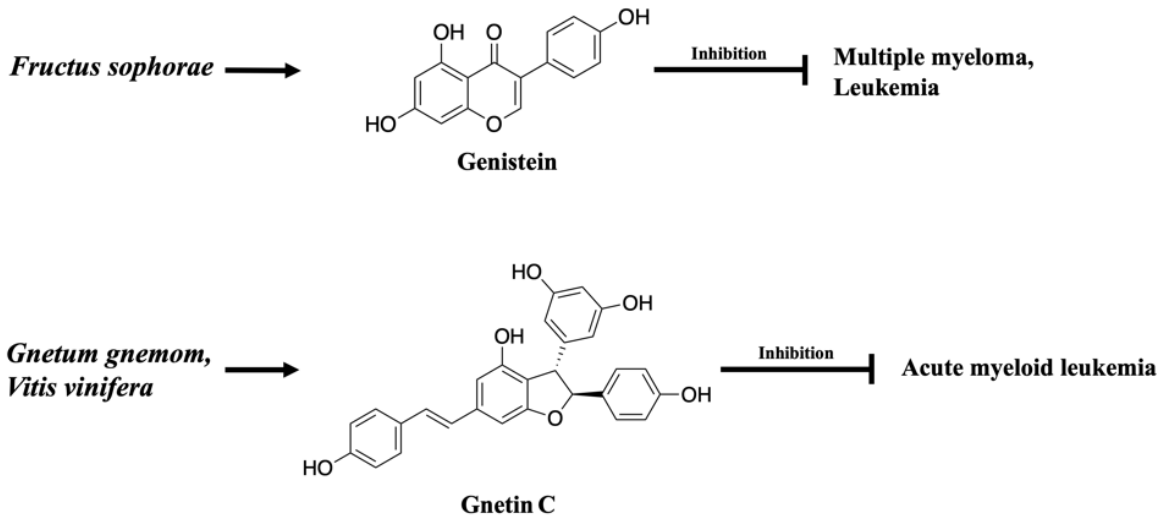

Figure 3. Anti-blood cancer substances derived from natural plants (Xie et al., 2016; Zadeh et al., 2022; Espinoza et al., 2017)

Although numerous plant species have shown their valuable pharmaceutical and medicinal properties, the overuse of these natural plants may lead to the loss of biodiversity (Teschke & Xuan, 2020). Therefore, the exploitation of selected plant objects for therapeutic purpose should also concern their available resources. Among plant sources, the family of Poaceae includes numerous plant species that have dominant biomass sources and revealed potentials for therapeutic uses (Moreira et al., 2010). In which, rice (*Oryza sativa*) has been acknowledged for their high valuable consumption during a long history. Besides, rice production remains an abundant source of rice by-products that should be exploited more properly. On the other hand, *Andropogon virginicus* is another species of Poaceae family, which is a valueless invasive weed with serious expansion all over the world (OEPP, 2019). Hitherto, there has been no strategy to take the advantages of this weed for human health purposes. Therefore, in this study, we selected *A. virginicus* and rice as the main objects. Notably, both rice and *A. virginicus* are monocot plants, which adapt to a wide range of environmental conditions (Simpson, 2010). Thus, they can be feasibly exploited for medicinal production and therapeutics with a dominant biomass availability. The study is expected to contribute to the development of anti-blood cancer treatments and solve the problems in biodiversity conservation and sustainable development.

1.3. Rice

1.3.1. Rice and rice by-products

Rice (*Oryza sativa* L.) is an important food crop that plays a crucial role in ensuring food security for the whole world. Rice grain has a long use history with high beneficial consumption as rich in nutrients (Esa & Ling, 2016; Sohail et al., 2017). In addition to valuable use of rice grain, rice by-products have recently attracted more and more attention from the pharmaceutical and food processing industries (Esa & Ling, 2016; Sohail et al.,

2017). Rice by-products including bran, husk, germ, and straw has been reported containing beneficial nutrients of proteins, vitamins, oryzanol, and phenolics etc. (Esa & Ling, 2016; Rahaie et al., 2014).

Theoretically, rice fields provide about 70% yield of white rice as major product. Besides, 30% yield of rice by-products such as husk and bran will be wasted without proper exploitation (Esa & Ling, 2016). Although rice by-products have been used for animal feed, biofuels, fertilizers, and nutrient media for mushrooms. However, the pharmaceutical and medicinal properties of isolated components from rice by-products have broad potentials that need to be elucidated. Additionally, there no toxicity of compounds derived from rice on human health. Therefore, bioactive compounds from rice and its by-products are a promising source to be exploited for medicinal and pharmaceutical purposes.

1.3.2. Momilactones

Momilactones were first isolated from rice husk (Kato et al., 1973). “Momilactone” was presented by Kato et al. (1973) (Figure 4). Of which, “momi” (籾 means the rice husk, while lactone is a group of compounds. Based on this term, every rice husk-derived lactone can be acknowledged as a momilactone compound.

Momilactones can be found in rice bran and rice by-products (husk, leaf, straw, and root). However, very few laboratories in the world can successfully isolate and purify momilactones from rice. Besides, momilactones are difficult to purchase from commercial sources. Therefore, the pharmaceutical and medicinal properties of momilactones have been least elucidated.

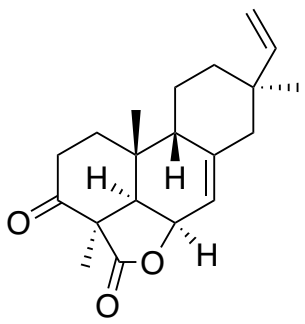

Momilactone A (MA)

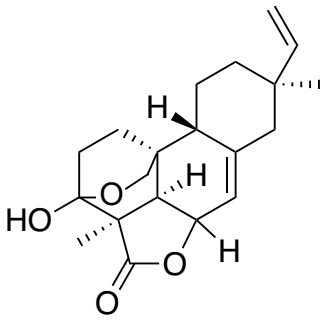

Momilactone B (MB)

Figure 4. Structures of momilactones A (MA) and B (MB)

In a preceding study, MA (150 mg) and MB (100 mg) were purified from a total of 200 kg of Koshihikari rice husks (Kato et al., 1973). Notably, an optimized isolation method (Figure 5) was conducted by Quan et al. (2019d) in our laboratory of Plant Physiology and Biochemistry, Hiroshima University, Japan to obtain a greater amount of momilactones from Koshihikari (11.7 and 8.3 mg/kg rice husk for MA and MB, respectively). Briefly, MA and MB were isolated from the ethyl acetate (EtOAc) extract of rice husks by repeated column chromatography over silica gel. The mobile phases of the first and the second column were hexane:EtOAc (v/v) and chloroform:methanol (v/v), respectively (Quan et al., 2019d). The identification and confirmation of such pure compounds applying thin-layer chromatography (TLC), high-performance liquid chromatography (HPLC), liquid chromatography-electrospray ionization-mass spectrometry (LC-ESI-MS), gas chromatography-mass spectrometry (GC-MS), and nuclear magnetic resonance (NMR) were described in the previous study of Quan et al. (2019d). Additionally, a specific technique in the preparation of samples and advanced ultra-performance liquid chromatography-electrospray ionization-mass spectrometry (UPLC-ESI-MS) method were improved to increase the detection sensitivity that helps quantify MA and MB in different rice organs with a minor amount. Those outstanding achievements may significantly contribute to the

in-depth studies aiming to exploit momilactones from rice and rice by-products for pharmaceutical purposes.

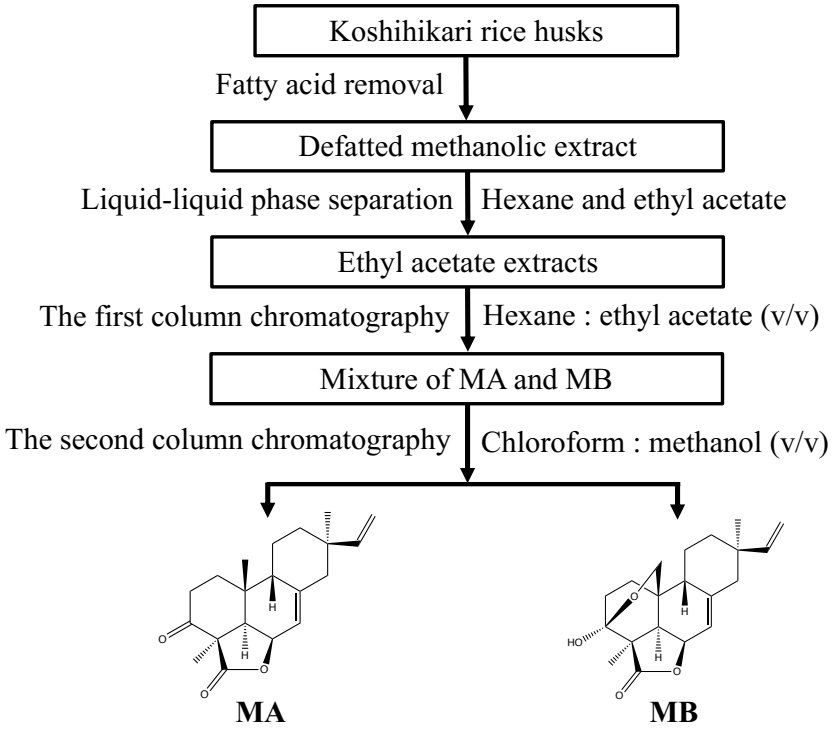

Figure 5. Momilactones isolated and purified from the laboratory of Plant Physiology and Biochemistry, Hiroshima University, Japan (Quan et al., 2019)

On the other hand, numerous diterpene lactones such as andrographolide, neoandrographolide, halimanolide, etc. were indicated having inhibitory effects against cancer cells (Silva et al., 2011) (Figure 6). Based on that, momilactones belonging to this group of compounds can be considered high potentials for anti-blood cancer properties.

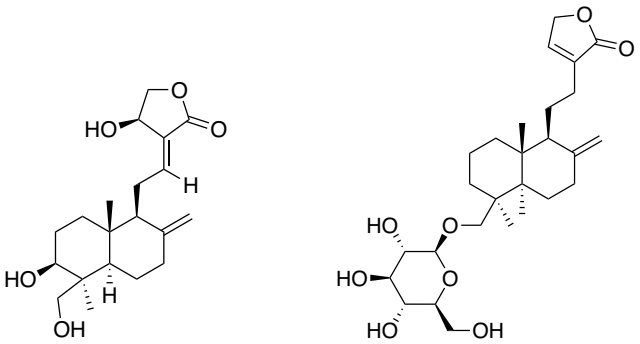

Andrographolide **Neoandrographolide**

Breast, central nervous system, colon, lung, melanoma, ovarian, prostate, renal cancers, and hepatoma

Figure 6. Anticancer potentials of diterpene lactones (Kumar et al., 2004; Ji et al., 2007)

1.3.3. Biological activities of momilactones

Allelopathic activity

Momilactones A (MA) and B (MB) exhibit a substantial allelopathic activity against natural enemies of plants such as problematic weeds (e.g., *Echinochloa crus-galli*, *Monochoria vaginalis, Solidago altissima*) (Fukuta et al., 2007; Kato-Noguchi et al., 2013; Quan et al., 2019e) and blast fungus (*Magnaporthe oryzae*) (Cartwright et al., 1980; Zhao et al., 2018). In which, MB displays a stronger allelopathic activity than that of MA. MA and MB were proven to inhibit the growth of barnyard grass (Fang et al., 2015) and Arabidopsis (Kato-Noguchi et al., 2013) through the related gene expression and transcription pathways. Whereas MA and MB presented a negligible effect on rice growth in the report of (Kato-Noguchi et al., 2013).

Antioxidant, antibacterial, anti-diabetes, anti-obesity, anti-skin aging, and anticancer potentials

MA (EC_{50} = 783.9 μg) and MB (EC_{50} = 790.7 μg) exhibited antiradical activity through 2,2-diphenyl-1-picrylhydrazyl (DPPH) assay (Fukuta et al., 2007). In the research of Quan

et al. (2019a), MA, MB, and their mixture MAB (1:1, v/v) present antiradical properties against 2,2′-azinobis-(3-ethylbenzothiazoline-6-sulfonic acid) (ABTS) radical cations with IC_{50} values of 2.84, 1.28, and 0.319 mg/mL, respectively.

MA and MB revealed antibacterial properties against 4 common strains, which cause problems in human digestion such as diarrhea and gastroenteritis. Accordingly, MB significantly inhibited the growths of *Pseudomonus ovalis*, *Bacillus cereus*, and *Bacillus pumilus* which is more potent than MA. Meanwhile, the inhibitory activity of MB was close to that of MA against *Escherichia coli* (Fukuta et al., 2007).

In previous study, MA (IC_{50} = 132.56 μg/mL) and MB (IC_{50} = 129.02 μg/mL) revealed a potent suppression on the key enzymes linked to type 2 diabetes (α-amylase and α-glucosidase) which were much stronger than the standard inhibitor γ-oryzanol (IC_{50} = 779.03 μg/mL). Besides, MA and MB showed inhibitory activity on an important enzyme associated with obesity (trypsin) with the IC_{50} values of 921.55 and 884.03 μg/mL, respectively. In another research, momilactones exhibited potentials for preventing skin wrinkles and freckles since these compounds inhibited the relevant enzymes including pancreatic elastase and tyrosinase through *in vitro* bioassays (Quan et al., 2019a).

Via cell viability (MTT) assay, MA and MB displayed a potent cytotoxicity on the murine P388 leukemia cells with IC_{50} of 0.85 and 0.07 μg/mL, respectively (Chung et al., 2005). In the research of Lee et al. (2008), MB suppressed the cell viability of human myeloblastic leukemia (HL-60), human leukemic T cells (Jurkat), basophilic leukemia (RBL-2H3), and mouse mastocytoma (p815) cell lines at concentration of less than 1.98 μg/mL. In which, MB prevent Jurkat cells by inducing cell apoptosis through the caspase and mitochondrial pathways (Lee et al., 2008). In other studies, the potential of MB in inhibiting colon cancer cells (HT-29 and SW620) was indicated via MTT, lactate dehydrogenase (LDH), and colony-forming ability assays (Kim et al., 2007). Besides, MB

suppressed human monocytic leukemia cell line U937 by stimulating apoptosis and the cell cycle arrest at G1 phase via the decrease in pRB phosphorylation and the upregulation of a CDK inhibitor $p21^{Waf1/Cip1}$ (Park et al., 2014). Since the potential of momilactones for preventing some cancers was previously indicated, the cytotoxic activity and mechanism of these compounds against many other cancer cell lines remain least elucidated.

1.4. *Andropogon virginicus*

Andropogon virginicus (Figure 7) is an invasive weed that distributes globally, threatening agriculture and economics in many countries. Until now, there has been no efficient way to remove once the weed has invaded (OEPP, 2019). However, different from rice, *A. virginicus* has hitherto received scant attention from scholars. To the best of our knowledge, there has been no strategies to exploit the dominant biomass source of this problematic invasive weed for pharmaceutical purposes. In a previous study, this weed was reported to exhibit strong allelopathic activities (Rice, 1972). Interestingly, some allelochemicals have been shown pharmaceutical properties including anticancer. Therefore, in this study, we expected to extract such potential compounds from *A. virginicus* for preventing blood cancer cell lines.

Figure 7. *Andropogon virginicus* in Higashi-Hiroshima Campus, Hiroshima University

1.4.1. Morphology

A. virginicus is a C4, herbaceous, perennial plant (Figure 7). It grows densely (cespitous form) with 50–200 cm high (Campbell, 2003). *A. virginicus* is a hemicryptophyte following the Raunkiaer life-form system (EPPO, 2019). The culm branches distally, with light green to reddish brown color during growth duration (EPPO, 2019). The leaf sheath is long. The leaf surface is scabrous. The ligule is yellow to brownish and membranous, 0.2–1 mm in size, with cilia 0.2–1.3 mm long (EPPO, 2019). The leaf blade is approximately 52 cm long and 6.5 mm wide. This blade has a variety of smooth and glabrous/or sparsely to densely pubescent spreading hairs. The inflorescence is racemes with up to 4 cm long containing spikelet (3.5–3.8 mm long).

1.4.2. Distribution

A. virginicus is original from the USA, presenting from the Central to the North of the USA. In the USA, *A. virginicus* mainly has an eastern and central native range. The weed also appears in California, where it is not native species. In 1924, *A. virginicus* was announced as invasive weed in Hawaii. This weed has been found naturally in Australia, New Zealand, Japan and South Korea. In other reports, *A. virginicus* has been found in Georgia, Russian Federation, and France. In 1940, *A. virginicus* was first reported a problematic invasive weed in Aichi Prefecture, Japan (NIES, 2017; Enomoto et al., 2007). This invasive weed is also detected in South Korea (Lee et al., 2008).

1.5. Main objectives

Considering the potentials of rice and the invasive weed *A. virginicus* for therapeutic purposes as well as their dominant biomass availability, the main objective of this study was:

(1) To explore potential phytochemicals and pharmaceutical properties of the invasive weed *A. virginicus* with focus on antioxidant, anti-blood cancer, anti-skin aging, and anti-diabetes activities.

(2) To determine the potentials of momilactones from rice for preventing different types of blood cancer.

CHAPTER 2: PHARMACEUTICAL PROPERTIES OF AN INVASIVE WEED *ANDROPOGON VIRGINICUS*

2.1. Introduction

Andropogon virginicus is a problematic invasive weed distributing widely in the world. *A. virginicus* is an herbaceous, perennial, C4 plant. This weed grows densely with up to 210 cm in height (EPPO, 2019). *A. virginicus* has been generally known with limited valuable use (EPPO, 2019). Moreover, this invasive weed is seriously threatening biodiversity with its strong invasiveness (EPPO, 2019). *A. virginicus* is problematically competing with endangered plant species such as *Tetramolopium remyi*, *Santalum freycinetianum* var. Lanaiense, and *Schiedea nuttallii* (EPPO, 2019). In addition, *A. virginicus* causes negative influence on horticultural systems because of its dense and robust growth. For example, the high competition of *A. virginicus* has been dealing a blow economically to the forage and timber production in the southeastern USA (EPPO, 2019). Besides, farmlands of Charmhaven apple in Australia have been being degraded due to its invasion (Weeds of Australia, 2020). The weed also affects the cycle of nitrogen and water content in soil which diminishing the abundance of native species (Balandier et al., 2006). Until now, there has been no efficient way to remove once the weed has invaded (Weeds of Australia, 2020). Despite the serious problem caused by *A. virginicus*, it has hitherto received scant attention from scholars. Therefore, an effective management of this natural resource is urgently needed, considering the potential of many other plants for therapeutic use, an attractive field of current research. Numerous plant species with antioxidant, anti-inflammatory, antibacterial, antiviral, anti-skin aging, and anticancer properties have been globally known (Xu et al., 2017). However, the pharmaceutical properties of the invasive weed *A. virginicus* have not been comprehensively investigated.

In humans, oxidative stress exists and contribute to several chronic diseases including diabetes, aging, and cancer through the correlation with inflammatory process (Collins, 1999). Thereby, an essential part of our study was to investigate the antioxidant capacities of extracted components from *A. virginicus*. Among chronic disorders, diabetes is a serious disease with various types requiring different treatment methods (Tarling et al., 2008). The most common diabetes is type 2, which causes the elevated level in bloodstream sugar. Of which, α-amylase is an important digestive enzyme acting on starch which involves in glucose formation. Therefore, inhibition of α-amylase is a crucial enzyme can be mentioned as a potential approach to mitigate type 2 diabetes (Tarling et al., 2008). On the other hand, freckles caused by hyperpigmentation are attributed to the upregulation of melanin formation through an abnormal tyrosinase activity (Demirseren et al., 2014). Accordingly, preventing tyrosinase can be an effective solution to avoid the symptom of skin hyperpigmentation. In blood cancer, chronic myeloid leukemia (CML) is a serious disease, caused by the unregular proliferation of myeloid cells in the bone marrow. In which, K562 and Meg-01 are typical cell lines, which are widely applied in anti-CML studies (NIH, 2020). Therefore, simultaneous inhibition of both K562 and Meg-01 can be a promising method in preventing CML. Furthermore, the synergic suppression against oxidative stress, tyrosinase and α-amylase enzymes, and K562 and Meg-01 cell lines can be considered a prospective approach for developing natural products which can be applied to treat multiple human health problems.

In this study, we aimed to investigate the pharmaceutical properties of the invasive weed *A. virginicus* targeting antioxidant, anti-skin aging, anti-diabetes, and anticancer properties. In addition, relevant phytochemicals to biological activities of this invasive species were identified using high-performance liquid chromatography-electrospray

ionization-tandem mass spectrometry (HPLC-ESI-MS/MS) and gas chromatography-mass spectrometry (GC-MS).

2.2. Materials and methods

2.2.1. Materials

Chemicals and cell lines

Solvents comprising methanol, hexane, ethyl acetate, butanol, and chloroform (Junsei Chemical Co., Ltd., Tokyo, Japan) and standards including gallic acid, rutin, butylated hydroxytoluene (BHT), kojic acid, (Kanto Chemical Co., Inc., Tokyo, Japan), palmitic acid (FUJIFILM Wako Pure Chemical Corporation) were used in this study.

Chemicals including Folin-Ciocalteu's reagent, aluminum chloride ($AlCl_3$), sodium carbonate (Na_2CO_3), sodium hypochlorite (NaClO), potassium persulfate ($K_2S_2O_8$), 2,2′-azinobis-(3-ethylbenzothiazoline-6-sulfonic acid) (ABTS), 2,2-diphenyl-1-picrylhydrazyl (DPPH), sodium acetate (CH_3COONa), β-carotene, linoleic acid, tween 40, dipotassium phosphate (K_2HPO_4), monopotassium phosphate (KH_2PO_4), trichloro acetic acid (CCl_3COOH), potassium ferricyanide ($K_3[Fe(CN)_6]$), ferric chloride ($FeCl_3$), dimethyl sulfoxide (DMSO), sodium chloride (NaCl), monosodium phosphate (NaH_2PO_4), hydrochloric acid (HCl) were purchased from Kanto Chemical Co., Inc., Tokyo, Japan. Besides, L-tyrosine, tyrosinase, starch, α-amylase, iodine, Iscove's Modified Dulbecco's Medium (IMDM), 3-(4,5-dimethylthiazolyl)2,5-diphenyl-tetrazolium bromide (MTT), and cell lysis buffer were obtained from Sigma-Aldrich, St. Louis, MO, USA.

The cell lines consisting of K562 and Meg-01 (American Type Culture Collection (ATCC), Virginia, United States) were applied in cell viability (MTT) assay.

Plant materials

A. virginicus' aerial parts were harvested in fields located inn Higashi-Hiroshima Campus, Hiroshima University, Hiroshima, Japan in October 2019. The identification was

based on the publication of European and Mediterranean Plant Protection Organization (EPPO, 2019), available database of the National Institute for Environmental Studies, Japan (NIES, 2020), Missouri Botanical Garden, United States (Tropicos, 2020), and the book entitled: "Invasive Weed" published by Japan Livestock Technology Association (JLTA, 1994). The specimen (voucher number: Anvi-J2019) was kept at the Laboratory of Plant Physiology and Biochemistry, Graduate School of Advanced Science and Engineering, Hiroshima University, Japan.

2.2.2. Sample preparation and extraction

A. virginicus' aerial plant parts were rinsed with 0.5% NaClO in water before placing in an oven at 40 °C for drying. After 1-week, the samples were blended into well powder. The obtained powder (10 g) was loaded into a Soxhlet extractor. An aliquot (400 mL) of methanol:ethyl acetate (2:8, v/v) was used as the extraction solvent. After 5 hours, the achieved extract was filtrated and concentrated using a rotary evaporator (Nihon Buchi K.K., Tokyo, Japan) to retrieve the total crude extract (T-Anvi). Subsequently, T-Anvi mixed with distilled water (50 mL) was subjected to liquid-liquid phase (1:1, v/v) extraction to obtain hexane (H-Anvi), ethyl acetate (E-Anvi), butanol (B-Anvi), and water (W-Anvi) extracts, respectively. The dried extracts were collected by evaporation at 50 °C under vacuum.

2.2.3. Total phenolic (TPC) and flavonoid (TFC) contents

The TPC of *A. virginicus'* extracts was determined applying Folin-Ciocalteu method (Elzaawely et al., 2007). The result was scanned at 765 nm and presented as milligrams of gallic acid equivalent per one gram of dry weight (mg GAE/g DW).

The TFC of *A. virginicus'* was evaluated using the aluminum chloride colorimetric method Tuyen et al. (2017). The result was recorded at 430 nm and expressed as milligrams of rutin equivalent per one gram of dry weight (mg RE/g DW).

2.2.4. Antioxidant activity

Anti-radical (ABTS and DPPH) assays

The procedures of ABTS and DPPH assays were described in the research of Quan et al. (2019f). The anti-radical capacities were observed as the discoloration of the final solution with samples and evaluated as the decreased percentage of absorbance over the negative control (MeOH) at 517 nm and 734 nm for DPPH and ABTS assays, respectively.

The anti-radical (ABTS and DPPH) ability was evaluated following the below formula:

$$\text{Anti-radical ability (\%)} = (A_C - A_S)/A_C \times 100$$

A_C: Absorbance of reaction with negative control (methanol) after subtracting control's blank (without radical solution), A_S: Absorbance of reaction with sample/or positive control (BHT) after subtracting sample's blank (without radical solution).

An established dose-dependent curve (linear equation) applying different concentrations of samples was used to calculate IC_{50} values (required concentration inhibiting 50% of radicals). A higher IC_{50} value indicates weaker inhibition.

β-Carotene bleaching assay

The reaction containing β-carotene (200 μg), chloroform (1 mL), linoleic acid (20 μL), and tween 40 (200 mg) was generated according to the protocol of Tuyen et al. (2017). The obtained solution was then concentrated under vacuum at 40 °C. Subsequently, 50 mL of oxygenated water were slowly mixed and shaken to obtain a stable emulsion. After that methanolic sample/or control (500 μg/mL) was added to the working emulsion (1:8, v/v) in a total of 225 μL of reaction solution. Similar to anti-radical assay, methanol and BHT were used as negative control and standard inhibitor, respectively. The absorbance was read every 15 min for a total of 180 min at 492 nm. The lipid peroxidation inhibition (LPI) was measured as follows:

$$LPI\ (\%) = A_{180}/A_0 \times 100$$

A_{180}: absorbance of reaction at the 180th min, A_0: absorbance of reaction at the beginning time point.

Reducing power assay

We followed the same protocol described in the study of Quan et al. (2019f). For preparation, the solutions including phosphate buffer (0.2 M, pH = 6.6); potassium ferricyanide (1 g/100 mL); trichloro acetic acid (10 g/100 mL); ferric chloride (0.01 g/10 mL) were prepared in distilled water.

The mixture of 0.1 mL of methanolic sample/or control, 0.25 mL of phosphate buffer (0.2 M, pH = 6.6), and 0.25 mL of potassium ferricyanide solution (1 g/100 mL) was incubated for 30 min at 50 °C. After that, 0.25 mL of trichloro acetic acid solution (10 g/100 mL) was supplied and centrifuged for 10 min at 4000 rpm. Subsequently, 100 µL of the supernatant was combined with 100 µL of distilled water, followed by adding 20 µL of ferric chloride solution (0.01 g/10 mL). The absorbance of obtained solution was scanned at 700 nm. BHT and methanol were tested as positive and negative controls, respectively. Sample/or control with different concentrations (10, 62.5, 125, 250, 500 µg/mL) was screened to establish the dose-responding curves.

2.2.5. Enzymatic inhibitory assays

Tyrosinase inhibition

The assay components included tyrosinase (500 units/mL in buffer), L-tyrosine substrate (2 mM in distilled water) solutions. Samples/or controls were prepared in DMSO.

Firstly, potassium phosphate buffer (20 mM, pH = 6.8) was prepared. At the beginning, 20 µL of sample/or control and 20 µL of tyrosinase solution (500 units/mL in buffer) were mixtured in 120 µL of buffer. The mixture was incubated (25 °C, 5 min). After that, the enzymatic reaction was performed by pipetting 50 µL of L-tyrosine (2 mM in distilled

water). After 10 min of incubation at 25 °C, the reaction's absorbance was read at 470 nm (Quan et al., 2019c). kojic acid and DMSO applied used as standard inhibitor and negative control, respectively. The inhibitory ability and IC_{50} values were evaluated with the same method with anti-radical assay.

α-Amylase inhibition

α-Amylase inhibitory activity was examined following the procedure presented by Quan et al. (2019f). Firstly, iodine (0.25 mM in distilled water), phosphate buffer saline (0.2 M, pH = 6.9), starch substrate (0.5% in distilled water), and α-amylase (5 units/mL in buffer) solutions were prepared. Initially, the mixture of sample/or control (20 μL) and enzyme (20 μL) was incubated (37 °C, 9 min). After that starch was (30 μL) added. The reaction was continued at 37 °C for 7 min before stopping by HCl 1M (20 μL). Finally, 100 μL of iodine was supplied. The outcome was recorded at 565 nm. Buffer:DMSO (1:1, v/v) and palmitic acid was negative control and standard inhibitor, respectively. The inhibitory activity was calculated as follows:

$$\% \text{ inhibition} = A_S/A_C \times 100$$

A_S: Absorbance of reaction with sample/or inhibitor after subtracting an absorbance of the enzymatic reaction without inhibitor, A_C: Absorbance of reaction without sample/or control and enzyme after subtracting an absorbance of the enzymatic reaction without inhibitors.

IC_{50} values were established in the same way with anti-radical assay to compare among samples.

2.2.6. Cytotoxic activity against K562 and Meg-01 cell lines

The effects of *A. virginicus'* extracts on tested cell viability were determined applying MTT assay. IMDM (Sigma-Aldrich, Missouri, United States) containing Penicillin (100 IU/mL), Streptomycin (100 μg/mL), L-glutamine (5 mM), and fetal bovine serum (10%) was used as cell culture. Samples were diluted in 0.1% DMSO (in culture media). 10 μL of

the cells (5×10^3) was seeded in each plate well filled with 90 µL of culture media and placed in an incubator (Thermo Fisher Scientific, Waltham, United States) (37 °C and CO_2 5%). After 24 h, 10 µL of sample were pipetted to each well and incubated for 40 h. Subsequently, 10 µL of MTT solution (5 mg/mL) were supplied and continuously incubated at 37 °C for 4 hours. Finally, 100 µL of cell lysis buffer (10% SDS in 0.01 M HCl) were added. The cell growth was observed using an inverted microscope (LabX, Midland, Canada). The cell viability was examined at 595 nm. 10 µL of DMSO (0.1% in culture media) was tested as negative control.

The inhibition percentage and IC_{50} value were calculated following the same method with anti-radical assay.

2.2.7. Identification of phytochemical component

GC-MS

Phytochemical profiles of H-Anvi were analyzed applying GC-MS (JMS-T100 GCV, JEOL Ltd., Tokyo, Japan). The column (DB-5MS, 30 m × 0.25 mm I.D. × 0.25 µm film thickness) (Agilent Technologies, J&W Scientific Products, Folsom, United States) was connected to GC-MS system. Sample (2 mg/mL) was automatically injected using an autosampler. Helium with the split ratio of 5:1 was performed. The temperature program of oven was scheduled as follows: Initial temperature was 50 °C without holding; Rushing temperature was 10 °C/min for 30 min then maintained for 20 min; Injector and detector temperatures were 300 °C and 320 °C, respectively. The scanned mass range (29 to 800 amu) was operated. The results of chromatogram, mass spectrum, linear retention index (LRI), and Kovats index (KI) of detected compound were collected. Identification of compound was conducted using standard sources comprising the library of JEOL's GC-MS Mass Center System Version 2.65a, and the online database of National Center for Biotechnology Information, U.S. National Library of Medicine, Bethesda MD, USA

(Pubchem-https://pubchem.ncbi.nlm.nih.gov), and the National Institute of Standards and Technology, U.S. Department of Commerce (NIST-https://webbook.nist.gov). Among detected compounds by GC-MS, palmitic acid was the most abundant compound in H-Anvi. Therefore, the quantity of palmitic acid was determined based on a calibration curve established with different concentrations of palmitic acid standard (0.1, 0.5, and 1 mg/mL). The result was expressed as milligrams per one gram of sample dry weight (mg/g DW).

HPLC-ESI-MS/MS

The phytochemical profiles of E-Anvi were identified based on the HPLC-ESI-MS/MS system equipping with LTQ Orbitrap XL mass spectrometers (Thermo Fisher Scientific, Waltham, United States) and an electrospray ionization (ESI) source. For analysis, 3.0 μL of sample (2 mg/mL) was injected into the XBridge® Shield RP18 (5 μm, 2.1 × 100 mm) column, with maintained temperature at 25 °C. The gradient program with the flow rate of 0.4 mL/min was set up as follows: 95% A and 5% B (0 – 2 min), then 30% A and 70% B (2 – 12 min), followed by 0% A and 100% B (12 – 22 min). From 22 – 34 min, the initial condition was performed. In which, solvent A was 0.1% formic acid in water and solvent B was pure acetonitrile. A negative FTMS mode (mass range from 100 to 700 m/z) was applied for mass scanning. The online database (Pubchem, National Center for Biotechnology Information, U.S. National Library of Medicine, Bethesda MD, USA) was used for reference to MS/MS spectra.

2.2.8. Data analysis

Data were analyzed applying one-way ANOVA in Minitab software version 16.2.3. Same group expresses insignificant differences (Turkey's test, $p < 0.05$). Pearson's correlation coefficients were evaluated using the same software.

2.3. Results

2.3.1. Yield and total phenolics (TPC) and flavonoids (TFC) of A. virginicus extracts

From 10 g of *A. virginicus* dried samples, the yields of total crude (T-Anvi), ethyl acetate (E-Anvi), hexane (H-Anvi), butanol (B-Anvi), and water (W-Anvi) extracts are 0.98 g (9.8%), 0.32 g (3.2%), 0.16 g (1.6%), 0.12 g (1.2%), and 0.11 g (1.1%), respectively (Table 1). The TPC results of T-Anvi, E-Anvi, H-Anvi, B-Anvi, and W-Anvi are 24.80, 25.34, 1.26, 3.26, and 0.49 mg GAE/g DW, respectively. T-Anvi contains the highest TFC (37.40 mg RE/g DW), followed by E-Anvi, H-Anvi, B-Anvi, and W-Anvi with TFCs are 25.44, 6.30, 4.91, and 0.25 mg RE/g DW, respectively (Table 1).

Table 1. Extraction yield and total phenolic (TPC) and flavonoid (TFC) contents

Samples	Extraction yield (%)	TPC (mg GAE/g DW)	TFC (mg RE/g DW)
T-Anvi	9.8	24.80 ± 0.51^{a}	37.40 ± 0.74^{a}
H-Anvi	1.6	1.26 ± 0.03^{c}	6.30 ± 0.13^{c}
E-Anvi	3.2	25.34 ± 0.47^{a}	25.44 ± 0.45^{b}
B-Anvi	1.2	3.26 ± 0.06^{b}	4.91 ± 0.08^{d}
W-Anvi	1.1	0.49 ± 0.01^{c}	0.25 ± 0.01^{e}

Data express means ± standard deviation (SD). Different superscript letters in a column indicate significant differences at $p < 0.05$. TPC, total phenolic content; TFC, total flavonoid content; T-Anvi, total crude extract; H-Anvi, hexane extract; E-Anvi, ethyl acetate extract; B-Anvi, butanol extract; W-Anvi, water extract. GAE, gallic acid equivalent; RE, rutin equivalent; DW, dry weight.

2.3.2. Antioxidant activity of extracts from A. virginicus

The antioxidant activity of *A. virginicus'* extracts is determined via ABTS, DPPH, β-carotene bleaching, and reducing power assays.

In the ABTS assay, the strongest sample inhibiting ABTS cations is E-Anvi (IC_{50} = 43.59 μg/mL), which is stronger than standard inhibitor BHT (IC_{50} = 63.51 μg/mL). The IC_{50} values of T-Anvi, B-Anvi, H-Anvi, and W-Anvi are 77.71, 86.73, 323.88, and 586.31 μg/mL, respectively (Figure 8).

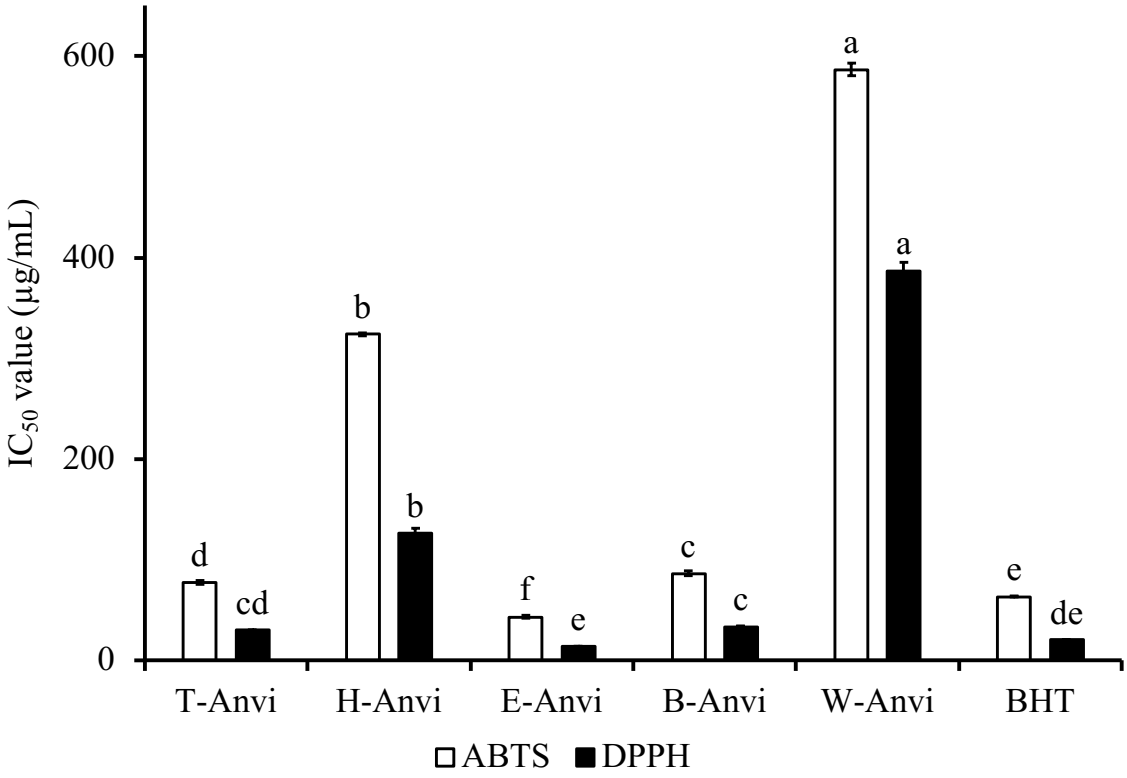

Figure 8. Anti-radical activities (ABTS and DPPH assays) of *A. virginicus* extracts. Different letters (a,b,c,d) enclosed with columns (same colors) express significant differences at $p < 0.05$ (one-way ANOVA). DPPH, 2,2-diphenyl-1-picrylhydrazyl; ABTS, 2,2′-azinobis-(3-ethylbenzothiazoline-6-sulfonic acid); T-Anvi, total crude extract; H-Anvi, hexane extract; E-Anvi, ethyl acetate extract; B-Anvi, butanol extract; W-Anvi, water extract; BHT, butylated hydroxytoluene.

In the DPPH assay, E-Anvi exhibit the most potent suppression against DPPH radicals with IC_{50} of 13.96 μg/mL, followed by T-Anvi, B-Anvi, H-Anvi, and W-Anvi with IC_{50} values of 30.54, 33.79, 126.27, and 386.91 μg/mL, respectively. Significantly, the

scavenging capacity against DPPH of E-Anvi is approximately twice stronger than that of BHT (Figure 8).

In the case of β-carotene bleaching model, the inhibition on lipid peroxidation of T-Anvi, E-Anvi, H-Anvi, B-Anvi, and W-Anvi are 90.81%, 90.85%, 92.05%, 90.17%, and 81.65%, respectively (Figure 9). Almost all samples show strong inhibition on lipid peroxidation which is close to BHT (LPI = 94.22%), except for W-Anvi.

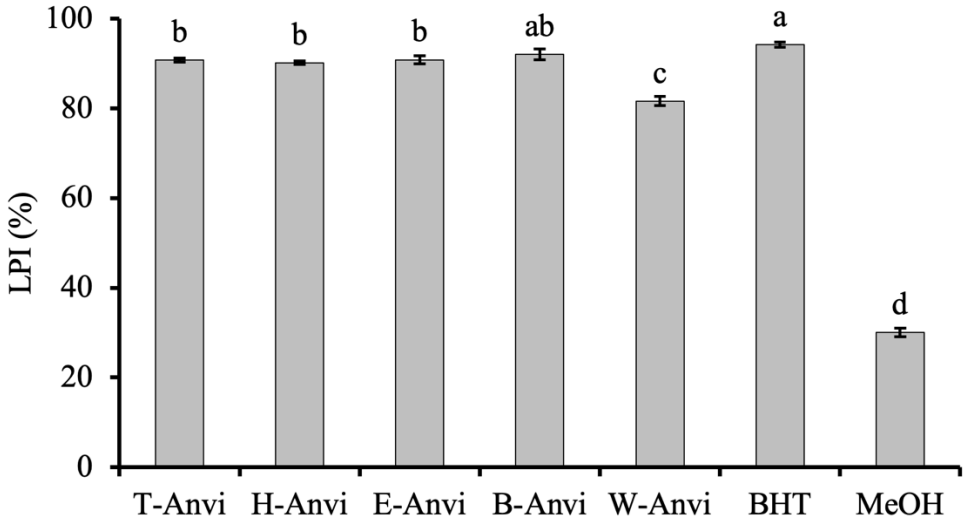

Figure 9. Inhibition on lipid peroxidation of *A. virginicus* extracts. Different letters (a,b,c,d) enclosed with columns indicate significant differences at $p < 0.05$ (one-way ANOVA). LPI, lipid peroxidation inhibition; T-Anvi, total crude extract; H-Anvi, hexane extract; E-Anvi, ethyl acetate extract; B-Anvi, butanol extract; W-Anvi, water extract; BHT, butylated hydroxytoluene.

In the reducing power assay, E-Anvi displays the most potent activity (IC_{50} = 124.11 μg/mL) which is 1.4-fold stronger than BHT (IC_{50} = 175.52 μg/mL). The following extracts are T-Anvi and B-Anvi with IC_{50} of 257.35 and 340.62 μg/mL, respectively. H-Anvi and W-Anvi exhibit negligible activity (Figure 10).

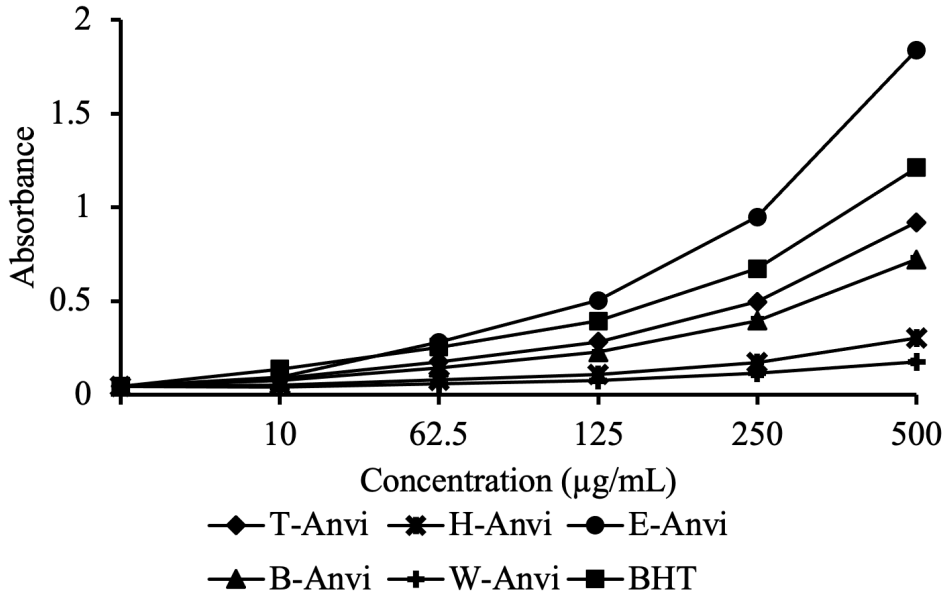

Figure 10. Potassium ferricyanide reducing power of *A. virginicus* extracts. T-Anvi, total crude extract; H-Anvi, hexane extract; E-Anvi, ethyl acetate extract; B-Anvi, butanol extract; W-Anvi, water extract; BHT, butylated hydroxytoluene.

2.3.3. Tyrosinase and α-amylase inhibitory activities of A. virginicus extracts

In the tyrosinase inhibitory results (Table 2), almost all samples reveal suppression effects. Among them, E-Anvi shows the most substantial activity (IC_{50} = 2.58 mg/mL), followed by T-Anvi, H-Anvi, and B-Anvi (IC_{50} = 4.57, 6.22, and 9.40 mg/mL, respectively). W-Anvi has no effect on the enzyme (Table 2).

In α-amylase inhibitory assay, H-Anvi and T-Anvi (IC_{50} values = 0.72 and 3.48 mg/mL, respectively) are the most potent extracts preventing α-amylase activity. Notably, the inhitory effects of H-Anvi is over twice stronger than that of palmitic acid, a well-known α-amylase inhibitor. E-Anvi and B-Anvi exhibit insignificant suppression on α-amylase (inhibition percentage = 31.93% and 17.52%, respectively at a concentration of 10 mg/mL. α-amylase is not affected by W-Anvi (Table 2).

Table 2. Tyrosinase and α-amylase inhibitory activities of *A. virginicus* extracts

Samples	Tyrosinase inhibition IC_{50} (mg/mL)	α-Amylase inhibition IC_{50} (mg/mL)
T-Anvi	4.57 ± 0.05^{c}	3.48 ± 0.07^{a}
H-Anvi	6.22 ± 0.08^{b}	0.72 ± 0.01^{c}
E-Anvi	2.58 ± 0.13^{d}	ne
B-Anvi	9.40 ± 0.02^{a}	ne
W-Anvi	na	na
Kojic acid	0.02 ± 0.00^{e}	-
Palmitic acid	-	1.57 ± 0.04^{b}

Data express mean ± standard deviation (SD). Different superscript letters in a column indicate significant differences at $p < 0.05$. T-Anvi, total crude extract; H-Anvi, hexane extract; E-Anvi, ethyl acetate extract; B-Anvi, butanol extract; W-Anvi, water extract; na, no activity; ne, negligible effect; -, not determined.

2.3.4. Cytotoxic activity of extracts from A. virginicus against K562 and Meg-01 cell lines

The dose-response curves of *A. virginicus* extracts for cytotoxic effects against K562 and Meg-01 cell lines are shown in Figure 11. For K562 cell line, E-Anvi is the most substantial extract inhibiting the viability of this cell line (IC_{50} = 112.01 µg/mL) which is twice strong than T-Anvi (IC_{50} = 247.88 µg/mL). Other extracts exhibit insignificant inhibitions on K562 cell expansion.

In the case of Meg-01 cell line, the extracts of T-Anvi, E-Anvi, and H-Anvi reveal substantial cytotoxicity with IC_{50} values of 91.40, 168.94, and 198.07 µg/mL, respectively. While B-Anvi and W-Anvi have negligible prevention against Meg-01 cell viability (Figure 11).

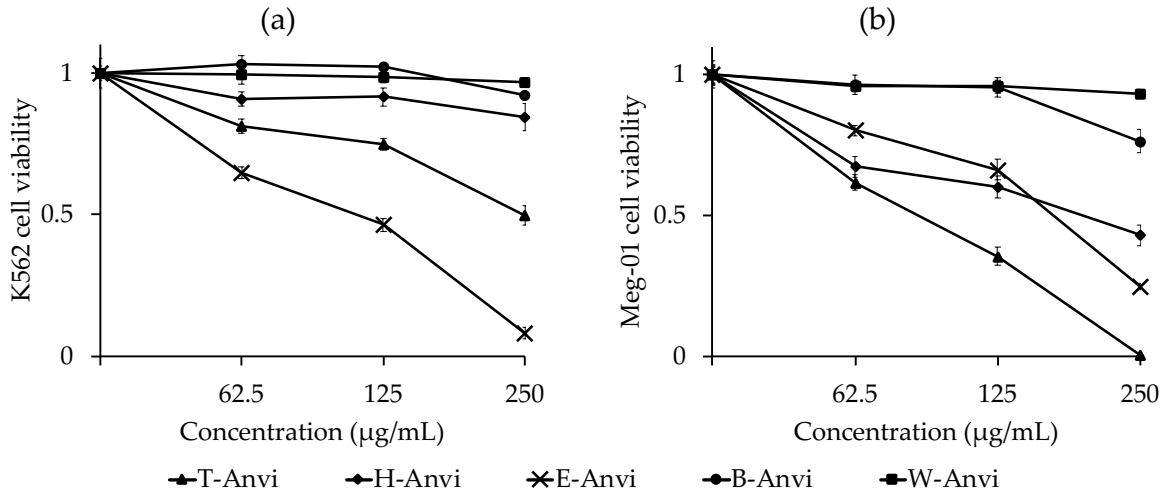

Figure 11. Dose-response curves of *A. virginicus* extracts for cytotoxicity against (a) K562 and (b) Meg-01 cell lines. T-Anvi, total crude extract; H-Anvi, hexane extract; E-Anvi, ethyl acetate extract; B-Anvi, butanol extract; W-Anvi, water extract.

2.3.5. Correlations between total phenolics (TPC) and flavonoids (TFC) and biological properties of A. virginicus extracts.

The results from Table 3 show that TPC and TFC have a strong correlation with antioxidant activity via ABTS, DPPH, and reducing power assays. On the other hand, these compounds might not be involved in lipid peroxidation and α-amylase inhibitory effects of *A. virginnicus* extracts. In contrast, flavonoids might contribute to the anti-tyrosinase potential of *A. virginicus*. Remarkably, the cytotoxicity on K562 and Meg-01 cell viability might be mainly determined by the presence of phenolics, especially flavonoid compounds in *A. virginicus'* extracts. The results show that the extract inhibiting K562 cell viability can feasibly suppress Meg-01 as well. Moreover, a close association between antioxidant, anti-tyrosinase, and K562, Meg-01 cytotoxic activities was recorded, suggesting that *A. virginicus'* extracts have synergic effects against various factors involving in human diseases.

Table 3. Pearson's correlation coefficients between total phenolic and flavonoid contents and biological activities of *A. virginicus* extracts

	TPC	TFC	ABTS	DPPH	β-Ca	RP	Tyro	α-Amy	K562
TFC	0.952*	-	-	-	-	-	-	-	-
ABTS	0.833*	0.674*	-	-	-	-	-	-	-
DPPH	0.813*	0.633*	0.993*	-	-	-	-	-	-
β-Ca	0.423	0.466	0.589*	0.549*	-	-	-	-	-
RP	0.843*	0.667*	0.987*	0.997*	0.523*	-	-	-	-
Tyro	0.479	0.525*	0.601*	0.572*	0.970*	0.555*	-	-	-
α-Amy	-0.236	-0.043	-0.439	-0.416	0.217	-0.391	0.302	-	-
K562	0.898*	0.736*	0.891*	0.914*	0.330	0.942*	0.393	-0.307	-
Meg-01	0.787*	0.913*	0.404	0.378	0.435	0.424	0.526*	0.351	0.554*

*, a significance at $p < 0.05$; TPC, total phenolic content; TFC, total flavonoid content; ABTS, 2,2′-azinobis-(3-ethylbenzothiazoline-6-sulfonic acid) assay; DPPH, 2,2-diphenyl-1-picrylhydrazyl assay; β-Ca, β-carotene bleaching assay; RP, reducing power assay; Tyro, tyrosinase inhibitory assay; α-Amy, α-amylase inhibitory assay; K562, K562 cytotoxic assay; Meg-01, Meg-01 cytotoxic assay.

2.3.6. GC-MS results

Based on the GC-MS results (Figure 12), four dominant compounds are detected in H-Anvi which are reported in Table 4. In which, palmitic acid is the most abundant compound (peak area accounts for 27.97%). The following dominant compound is phytol, 8-methyl-1-undecene, and γ-sitosterol with peaks areas of 16.42%, 10.77%, and 7.38%, respectively. The linear retention index (LRI) and Kovats index (KI) of detected compounds are compared to the literature. The quantity of palmitic acid is 0.86 mg per 1 g of *A. virginicus* dry weight and 0.05 mg per 1 g of H-Anvi dried extract (Table 4).

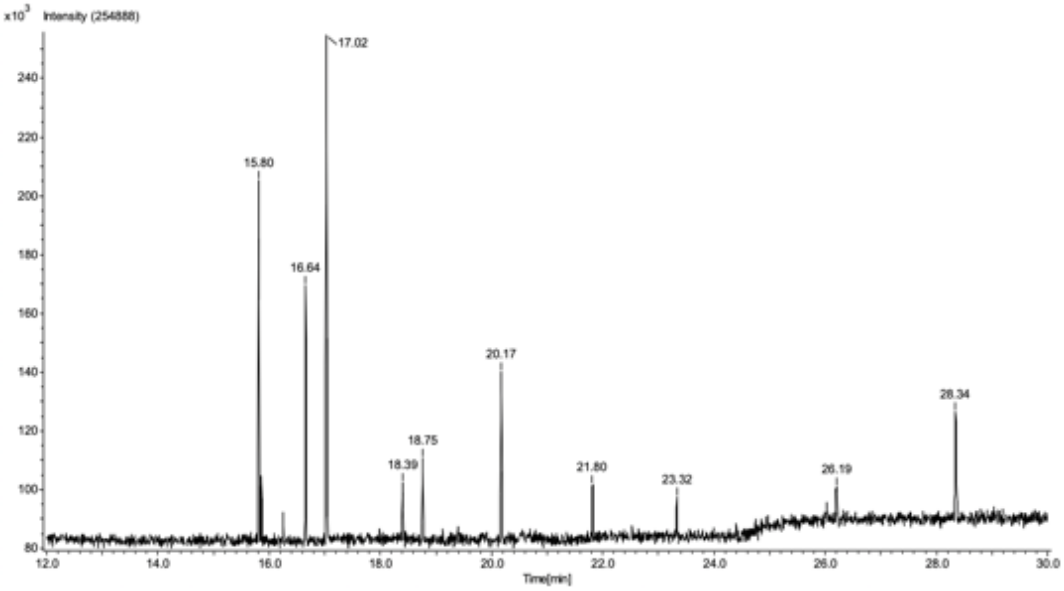

Figure 12. GC-MS chromatogram of H-Anvi extract

Table 4. Dominant phytochemicals in H-Anvi extract from *A. vigirnicus* identified by GC-MS

No.	Identified compound	RT (min)	MW	Formula	Classification	Peak area (%)	LRI	KI	Content (mg/g DW)
1	Phytol	15.80	296	$C_{20}H_{40}O$	Diterpenoids	16.42	1835	1835	-
2	8-Methyl-1-undecene	16.64	168	$C_{12}H_{24}$	Alkenes	10.77	1916	1917	-
3	Palmitic acid	17.02	256	$C_{16}H_{32}O_2$	Fatty acids	27.97	1955	1955	0.86
4	γ-Sitosterol	28.34	414	$C_{29}H_{50}O$	Steroids	7.38	-	-	-

RT, retention time; LRI, linear retention index; KI, Kovats index; DW, dry weight; -, not determined.

2.3.7. HPLC-ESI-MS/MS results

The results of HPLC-ESI-MS/MS in Figure 13 indicate eight tentative compounds in E-Anvi. Among them, five compounds can be classified as flavonoids including genistin,

kaempferol-O-galactopyranoside, eupatilin, quercetin-3-O-β-d-glucopyranoside, and kaempferol 3-O-β-d-glucopyranoside. The groups of benzophenones (annulatophenonoside), phenolic glycosides (dihydroferulic acid 4-O-glucuronide), proanthocyanidins (prodelphinidin B6) are also identified (Table 5).

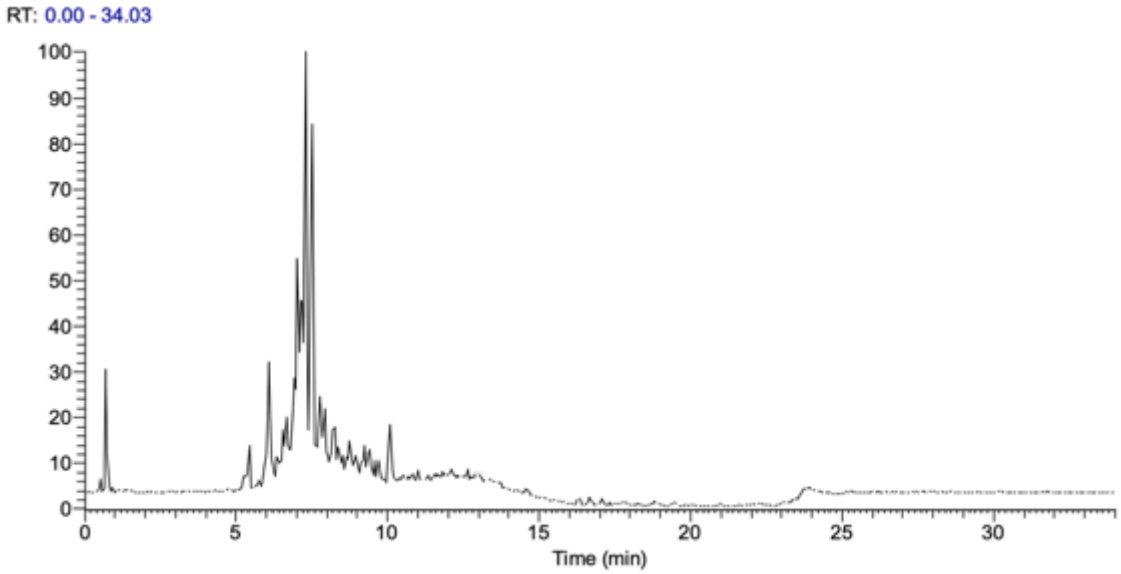

Figure 13. HPLC chromatogram of E-Anvi extract

Table 5. Phytocompounds in E-Anvi extract from *A. virginicus* detected by HPLC-ESI-MS/MS

No. Signals	RT (min)	$[M+H]^-$ (m/z)	Chemical classification	Tentative identity	Molecular formula	Exact mass	Fragment ions (m/z)
1	0.68	377.086	Benzophenones	Annulatophenonoside	$C_{18}H_{18}O_9$	378.3	89.024(100); 119.086(53); 143.036(45); 149.099(28)
2	5.74	371.098	Phenolic glycosides	Dihydroferulic acid 4-O-glucuronide	$C_{16}H_{20}O_{10}$	372.3	231.158(100); 243.293(23); 225.296(19); 121.105(14)
3	6.08	447.093	Flavonoids	Kaempferol-O-galactopyranoside	$C_{21}H_{20}O_{11}$	448.4	327.154(100); 357.141(48); 429.155(5); 369.242(4)
4	6.35	431.098	Flavonoids	Genistin	$C_{21}H_{20}O_{10}$	432.4	311.140(100); 341.117(6); 283.142(2)
5	6.54	463.088	Flavonoids	Quercetin-3-O-β-d-glucopyranoside	$C_{21}H_{20}O_{12}$	464.4	445.145(100); 343.148(92); 427.169(75); 373.161(48)
6	6.67	447.093	Flavonoids	Kaempferol 3-O-β-d-glucopyranoside	$C_{21}H_{20}O_{11}$	448.4	285.167(100); 402.158(6); 428.144(5); 374.128(3)

7	8.37	413.088	Proanthocyanidins	Prodelphinidin B6	$C_{21}H_{18}O_9$	414.4	313.135(100); 297.155(73); 369.145(70); 285.154(20)
8	9.71	343.082	Flavonoids	Eupatilin	$C_{18}H_{16}O_7$	344.3	311.153(100)

RT, retention time.

2. 4. Discussion

Recently, the impacts of oxidative stress on many human diseases have been proposed though rarely established (Ambade & Mandrekar, 2012; Biswas et al., 2007; Cachofeiro et al., 2008; Tucker et al., 2015). Numerous studies were carried out worldwide to evaluate the contribution of antioxidant substances to several chronic disorders, for example, skin aging, cancer, diabetes, etc. However, the application on human through clinical tests have shown failure (Sesso, 2008; Zhang et al., 2008a, 2008b). This unsuccessful result may be due to select only potent antioxidant compounds to inhibit varuous diseases (Biswas, 2016). Therefore, in our study, the synergic effects of antioxidant, anti-tyrosinase, anti-α-amylase, and cytotoxic potentials were investigated on *A. virginicus*, an invasive weed that was once thought to be of no use.

Basically, plant's biological properties are determined by their chemical profile. Therefore, potential phytocompounds of *A. virgnicus* are determined in this study. The results of total phenolics (TPC) and flavonoids (TFC) indicate that E-Anvi contains the highest TPC and TFC. The most dominant compounds in E-Anvi belong to the groups of flavonoids and flavonoid glycosides. Theoretically, such compounds show a higher affinity for water or butanol fractions. Therefore, other studies tend to choose polar solvents and extraction procedures such as hexane, ethyl acetate, butanol, 50% ethanol, and water, which are more effective in extracting flavonoid glycosides, and their solubility in ethyl acetate is rather law (Tagousop et al., 2018; Thavamoney et al., 2018). In fact, the identification and characterization of the phytocompound composition of each plant sample is affected by numerous factors such as plant species and extraction methods. The TPC and TFC in ethyl acetate extracts were found to be equal to or higher than those obtained from aqueous and butanol solutions in the case of some species including *Euphorbia splendida* (Kefayati et al., 2017) or *Ziziphus jujube* (Al-Saeedi et al., 2016). On the other hand, Soxhlet extraction applied in this study with methanol:ethyl acetate (2:8, v/v) could collect flavonoid glycoside components. This suggests that the mentioned extraction procedure may be suitable for extracting flavonoid glycosides from *A. virginicus*. However, further extraction and isolation protocols should be performed to improve the purification of potential compounds from this weed.

In antioxidants, the potent activities of phenolics and flavonoids such as radical scavenging and metal ion chelation have been widely reported. It can be explained via their specific structure of aromatic ring, and especially the number of hydroxyl (-OH) groups (Pandey & Mishra, 2012; Heim et al., 2002; Kumar & Pandey, 2013; Soobrattee et al., 2005). The correlation among TPC, TFC, and antioxidant ability of *A. virginicus* reinforces the above statement (Table 3). Remarkably, the strongest samples of antioxidant activities

include the total crude and ethyl acetate extracts, which are recorded to contain high levels of phenolic compounds, particularly flavonoids (Table 1). Notably, the ethyl acetate extract exhibits stronger radical scavenging capacities via ABTS, and DPPH assays and higher reducing power than BHT, a well-known antioxidant agent (Figure 8). Hence, the HPLC-ESI-MS/MS method was applied to analyze the chemical profiles in this extract. Accordingly, the ethyl acetate extract is found rich in flavonoid content, which may determine the potent antioxidant ability of this extract (Table 5).

Besides the antioxidant activity, flavonoids in *A. virginicus* may be a main contributor to anti-tyrosinase ability of the total crude and ethyl acetate extracts in this study (Tables 2, 3, and 5). Previously, flavonoids were recorded having inhibitory effects against tyrosinase through *in silico* and *in vitro* screenings (Şöhretoğlu et al., 2018). However, unlike the antioxidant capacities, the enzymatic reactions are much more complicated and difficult to predict, which are influenced by various features in chemical structures (Quan et al., 2019f). For example, the rings A and C, (-OH) substituent at the position of 7, and the ring B linked to (-OH) groups at the position of para or para and meta in the flavonoid structures lead to the competitive inhibition against tyrosinase (Şöhretoğlu et al., 2018). In the case of anti-α-amylase activity, the inhibition may depend on different factors such as the position of (-OH) substituents, methoxy groups, lactone rings, or the interaction between compounds in the mixture (Quan et al., 2019f). Via the results of α-amylase inhibitory assay (Table 2), the hexane extract from *A. virginicus* shows the strongest suppression. Thus, the GC-MS analysis was performed to find out the major compounds involving in the prevention against α-amylase in this extract. Among the most dominant compounds, palmitic acid shows the highest peak area and accounts for 0.86 and 0.05 mg per 1 g of *A. virginicus* dry weight and hexane dried extract, respectively (Table 4), whilst other compounds in Table 4 were neither successfully isolated nor be purchased, thus need further clarification. Notably, palmitic acid

is an acknowledged α-amylase inhibitor (Anh et al., 2020; Su et al., 2013a, 2013b), thus it was used as a positive control in this study. Remarkably, the hexane extract reveals over twice stronger inhibitory effect than palmitic acid by comparing their IC_{50} values. Because palmitic acid is a major compound (Table 4) in the plant, it is suggested that this compound may play an important role in the biological potential of the invasive weed, beside the α-amylase inhibitory effect as shown in this study. The hexane extract's activity may be strengthened due to the interaction between four dominant compounds consisting of palmitic acid, γ-sitosterol, phytol, and 8-methyl-1-undecene (Table 4). In which, γ-sitosterol is also a high potential anti-diabetes substance, which has been affirmed through *in vitro* and *in vivo* tests on rats in recent studies (Kumar et al., 2013). Therefore, this compound may play an influential role in the anti-α-amylase ability of the hexane extract.

The detected flavonoids in the *A. virginicus*'s total crude and ethyl acetate extracts may be also the primary agents for the cytotoxic activities against K562 and Meg-01 cell lines. According to the previous studies including laboratory bioassays, epidemiological investigations, and clinical trials, flavonoids have shown important chemotherapy roles for cancer. The anticancer property of flavonoids has been comprehensively explained through various biological pathways such as antioxidants, enzymatic activities, genetic factors, and cell-related mechanisms, or synergic effects of these mentioned factors (Sharma et al., 2011). Remarkably, the antioxidant activity of flavonoids is closely associated with anticancer regulation (Kopustinskiene et al., 2020). Meanwhile, phytoflavonoids are not harmful to normal myeloid, peripheral blood, and epithelial cell lines (Veeramuthu et al., 2017). In our research, we also find a strong correlation between total phenolics and flavonoids, antioxidant and cytotoxic capacities in the ethyl acetate extract (Table 3). On the other hand, the hexane extract's cytotoxic activity against Meg-01 cell line may be due to the presence of phytol and γ-sitosterol or the combined influence of the found compounds in this extract

(Figure 11 and Table 4). Particularly, phytol is a popular anticancer agent, which has been mentioned in numerous recent studies. The inhibition of this compound on different types of cancer cells and relevant modes of action have been globally published (Alencar et al., 2019; de Alencar et al., 2019; Pejin et al., 2014; Sakthivel et al., 2018). Whilst γ-sitosterol has been also known to be an antitumor agent, its specific mechanism has been reported in other studies (Endrini et al., 2015; Sundarraj et al., 2012; Teschke & Xuan, 2020).

In addition to finding out potential therapeutic properties and phytocompounds, the specific direction of developing natural-based drugs is essentially considered to come up with the most effective approach (Teschke & Xuan, 2020). For example, clinical tests through randomized controlled trials are required before the products are registered as drugs. One of the critical factors is that natural products must satisfy the safety requirements. In fact, some of them have shown hepatotoxicity with high application dose in clinical trials on humans (Teschke et al., 2016, 2018; Teschke & Xuan, 2020). Therefore, although numerous plant products have proven their potentials for therapeutic uses, very few of them have been officially registered and widely applied. An effective approach can be addressed such as investigating the biological properties of folk medicines and traditional food stuffs. Ginger shell (*Alpinia zerumbet*) can be an example, which is considered as a significant contributor to human longevity in Japanese Okinawa (Teschke & Xuan, 2018, 2020). This plant species is popularly used with even no clinical data available. However, the overuse of these natural plants also leads to the loss of biodiversity (Teschke & Xuan, 2020). Therefore, changing the conventional objects to other available resources, especially problematic invasive species, is a prospective direction. The exploitation of invasive weed for medicinal purposes can simultaneously solve the problems in biodiversity conservation and sustainable development.

In general, the invasive weed *A. virginicus* shows the potential for antioxidant, anti-diabetes, anti-skin aging, and anti-CML properties via *in vitro* approaches. Therefore, *in vivo* tests and clinical trials should be further performed to develop novel natural-based drugs. Additionally, the screening results by GC-MS (Table 4) and HPLC-ESI-MS/MS (Table 5) indicate the most dominant compounds including palmitic acid, γ-sitosterol, phytol, and 8-methyl-1-undecene, flavonoids, and flavonoid glycosides, which might be the main contributors to the biological activities of this plant. Based on that, the research on confirmation of their role in biological and pharmaceutical properties of *A. virginicus* should be conducted. Furthermore, the quantification of bioactive compounds in mixtures and extracts showing the potent activity should be also carried out. Palmitic acid has been reported as an inhibitor for anti-diabetes (Anh et al., 2020; Su et al., 2013a, 2013b), phytol and γ-sitosterol are popularly known as anticancer agents (Alencar et al., 2019; de Alencar et al., 2019; Pejin et al., 2014; Sakthivel et al., 2018). While flavonoids and flavonoid glycosides can be used as antioxidant agents and applied in treatment for numerous diseases (Pandey & Mishra, 2012; Heim et al., 2002; Kumar & Pandey, 2013; Sharma et al., 2011; Soobrattee et al., 2005). The quantification of dominant and specific bioactive compounds should use advantage analytical instruments such as LC-MS and LC-ESI-MS/MS rather than the estimation of total flavonoids and phenols and quantification by only GC-MS. Future studies focusing on isolation, purification, and quantification of bioactive compounds from *A. virginicus* should be performed to explore the medicinal and pharmaceutical potential of this invasive species. This could help farmers in developing countries to improve their income from the utilization of this problematic weed as a source of antioxidants, anti-skin aging, anti-diabetes, and anticancer.

2.5. Conclusions

This is the first investigation of the biological properties of the invasive weed *A. virginicus* including antioxidants, anti-α-amylase, and anti-tyrosinase abilities, and cytotoxicity against CML cell lines. The results show that the ethyl acetate extract from *A. virginicus* exhibits the highest antioxidant activity via ABTS, DPPH, reducing power assays, and β-carotene bleaching models. In addition, this extract reveals potential anti-tyrosinase capacity and potent cytotoxicity against K562 and Meg-01 cell lines. Meanwhile, the hexane extract displays strong α-amylase and Meg-01 inhibitory effects. The chemical analysis results indicate that *A. virginicus* aerial parts are rich in flavonoids, palmitic acid, phytol, and γ-sitosterol, which may principally play a vital role in biological activities of the respective extracts. The finding suggests that *A. virginicus* is a promising source of antioxidant, anti-diabetic, anti-tyrosinase, and antitumor agents. Further *in vivo* and clinical tests should be performed to confirm and develop the natural functional products from *A. virginicus* for pharmaceutical purposes.

CHAPTER 3: CYTOTOXIC ACTIVITIES OF MOMILACTONES AGAINST LEUKEMIA, LYMPHOMA, AND MULTIPLE MYELOMA CELL LINES

3.1. Introduction

Hematological disorder is a serious type of cancer, causing 688,464 deaths worldwide in 2020 (approximately 60%) (Sung et al., 2021). Among hematological cancers, lymphoma is the most common type, which achieved in 544,352 cases and 48% of deaths (Sung et al., 2021). In which, mantle cell lymphoma is a subtype of non-Hodgkin's lymphoma, resulting in a short survival time of 3 to 5 years for patient (Cheah et al., 2016). Leukemia including acute and chronic conditions is another dangerous blood cancer type that accounted for 474,519 new cases with mortality rate of 66% (Sung et al., 2021). The overgrowth of white blood cell and the loss of their functional activities are happened in leukemia, leading to adverse problems for human health (Sung et al., 2021). Besides, multiple myeloma was reported 176,404 new cases with 66% of deaths (Sung et al., 2021). Patients affected by this disease can be suffered from the disruption of bone structure and function (Hanamura, 2021). In the context of blood cancer has been becoming serious and complicated problems over the years without any signal of stopping, promising candidates are needed to generate effective treatments for patients suffering from this cancer.

In the last few decades, numerous studies were carried out aiming to develop anticancer agents from plant-based products (Anh et al., 2020; Lam et al., 2022; Quan et al., 2022; Un et al., 2022). These natural products have been reported having therapeutic properties with less toxicity compared to synthetic drugs (Teschke & Xuan, 2020). Interestingly, simultaneous application of herbal medicines and modern drugs has exhibited certain effects to the treatment (Ameade et al., 2018). Among valuable compounds isolated from plants, diterpene lactones namely, momilactones, have been detected only in rice (*Oryza sativa*) and the *Hypnum* moss (*Hypnum plumaeforme*). These compounds were

reported that play an important role in rice responses to biotic and abiotic stresses (Kato-Noguchi, 2009; Kato-Noguchi et al., 2010; Kato-Noguchi & Peters, 2013; Quan et al., 2019e; Xuan et al., 2016; Zhao et al., 2018). In other studies, momilactones have shown potentials for preventing oxidative stress, diabetes (Quan et al., 2019a, 2019b, 2019d), obesity (Quan et al., 2019d), and skin aging (Quan et al., 2019a). Notably, momilactone B was reported suppressing colon cancer (Kim et al., 2007), monocytic leukemia (Park et al., 2014), leukemic T cell lines (Lee et al., 2008). However, the cytotoxic potentials of momilactones against chronic myeloid leukemia (CML), acute promyelocytic leukemia (APL), mantle cell lymphoma (MCL), and multiple myeloma (MM) have been remained least elucidated.

In metabolic control of cell death, apoptosis is a natural mechanism to kill unnecessary or unwanted cells. Accordingly, numerous studies have been targeted the activation of the apoptotic process to suppress the undisciplined invasion of cancer cells (Pfeffer & Singh, 2018). In cancer therapy, apoptosis enhancement can represent the most effective non-surgical approaches for all cases (Pfeffer & Singh, 2018). Therefore, in this study, we investigated, for the first time, the cytotoxic potentials of momilactones A (MA) and B (MB) and their mixture MAB (1:1, w/w) against CML (Meg-01 and K562), APL (HL-60), MCL (Mino), and MM (U266 and KMS-11) cell lines through apoptotic pathways.

3.2. Materials and methods

3.2.1. Materials

Purified momilactones A (MA) and B (MB) were obtained from previous study conducted in our laboratory of Plant Physiology and Biochemistry, Hiroshima University, Japan (Quan et al., 2019b). In brief, MA and MB were isolated and purified from rice husks (*Oryza sativa* var. Koshihikari) by column chromatography over silica gel. The identification

and confirmation of pure MA and MB using TLC, HPLC, LC-ESI-MS, GC-MS, and ^{1}H-NMR, and ^{13}C-NMR were presented by Quan et al. (2019b).

The tested cell lines in the current investigation included normal cell MeT-5A (CRL-9444™), chronic myeloid leukemia (CML) Meg-01 (CRL-2021™) and K562 (CCL-243™), acute promyelocytic leukemia (APL) HL-60 (CCL-240™), mantle cell lymphoma (MCL) Mino (CRL-3000™), and multiple myeloma (MM) U266 (TIB-196™) were purchased from American Type Culture Collection (ATCC), Virginia, United States. Another MM cell line KMS-11 (JCRB1179) was obtained from Japanese Collection of Research Bioresource Cell Bank.

3.2.2. Cell viability (MTT) assay

Cell culture media was prepared in the same method described in Chapter 2. The cells (10 µL) were seeded into a 96-well plate filled with culture media (90 µL) and placed in a CO_2 incubator at 37 °C. After 24 h, the cells were treated with MA, MB, and MAB (10 µL) with different concentrations (0.5, 1, 5, and 10 µM) for 48 h. Subsequently, 10 µL of the MTT solution (5 mg/mL, Sigma-Aldrich) was pipetted into each well. The cells were continuously incubated for 4 h. Finally, 100 µL of cell lysis buffer (10% SDS in 0.01 M HCl) was applied to dissolve the colored formazan crystals. Culture media instead of momilactones was used as the negative control. Meanwhile the well-known medicines comprising Doxorubicin, Imatinib, and Ibrutinib were tested as the standard inhibitors. The absorbance at 595 nm was scanned to determine the cell growth rate in value using a spectrophotometer (SpectraMAX M5, Molecular Devices, Sunnyvale, CA, USA) (Anh et al., 2020). The cytotoxic activity (% inhibition) of momilactones/or inhibitors on the tested cell lines was as follows:

$$\text{Inhibition (\%)} = (A_{NC} - A_S)/A_{NC} \times 100$$

A_{NC}: Absorbance of reaction with negative control, A_S: Absorbance of reaction with momilactone/or inhibitor.

Dose-responding curves and IC_{50} values of the momilactones and standard inhibitors for cytotoxicity against tested cell lines were established. A higher IC_{50} indicates a weaker cytotoxicity activity.

3.2.3. Cell apoptosis (annexin V) assay

The procedure was conducted following Lam et al. (2022). In brief, the cells were seeded into a 6-well plate and cultured in a CO_2 incubator for 24 h with the same condition as mentioned in MTT assay. The cells were then treated with momilactones for 24 h and 48 h. The non-treated cells were used as a control. After that, the control and treated cells were incubated with annexin V-conjugated fluorescein isothiocyanate (FITC) (Biolegend, San Diego, CA, USA) and propidium iodide (PI) for 15 min at 25 °C. The intensities of annexin V-FITC and PI, and the percentages of apoptotic cells were determined by a flow a flow cytometer (BD, Franklin Lakes, NJ, USA).

3.3. Results

3.3.1. Effects of momilactones A (MA) and B (MB) and their mixture (MAB) on cell viability of blood cancer cell lines

The *in vitro* cytotoxic activities of momilactones A (MA) and B (MB) and their mixture (MAB) (1:1, w/w) against blood cancer cell lines, including the chronic myeloid leukemia (CML) Meg-01 and K562, acute promyelocytic leukemia (APL) HL-60, mantle cell lymphoma (MCL) Mino, and multiple myeloma (MM) U266 and KMS-11 cell lines are expressed as IC_{50} values in Table 6. The mesothelium cell line MeT-5A was tested as the non-cancerous control. In addition, Doxorubicin, Imatinib, and Ibrutinib were applied as the standard inhibitors.

Table 6. Cytotoxic activities of momilactones A and B against non-cancerous (MeT-5A), chronic myeloid leukemia (Meg-01 and K562), acute promyelocytic leukemia (HL-60), mantle cell lymphoma (Mino), and multiple myeloma (U266 and KMS-11) cell lines

Compounds	MeT-5A (% Inhibition at 10 µM)	Meg-01 IC_{50} (µM)	K562 IC_{50} (µM)	HL-60 IC_{50} (µM)	Mino IC_{50} (µM)	U266 IC_{50} (µM)	KMS-11 IC_{50} (µM)
MA	28.52 ± 2.93^{a}	7.19 ± 0.39^{a}	8.18 ± 0.33^{a}	ne	ne	ne	ne
MB	38.00 ± 2.29^{b}	4.39 ± 0.32^{b}	5.02 ± 0.56^{b}	4.49 ± 0.34^{a}	5.89 ± 0.14^{a}	5.09 ± 0.58^{b}	4.97 ± 0.10^{b}
MAB	37.82 ± 3.64^{b}	4.30 ± 0.55^{b}	4.13 ± 0.38^{b}	4.61 ± 0.10^{a}	5.19 ± 0.39^{b}	5.59 ± 0.17^{b}	5.36 ± 0.10^{a}
Doxorubicin	49.23 ± 6.17^{c}	3.34 ± 0.42^{c}	3.13 ± 0.21^{c}	5.22 ± 0.15^{b}	0.64 ± 0.03^{d}	0.24 ± 0.01^{c}	0.46 ± 0.01^{c}
Imatinib	ne	0.61 ± 0.01^{d}	0.67 ± 0.01^{d}	ne	-	-	-
Ibrutinib	ne	-	-	-	0.85 ± 0.03^{c}	7.97 ± 0.34^{a}	ne

Outcomes are presented as means ± standard deviations (SD). Means within a column followed by similar superscript letters (^{a,b,c,d}) are insignificantly different at $p < 0.05$. MA, momilactone A; MB, momilactone B; MAB, the mixture of MA and MB (1:1, w/w); ne, negligible effect; -, not determined.

According to Table 6, MA, MB, and MAB exhibit a slight inhibition on the non-cancerous cell line MeT-5A with the percentages of 28.52%, 38.00%, and 37.82% which are weaker than Doxorubicin (% inhibition = 49.23%) at a concentration of 10 µM. Imatinib and Ibrutinib are observed as having insignificant effects on MeT-5A.

The proliferation of typical CML cell lines including Meg-01 and K562 is remarkably prevented by MA, MB, and MAB (IC_{50} = 7.19, 4.39, and 4.30 μM, respectively for Meg-01 and IC_{50} = 8.18, 5.02, and 4.13 μM, respectively for K562). For APL cell line HL-60, MA shows negligible inhibition. Meanwhile, MB and MAB display a strong cytotoxicity with IC_{50} values of 4.49 and 4.61 μM, respectively. Besides, Doxorubicin and Imatinib reveal a potent suppression against Meg-01 (IC_{50} = 3.34 and 0.61 μM, respectively) and K562 (IC_{50} = 3.13 and 0.67 μM, respectively). Significantly, Imatinib presents a negligible effect on HL-60, while Doxorubicin (IC_{50} = 5.22 μM) exhibits a lower cytotoxic activity than MB (IC_{50} = 4.49 μM) and MAB (IC_{50} = 4.61 μM).

In the case of MCL, the expansion of Mino is negligibly diminished by MA. Whereas MB and MAB exhibit a strong inhibition (IC_{50} = 5.89 and 5.19 μM, respectively). While the cell line is dramatically suppressed by the drug Doxorubicin (IC_{50} = 0.64 μM), followed by Ibrutinib (IC_{50} = 0.85 μM).

The cytotoxic effects on MM cell lines consisting of U266 and KMS11 indicate that all the tested samples significantly inhibit the cell growth, except for MA. Among them, Doxorubicin displays the strongest prevention against U266 and KMS11 (IC_{50} = 0.24 and 0.46 μM, respectively), followed by MB (IC_{50} = 5.09 and 4.97 μM, respectively), and MAB (IC_{50} = 5.59 and 5.36 μM, respectively). Remarkably, Ibrutinib shows a weaker cytotoxic activity compared to MB and MAB when the IC_{50} value is 7.97 μM for U266. Meanwhile Ibrutinib reveals negligible inhibition on KMS-11.

The dose–responding curves of MA, MB, and MAB against non-cancerous (MeT-5A), CML (Meg-01 and K562), APL (HL-60), MCL (Mino), and MM (U266 and KMS-11) cell lines are presented in Figure 14.

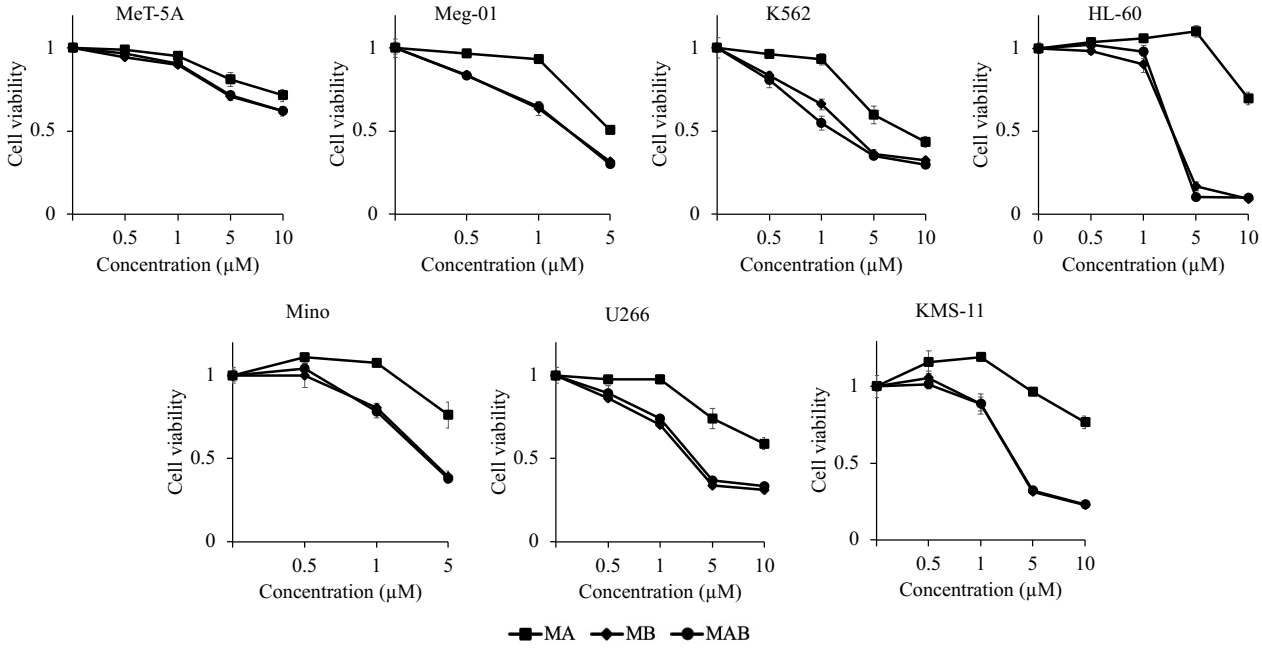

Figure 14. Dose-responding curves of momilactones A and B for cytotoxic activities against non-cancerous (MeT-5A), chronic myeloid leukemia (Meg-01 and K562), acute promyelocytic leukemia (HL-60), mantle cell lymphoma (Mino), and multiple myeloma (U266 and KMS-11) cell lines. MA, momilactone A; MB, momilactone B; MAB, the mixture of momilactones A and B (1:1, w/w).

Following the results shown in Table 6 and Figure 14, MA is the weakest compound inhibiting tested cancer cell lines. While MB and MAB substantially suppress these cell lines at around 5 μM. Therefore, MB and MAB at a concentration of 5 μM were selected for further investigation of their effects on tested cancer cell apoptosis.

3.3.2. Apoptosis-inducing activities of momilactones against blood cancer cell lines

Through annexin V assay, only MB-48 h slightly increases MeT-5A cell apoptosis. Meanwhile MB-24 h, MAB-24 h and -48 h exhibit no effect on apoptosis of this cell line. Particularly, MeT-5A apoptotic cells account for 3.86%, 2.87%, 2.44%, 10.3%, 4.73% in the untreated control and the treatments of MB-24 h, MAB-24 h, MB-48 h, and MAB-48 h, respectively (Figure 15).

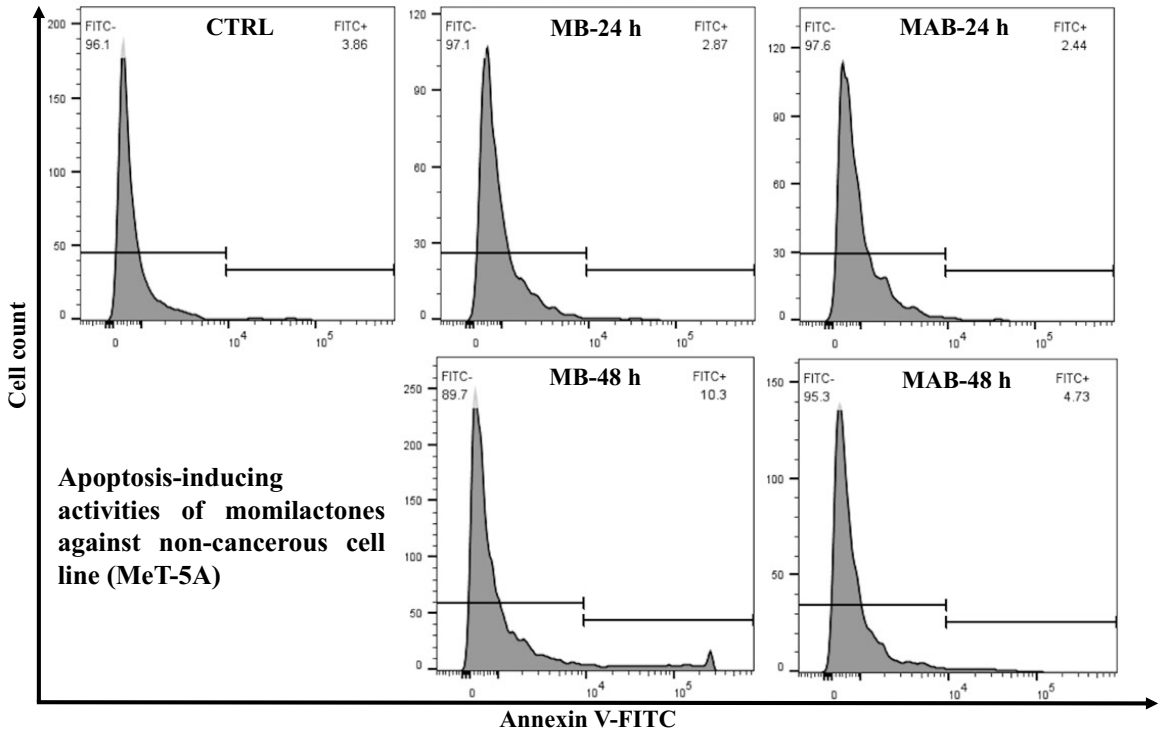

Figure 15. Apoptosis-inducing effects of momilactone B (MB) and the mixture of momilactone A and B (MAB) (1:1, w/w) at 5 μM against non-cancerous MeT-5A cell line after 24 h and 48 h.

Regarding CML cell line Meg-01, MB and MAB have insignificant influences on the apoptosis of this cell line after 24 h, whereas these compounds increase the apoptotic process in Meg-01 after 48 h (% apoptosis = 26.2% and 21.7% for the treatments with MB and MAB, respectively) (Figure 16). In another CML cell line K562, the tested compounds significantly increase cell apoptosis after 24 h (7.96- and 10.28-fold for MB and MAB, respectively) and 48 h (18.44-fold for both MB and MAB), compared to the untreated control (Figure 16).

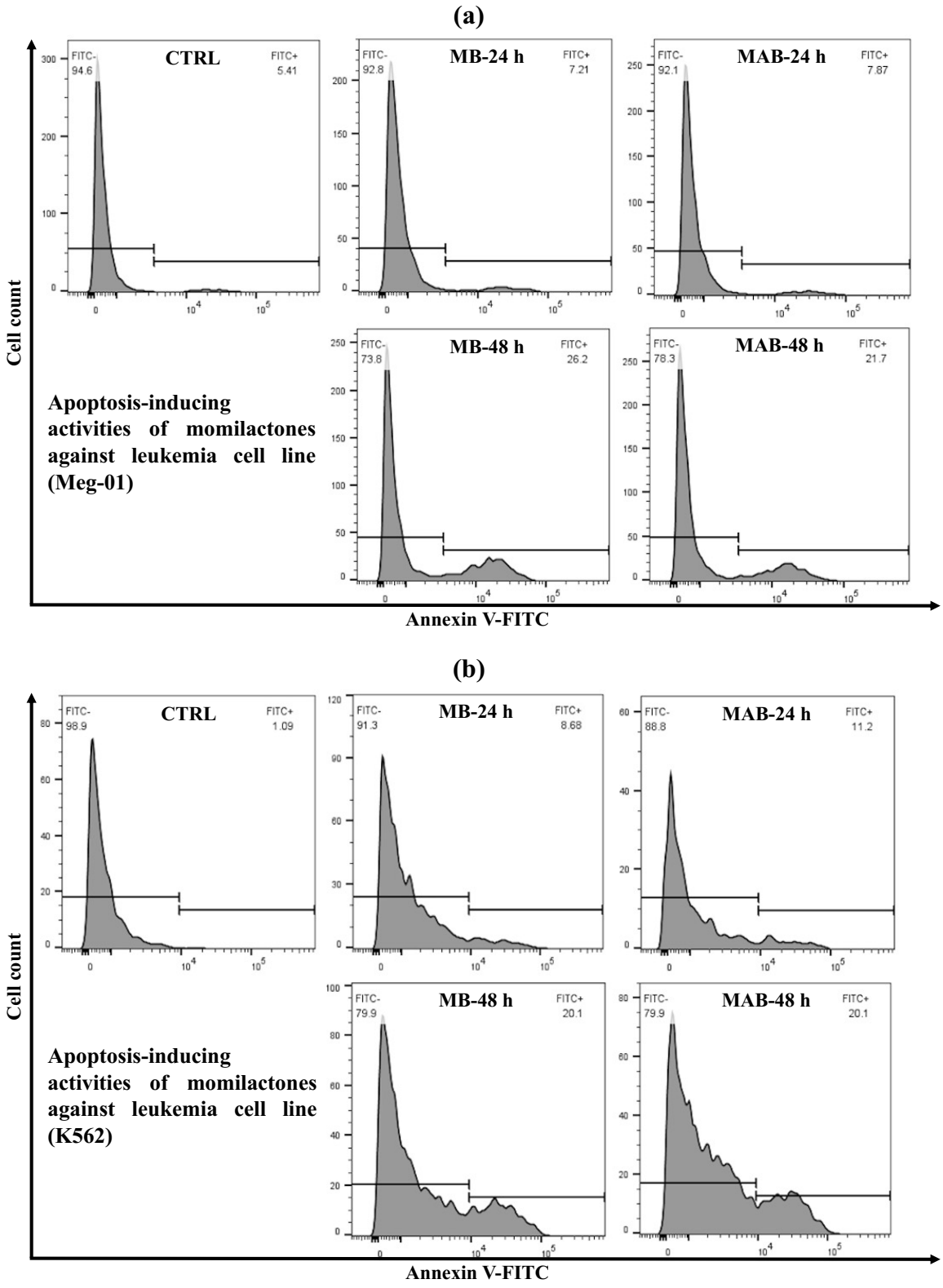

Figure 16. Apoptosis-inducing effects of momilactone B (MB) and the mixture of momilactone A and B (MAB) (1:1, w/w) at 5 μM against chronic myeloid leukemia (CML) (a) Meg-01 and (b) K562 cell lines after 24 h and 48 h.

For APL cell line, MB and MAB enhance HL-60 cell apoptosis after 24 h by 1.30 and 3.26 times, respectively, over the control (Figure 17). Significantly, after 48 h, HL-60 apoptotic process significantly increases to 40.5% and 42.1% in the cell affected by MB and MAB, respectively which are much higher than the control (% apoptosis = 0.86%) (Figure 17).

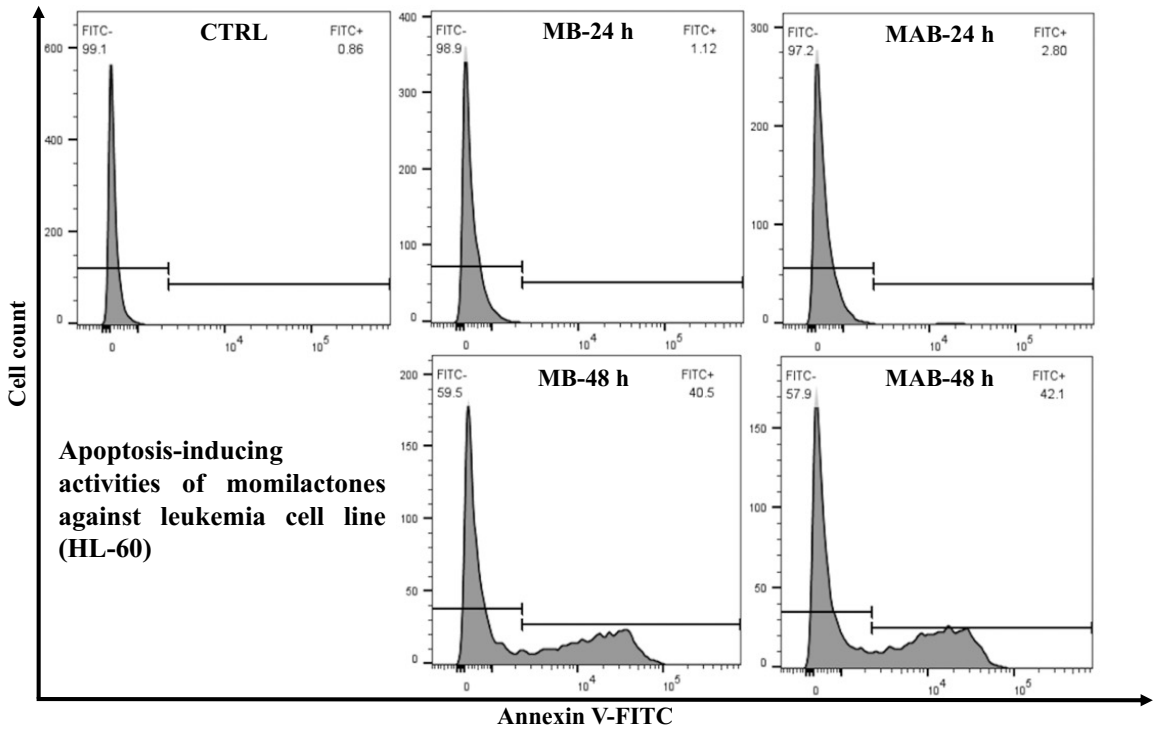

Figure 17. Apoptosis-inducing effects of momilactone B (MB) and the mixture of momilactone A and B (MAB) (1:1, w/w) at 5 μM against acute promyelocytic leukemia (APL) HL-60 cell line after 24 h and 48 h.

For the tested MCL cell line, MB and MAB substantially promote Mino cell apoptosis after both 24 h- and 48 h-treatment. The percentages of apoptosis achieve in 4.06%, 35.7%, 32.3%, 51.6%, and 44.1%, respectively, in the control and the treatments comprising MB-24 h, MAB-24 h, MB-48 h, and MAB-48 h, respectively (Figure 18).

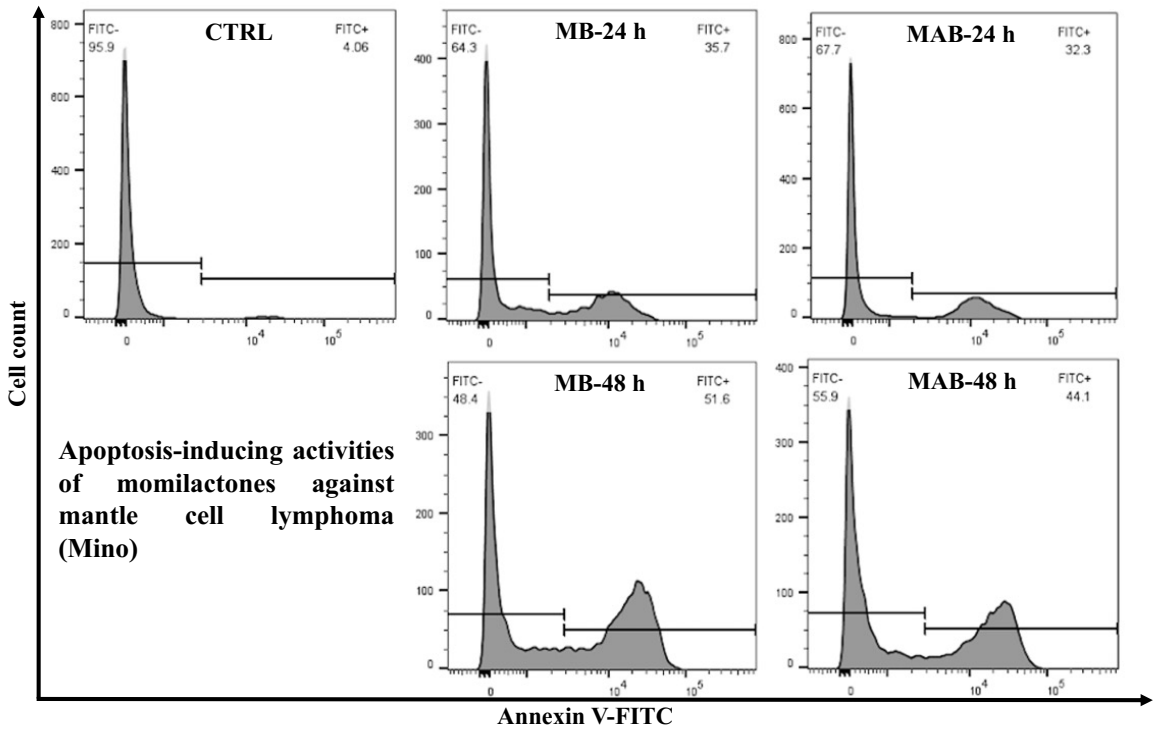

Figure 18. Apoptosis-inducing effects of momilactone B (MB) and the mixture of momilactone A and B (MAB) (1:1, w/w) at 5 μM against mantle cell lymphoma (MCL) Mino cell line after 24 h and 48 h.

In the case of MM cell line, the apoptotic cells of U266 are recorded increasing by 7.44%, 6.32%, 9.31%, and 9.62%, respectively, under the effects of MB-24 h, MAB-24 h, MB-48 h, and MAB-48 h, in comparison with the non-treated control (Figure 19). Similarly, MB and MAB remarkably activate the apoptotic process in KMS-11 (Figure 19). The number of KMS-11 apoptotic cells account for 22.4%, 20.3%, 55.7%, 44.4% under the treatments of MB-24 h, MAB-24 h, MB-48 h, and MAB-48 h, respectively, while the percentage of apoptosis is 1.58% in the control.

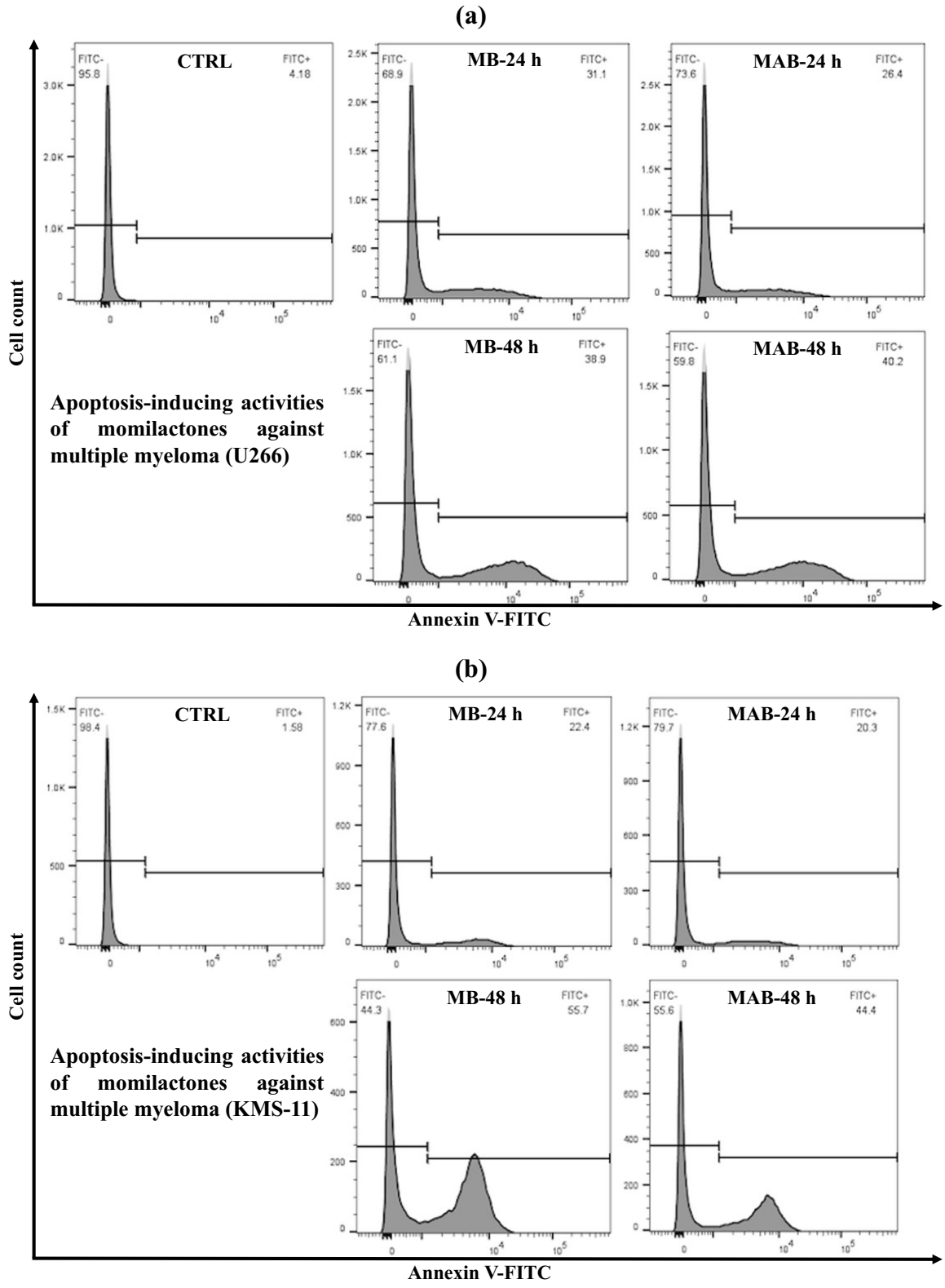

Figure 19. Apoptosis-inducing effects of momilactone B (MB) and the mixture of momilactone A and B (MAB) (1:1, w/w) at 5 μM against multiple myeloma (MM) (a) U266 and (b) KMS-11 cell lines after 24 h and 48 h.

Overall, MB and MAB inhibit the tested blood cancer cell lines by inducing apoptotic process. Meanwhile, these compounds exhibit an insignificant effect on normal cells.

3.4. Discussion

In recent years, a vast number of studies have been conducted to exploit anticancer potentials of plant-based products (Anh et al., 2020; Lam et al., 2022; Quan et al., 2022; Un et al., 2022). In these studies, the cell viability (MTT) assay was an integral part to examine the potentials of a promising candidate. Principally, the cytotoxic activity of derived compounds from plants is dose-dependent (Lam et al., 2022). Therefore, we investigated the effects of momilactones in increased concentrations on selected blood cancer cell lines. Importantly, a promising candidate should inhibit tumors with an IC_{50} of less than or equal to 5 μM (Lichota & Gwozdzinski, 2018). Accordingly, MB and MAB with IC_{50} of around 5 μM against tested blood cancer cells might be useful for developing novel medicines. Besides, the cytotoxic ability of momilactones is compared to that of widely applied medicines consisting of Doxorubicin, Imatinib, and Ibrutinib in our study. In which, Doxorubicin is commonly used to treat lymphoma and MM (Thorn et al., 2011). Especially, Doxorubicin was widely applied as a positive control in the research on cytotoxic activity against HL-60 cell line (Rodrigues et al., 2021). Imatinib is popularly used for leukemia patients (Moen et al., 2007). On the other hand, Ibrutinib has been announced as anti-MM agent via *in vitro*, *in vivo*, and clinical tests (Li, 2021; Richardson et al., 2018). Based on the MTT results, the cytotoxicity of MB and MAB is close to that of Doxorubicin against Meg-01 and K562. Significantly, MB and MAB are stronger than Doxorubicin in preventing HL-60 cells and Ibrutinib in inhibiting U266 cells. Interestingly, momilactones are less toxic to normal cell line MeT-5A compared to Doxorubicin, implying that they may be promising candidates for anti-blood cancer therapy.

In cancer, the loss of apoptosis occurs in all cases which allow cancer cells to avoid death, leading to their continuous proliferation and expansion (Pfeffer & Singh, 2018). Interestingly, chain events of apoptosis can be promoted by decreasing the activities of antiapoptotic factors and/or enhancing the activities of proapoptotic factors which can subsequently eliminate cancer cells (Pfeffer & Singh, 2018). Accordingly, apoptosis is considered a major target in the development of effective anticancer therapy (Pfeffer & Singh, 2018). Through the annexin V assay, we determined, for the first time, that MB and MAB at a concentration of 5 μM can suppress blood cancer cells by promoting cell apoptosis. Notably, apoptosis induction is regulated by relevant protein expressions. For example, in intrinsic pathway, an anti-apoptotic family, namely BCL-2, can inhibit apoptotic process (Pfeffer & Singh, 2018), while a pro-apoptotic member, namely caspase, can decompose proteins, resulting in cell death (Pfeffer & Singh, 2018). Based on that, further studies on cytotoxic mechanism of momilactones against blood cancer cells through the alteration of regulatory proteins related to the apoptotic process such as BCL-2 and caspase should be conducted.

In other studies, momilactone B was reported to suppress colon cancer (Kim et al., 2007), monocytic leukemia (Park et al., 2014), leukemic T cell lines (Lee et al., 2008). However, the cytotoxic ability of momilactones was compared to that of widely applied drugs in our research which has not been reported in other studies. Besides, this is the first reports that MB and MAB can inhibit chronic myeloid leukemia (CML), acute promyelocytic leukemia (APL), mantle cell lymphoma (MCL), and multiple myeloma (MM) cell lines by inducing cell apoptosis. Interestingly, the antioxidant capacity of momilactones was also previously indicated. In which, synergistic effect of MA and MB revealed stronger antioxidant capacity than individual compounds (Quan et al., 2019a). This may be an effective approach in cancer treatment since the negative effects of medicines (e.g.,

Doxorubicin) relate to oxidative stress by enhancing free radicals (Thorn et al., 2011). Thereby, candidates simultaneously exhibiting antioxidant and cytotoxicity against tumors may be useful for developing cancer therapies. Moreover, a correlation between chronic disorders including diabetes, obesity, aging, and cancer through the central role of inflammation and oxidative stress has been acknowledged (Collins, 1999). Interestingly, momilactones have exhibited potential for anti-diabetes, anti-obesity, and anti-skin aging activities (Quan et al., 2019a, 2019b, 2019d). Thereby, these compounds can be considered a promising source for improving blood cancer treatments, especially for patients complicated with oxidative stress and chronic diseases.

MA and MB were principally found in rice husk (Kang et al., 2017; Kato-Noguchi et al., 2010; Lee et al., 1999; Minh et al., 2018), leaf (Xuan et al., 2016), root and root exudates (Kato-Noguchi, 2011; Kato-Noguchi et al., 2010). Recently, liquid chromatography-electrospray ionization-mass spectrometry (LC-ESI-MS) method was improved to determine MA and MB content in white rice bran (Quan et al., 2019b). Therefore, our finding may support forthcoming strategies to take the advantages of rice bran and rice by products as a potential source for anti-blood cancer. Notably, rice is monocot plants, which adapt to a wide range of environmental conditions (Simpson, 2010). Thus, rice organs can be feasibly exploited for pharmaceutical purposes with an abundant biomass source.

In another concern, the bioaccessibility of bioactive compounds can be regulated through human digestion (Un et al., 2022). Thus, future research should be conducted to clarify the effects of digestive process on the bioaccessibility and bioavailability of momilactones. Besides, a natural-based drug must have benefits over risks (Teschke & Xuan, 2020). Therefore, the optimized dose of momilactones should be established to supress substantially tumors without harmful effects on normal blood cells. On the other hand, the potential risk such as neurotoxicity and hepatotoxicity by using herbal products

should be seriously considered and thoroughly evaluated (Quan et al., 2020). Accordingly, *in vivo* tests and clinical trials should be further conducted for the development of momilactones as novel anti-CML, anti-APL, anti-MCL, and anti-MM drugs.

3.5. Conclusions

This is the first study indicate that MB and MAB can inhibit chronic myeloid leukemia (CML) Meg-01 and K562, acute promyelocytic leukemia (APL) HL-60, mantle cell lymphoma (MCL) Mino, and multiple myeloma (MM) U266 and KMS-11 cell lines with IC_{50} of around 5 μM via MTT test. The cytotoxic activity of MB and MAB is close to that of Doxorubicin in preventing Meg-01 and K562. Meanwhile, MB and MAB are stronger than Doxorubicin and Ibrutinib in inhibiting HL-60 and U266, respectively. Through annexin V assay, momilactones suppress the tested cancer cell lines by promoting their cell apoptosis. Significantly, these compounds exhibit negligible effects on non-cancerous MeT-5A cell line. The finding implies that momilactones may be a promising source for the development of novel anti-CML, anti-APL, anti-MCL, and anti-MM medicines.

CHAPTER 4: CYTOTOXIC MECHANISM OF MOMILACTONES A AND B AGAINST ACUTE PROMYELOCYTIC LEUKEMIA AND MULTIPLE MYELOMA CELL LINES

4.1. Introduction

Blood cancer is a serious human disorder, accounting for over 1.2 million cases annually in the world (Sung et al., 2021). Among blood cancer types, the incidence of worldwide leukemia was reported 474,519 new cases with 311,594 deaths in 2020 (Sung et al., 2021). Of which, acute promyelocytic leukemia (APL) regularly gets aggravation during chemotherapy and has a poor prognosis with a high level of early death because of bleeding from coagulopathy. On the other hand, multiple myeloma (MM) was achieved in 176,404 cases with 117,007 deaths in 2020 (Sung et al., 2021). In MM patients, the accumulated cells in bone marrow can lead to bone lesions with the disruption of structure and function (Hanamura, 2021). APL and MM have been becoming serious and complicated problems over the years without any signal of stopping. Therefore, pharmaceutical and medicinal candidates are urgently needed to develop effective treatments for patients suffering from these cancers.

In anticancer studies, numerous strategies have been conducted to promote the apoptotic process, which is a natural mechanism for cell death to control or eliminate the undisciplined expansion of tumor (Pfeffer & Singh, 2018). Enhanced apoptosis is one of the most effective approaches for developing specific anticancer therapy and represents the most successful non-surgical treatment for all cancer cases (Pfeffer & Singh, 2018). Another potential target in anticancer research is the cell cycle, which strictly regulates cell division through multiple control mechanisms (Matthews et al., 2022). Cancer-associated mutations lead to abnormal regulation that prevents cells from exiting the cell cycle, followed by continuous cell division (Matthews et al., 2022). Therefore, inducing cell cycle arrest is a

promising method for inhibiting tumor's proliferation and expansion. Interestingly, both apoptotic and cell cycle processes can be regulated by regulatory proteins (Otto & Sicinski, 2017; Pfeffer & Singh, 2018). Therefore, substances with synergistic effects on apoptosis induction and cell cycle arrest through mediating the activities of relevant protein may be excellent candidates for developing efficient cancer therapies.

In recent years, a vast number of studies have been conducted considering the anticancer potentials of plant-based products (Anh et al., 2020; Lam et al., 2022; Quan et al., 2022; Un et al., 2022) which have exhibited benefits for therapeutic purposes with less toxicity than synthetic medicines (Teschke & Xuan, 2020c). Reality also shows that the simultaneous use of herbal remedies and modern medicine has brought certain effectiveness to the treatment (Ameade et al., 2018). Among valuable plant-derived analytes, momilactones, diterpene lactones, have been found only in rice (*Oryza sativa*) and the *Hypnum* moss (*Hypnum plumaeforme*). These compounds were first known as phytoalexins which principally play a role in the defense system of rice against pathogens (Zhao et al., 2018). Recently, momilactones have exhibited antioxidant, anticancer (leukemia (Park et al., 2014), lymphoma (Lee et al., 2008), and colon cancer (Kim et al., 2007), anti-diabetes (Quan et al., 2019b, 2019d), anti-obesity (Quan et al., 2019d), and anti-skin aging properties (Quan et al., 2019a). Hitherto, the mechanism of cytotoxic and anticancer actions of momilactones has not been scrutinized comprehensively. The limitation of in-depth studies about anticancer activity of momilactones may be due to the confined availability on the market as well as the difficulty in isolation and purification (Quan et al., 2019b). Our laboratory is one of the few laboratories in the world can purify momilactones from natural sources. In preceding reports, we successfully established a method to achieve a remarkable amount of momilactones A and B from rice by-products (Quan et al., 2019b).

The aforementioned rationales prompted us to investigate the cytotoxic mechanism of momilactones A (MA) and B (MB) and their mixture MAB (1:1, w/w) on HL-60 (a typical cell line isolated from APL patients) and U266 (a well-known cell line derived from MM patients) through apoptotic and cell cycle pathways, and the expressions of relevant regulatory proteins.

4.2. Materials and methods

4.2.1. Materials

Momilactones A (MA) and B (MB) were previously isolated and purified from rice husk in our laboratory of Plant Physiology and Biochemistry, Hiroshima University, Japan (Quan et al., 2019b). Briefly, MA and MB were isolated from the ethyl acetate (EtOAc) extract of rice husks (*Oryza sativa* var. Koshihikari) by column chromatography over silica gel with the mobile phase of hexane:EtOAc (8:2). The identification and confirmation of such pure compounds applying TLC, HPLC, LC-ESI-MS, GC-MS, and ^{1}H-NMR, and ^{13}C-NMR were described in the previous study of Quan et al. (2019b).

The cell lines including non-cancerous MeT-5A (CRL-9444™), acute promyelocytic leukemia HL-60 (CCL-240™), and multiple myeloma U266 (number: TIB-196™) were purchased from ATCC (Manassas, VA, USA).

4.2.2. Cell viability (MTT) assay

In this assay, culture media was prepared by adding fetal bovine serum (10%), L-glutamine (5 mM), penicillin (100 IU/mL), and streptomycin (100 µg/mL) to IMDM (Sigma-Aldrich, Missouri, United States). The cells (5×10^3 cells/well) were seeded into a 96-well plate filled with 90 µL of culture media and placed in a CO_2 incubator at 37 °C. After 24 h, the cells were treated with MA, MB, and MAB (10 µL) with different concentrations (0.5, 1, 5, and 10 µM) for 48 h. Subsequently, 10 µL of the MTT solution (5 mg/mL, Sigma-Aldrich) was pipetted into each well. The cells were continuously incubated

for 4 h. Finally, 100 µL of cell lysis buffer (10% SDS in 0.01 M HCl) was applied to dissolve the colored formazan crystals. Culture media instead of momilactones was used as the negative control. Meanwhile the drugs consisting of Doxorubicin, Ibrutinib, all-trans retinoic acid (ATRA), arsenic trioxide (ATO), and Bortezomib were tested as the standard inhibitors. The absorbance at 595 nm was scanned to determine the cell growth rate in value using a spectrophotometer (SpectraMAX M5, Molecular Devices, Sunnyvale, CA, USA) (Anh et al., 2020). All tests were performed with 3 replications. The cytotoxic activity (% inhibition) of momilactones/or inhibitors on the tested cell lines was as follows:

$$\text{Inhibition (\%)} = (A_{NC} - A_S)/A_{NC} \times 100$$

A_{NC}: Absorbance of reaction with negative control, A_S: Absorbance of reaction with momilactone/or inhibitor.

Dose-responding curves and IC_{50} values of the momilactones and standard inhibitors for cytotoxicity against tested cell lines were established. A lower IC_{50} indicates a stronger cytotoxicity activity.

4.2.3. Cell apoptosis (annexin V) assay

The procedure was conducted in triplicate following Lam et al. (2022). In brief, the cells (5×10^5 cells/well) were seeded into a 6-well plate filled with 1.5 mL of culture media and cultured in a CO_2 incubator for 24 h with the same condition as mentioned in MTT assay. The cells were then treated with momilactones at a concentration of 5 µM for 24 h and 48 h. The non-treated cells were used as a control. Harvested cells were washed twice with cold phosphate-buffered saline (PBS). After that, the control and treated cells were incubated with annexin V-conjugated fluorescein isothiocyanate (FITC) (Biolegend, San Diego, CA, USA) and propidium iodide (PI) for 15 min at 25 °C. The obtained cells were dissolved in 450 µL of PBS. The solution was filtered by a nylon membrane to prevent cell clumping and kept on ice until analysis. The intensities of annexin V-FITC and PI, and the

percentages of apoptotic cells were instantly determined by a flow a flow cytometer (BD, Franklin Lakes, NJ, USA).

4.2.4. Cell cycle assay

The cells (5×10^5 cells/well) were cultured and treated in triplicate following the same methods with apoptosis assay. The FxCycle PI/RNase staining solution was applied according to the manufacturer's instructions (Calbiochem, Darmstadt, Germany). The cell cycle distribution at each phase of G1, S, and G2 was determined based on the cell's DNA content. The percentages of cells in different phases of the cell cycle were quantified by a flow cytometer (BD, Franklin Lakes, NJ, USA). In brief, the collected cells were washed with ice-cold PBS. Subsequently, ice-cold PBS in pure ethanol was added to disperse the cells. The obtained solution was stored at 4 °C for 24 h for fixing. For analysis, the cells were incubated with 10 mg/ml RNase A (Sigma-Aldrich) for 5 min on ice. The following step was conducted by adding 1 mg/mL PI (in PBS). After incubating for 10 min at room temperature, the cells were dissolved in 450 μL of PBS. The solution was then filtered using a nylon membrane to remove cell clumping before analysis. Subsequently, the flow cytometric measurement was immediately performed.

4.2.5. Western blotting assay

The cells (5×10^5 cells/well) were cultured and treated in triplicate following the same methods with apoptosis and cell cycle assays. The cell lysates were conducted by rinsing cells with PBS, followed by adding two times of 2x loading buffer (4% SDS, 10% 2-mercaptoethanol, 20% glycerol, 0.004% bromophenol blue, 0.125 M Tris-HCl, pH 6.8). The extracted protein (200 pg) was subjected to sodium dodecyl sulfate (SDS)-polyacrylamide gels applying 10% acrylamide and subsequently transferred to a polyvinylidene fluoride membrane (Takara Bio, Shiga, Japan) by electroblotting. The membrane was blocked using 3% skim milk in PBS-0.05% Tween 20 (PBS-T) at 25 °C for 1 h. The incubation with each

antibody (2 μg/mL) against anti-rabbit total p-38/MAPK, phosphorylated p-38/MAPK, BCL-2, procaspase-3, cleaved caspase-3, CDK1/cdc2, cyclin B1, and GAPDH (BioLegend, California, United States) in blocking buffer was conducted overnight at 4 °C. The following step was performed by washing the membrane with PBS-T in triplicate. The collected membrane was incubated with a secondary antibody of horseradish peroxidase-labeled goat anti-rabbit IgG (20 ng/mL) (IBL, Gunma, Japan) at 37 °C for 1 h. Protein bands were visualized with the use of the LAS-4000 image analyzer (GE Healthcare, Tokyo, Japan). The relative expression (RE) was calculated by normalizing the intensity of targeted proteins to the intensity of the housekeeping protein GAPDH.

4.2.6. Statistical analysis

Data are displayed as mean ± standard deviation (SD) (n = 3). Student's t-test or one-way ANOVA was used to compare groups. Differences were considered significant at $p < 0.05$ (Minitab 16.0 software, Minitab Inc., State College, United States).

4.3. Results

4.3.1. Effects of momilactones on cell viability of non-cancerous (MeT-5A), acute promyelocytic leukemia (HL-60), and multiple myeloma (U266) cell lines

The cytotoxic activities of momilactones A (MA) and B (MB) and their mixture (MAB) (1:1, w/w) in increased concentrations against the cell viability of non-cancerous MeT-5A, acute promyelocytic leukemia (APL) HL-60, and multiple myeloma (MM) U266 cell lines after 48 h of treatments are displayed in Figure 20. In addition, the cytotoxicity of momilactones is compared with that of well-known inhibitors including Doxorubicin, Ibrutinib, all-trans retinoic acid (ATRA), arsenic trioxide (ATO), and Bortezomib.

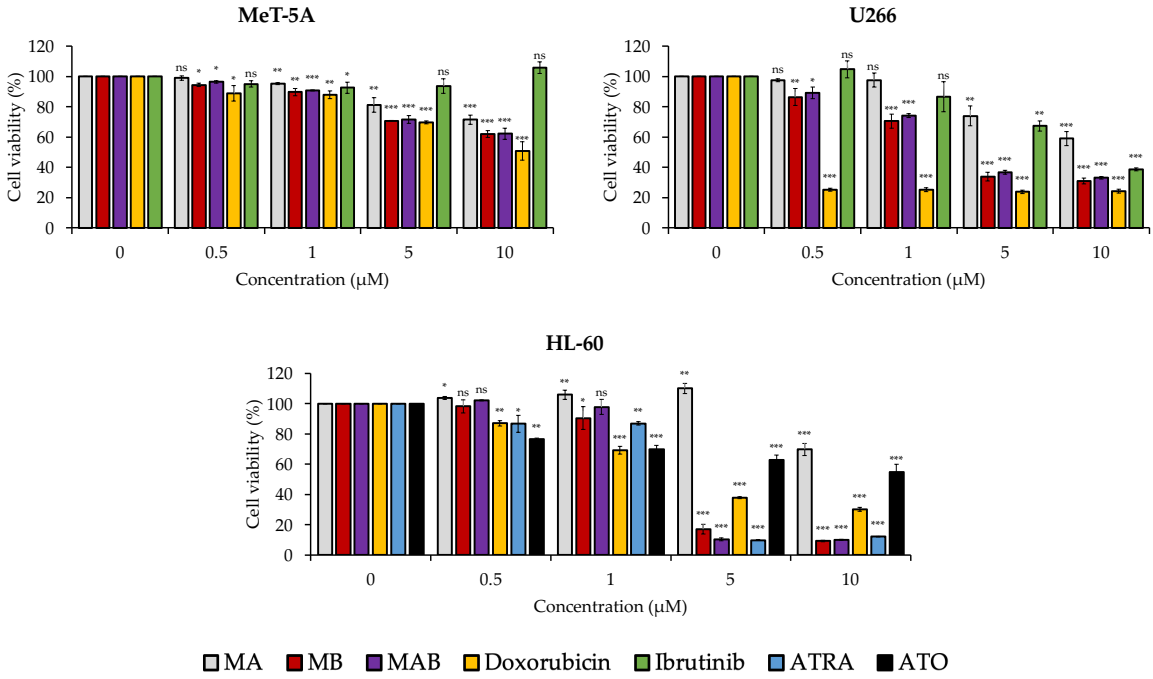

Figure 20. Effects of momilactones A (MA) and B (MB) and their mixture (MAB) (1:1, w/w) on cell viability of non-cancerous (MeT-5A), acute promyelocytic leukemia (HL-60), and multiple myeloma (U266) cell lines after 48 h. Data are expressed as mean ± standard deviation (SD). Statistical significance was determined by *t*-test. $^{*}p < 0.05$ versus control (0 μM); $^{**}p < 0.01$ versus control (0 μM); $^{***}p < 0.001$ versus control (0 μM); ATRA, all-trans retinoic acid; ATO, arsenic trioxide; ns, not significant versus control (0 μM).

According to Figure 20 and Table 7, MA, MB, and MAB exhibit a minor inhibition on normal cell line MeT-5A with percentages of 28.52%, 38.00%, and 37.82%, respectively which are lower than Doxorubicin (inhibition percentage = 49.23%) at a concentration of 10 μM (Figure 20).

The APL cell line HL-60 is least inhibited by MA with a percentage of 30.25% at 10 μM (Figure 20). Meanwhile, MB and MAB display a potent cytotoxic capacity against HL-60 (IC_{50} = 4.49 and 4.61 μM, respectively) which is more substantial than Doxorubicin and ATO (IC_{50} = 5.22 μM and 13.80, respectively) (Table 7 and Figure 20). The inhibitory effects of MB and MAB on HL-60 are close to that of ATRA (IC_{50} = 3.99 μM) (Table 7 and Figure 20).

In the case of MM cell line, MA exhibits the lowest effect on U266 cell proliferation (inhibition percentage = 40.97%) at 10 μM (Figure 20). On the other hand, Doxorubicin reveals the strongest prevention against U266 (IC_{50} = 0.24 μM), followed by MB and MAB (IC_{50} = 5.09 and 5.59 μM, respectively) (Table 7 and Figure 20). Notably, MB and MAB show higher cytotoxicity against U266 cells than Ibrutinib (IC_{50} = 7.97 μM) (Table 7 and Figure 20). Whereas the widely applied drug Bortezomib for MM shows an outstanding cytotoxicity on U266 with an IC_{50} value of 7.97 nM (Supplementary Data, Figure S11).

Table 7. Cytotoxic activities (IC_{50}) of momilactones A and B against MeT-5A, HL-60, and U266 cell lines (Obtained results from Chapter 3)

Compounds	**MeT-5A** (% Inhibition at 10 μM)	**HL-60** IC_{50} (μM)	**U266** IC_{50} (μM)
MA	28.52 ± 2.93^{a}	-	-
MB	38.00 ± 2.29^{b}	4.49 ± 0.34^{b}	5.09 ± 0.58^{b}
MAB	37.82 ± 3.64^{b}	4.61 ± 0.10^{b}	5.59 ± 0.17^{b}
Doxorubicin	49.23 ± 6.17^{c}	5.22 ± 0.15^{b}	0.24 ± 0.01^{c}
Ibrutinib	-	-	7.97 ± 0.34^{a}
ATRA	-	3.99 ± 0.16^{b}	-
ATO	-	13.80 ± 1.77^{a}	-

Outcome is presented as mean ± standard deviation (SD). Means within a column followed by similar superscript letters (^{a,b,c,d}) are insignificantly different at $p < 0.05$ (one-way ANOVA). MA, momilactone A; MB, momilactone B; MAB, the mixture of MA and MB (1:1, w/w); ATRA, all-trans retinoic acid; ATO, arsenic trioxide; -, not determined.

In general, MA is the weakest compound inhibiting tested cancer cell lines. While MB and MAB substantially suppress these cell lines at around 5 μM. Therefore, MB and MAB

at a concentration of 5 μM were selected for further investigation of their cytotoxic mechanism.

4.3.2. Apoptosis-inducing activities of momilactones against non-cancerous (MeT-5A), acute promyelocytic leukemia (HL-60), and multiple myeloma (U266) cell lines

In this assay, the annexin V method was applied to evaluate the effects of MB and MAB at 5 μM on the cell apoptosis of non-cancerous MeT-5A, acute promyelocytic leukemia (APL) HL-60, and multiple myeloma (MM) U266 cell lines (Figure 21).

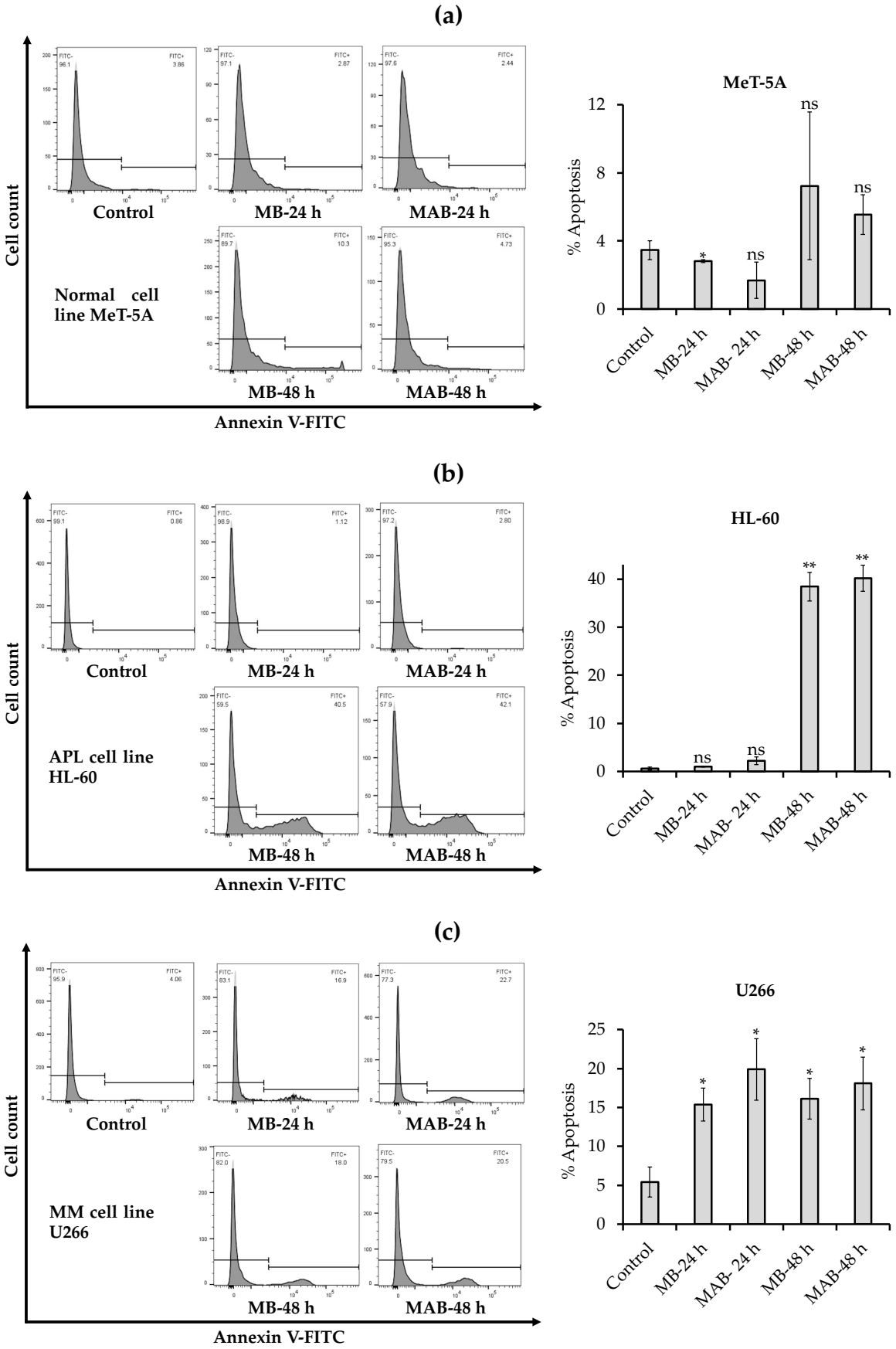
(a)
Cell count
Control
MB-24 h
MAB-24 h
Normal cell line MeT-5A
MB-48 h
MAB-48 h
Annexin V-FITC
MeT-5A
% Apoptosis
ns
*
ns
ns
Control
MB-24 h
MAB- 24 h
MB-48 h
MAB-48 h
(b)
Cell count
Control
MB-24 h
MAB-24 h
APL cell line HL-60
MB-48 h
MAB-48 h
Annexin V-FITC
HL-60
% Apoptosis
ns
ns
**
**
Control
MB-24 h
MAB- 24 h
MB-48 h
MAB-48 h
(c)
Cell count
Control
MB-24 h
MAB-24 h
MM cell line U266
MB-48 h
MAB-48 h
Annexin V-FITC
U266
% Apoptosis
*
*
*
*
Control
MB-24 h
MAB- 24 h
MB-48 h
MAB-48 h

Figure 21. Apoptosis-inducing effects of momilactone B (MB) and the mixture of momilactone A and B (MAB) (1:1, w/w) at 5 μM against **(a)** non-cancerous MeT-5A, **(b)** acute promyelocytic leukemia (APL) HL-60, and **(c)** multiple myeloma (MM) U266 cell lines after 24 h and 48 h. Statistical significance was determined by *t*-test. $^{*}p < 0.05$ versus control; $^{**}p < 0.01$ versus control; ns, not significant versus control.

The effects of MB and MAB at 5 μM on cell apoptosis of normal cells (MeT-5A) are presented in Figure 21a. The results obtain that after 24 h, MB and MAB reveal a mild decrease in cell apoptosis of MeT-5A (% apoptosis = 2.87% and 2.44%, respectively), while apoptotic cells in the non-treated control account for 3.86% (Figure 21a). After 48 h, a slight increase in cell apoptosis of MeT-5A is recorded under the influences of MB and MAB (2.67- and 1.23-fold, respectively) compared to the non-treated control (Figure 21a).

Regarding APL cell line, MB and MAB reveal an insignificant increase in the apoptotic process of HL-60 after 24 h (1.30- and 3.26-fold, respectively over the control) (Figure 21b). Remarkably, after 48 h, the number of HL-60 apoptotic cells is dramatically enhanced to 40.50% and 42.10% under MB and MAB effects, respectively which are much higher than the control (% apoptosis = 0.86%) (Figure 21b).

For the tested MM cell line, MB and MAB remarkably promote U266 cell apoptosis after 24 h and 48 h. Apoptotic cells account for 4.06%, 16.90%, 22.70%, 18.0%, and 20.5% in the control and the treatments of MB-24 h, MAB-24 h, MB-48 h, and MAB-48 h, respectively (Figure 21c).

Overall, MB and MAB promote apoptosis in cancer cells (HL-60 and U266) and exhibit a minor effect on normal cells (MeT-5A).

4.3.3. Effects of momilactones on inducing cell cycle arrest of non-cancerous (MeT-5A), acute promyelocytic leukemia (HL-60), and multiple myeloma (U266) cell lines

The effects of MB and MAB at 5 μM on the cell cycle of MeT-5A, HL-60, and U266 cell lines after 24 h and 48 h are displayed in Figure 22.

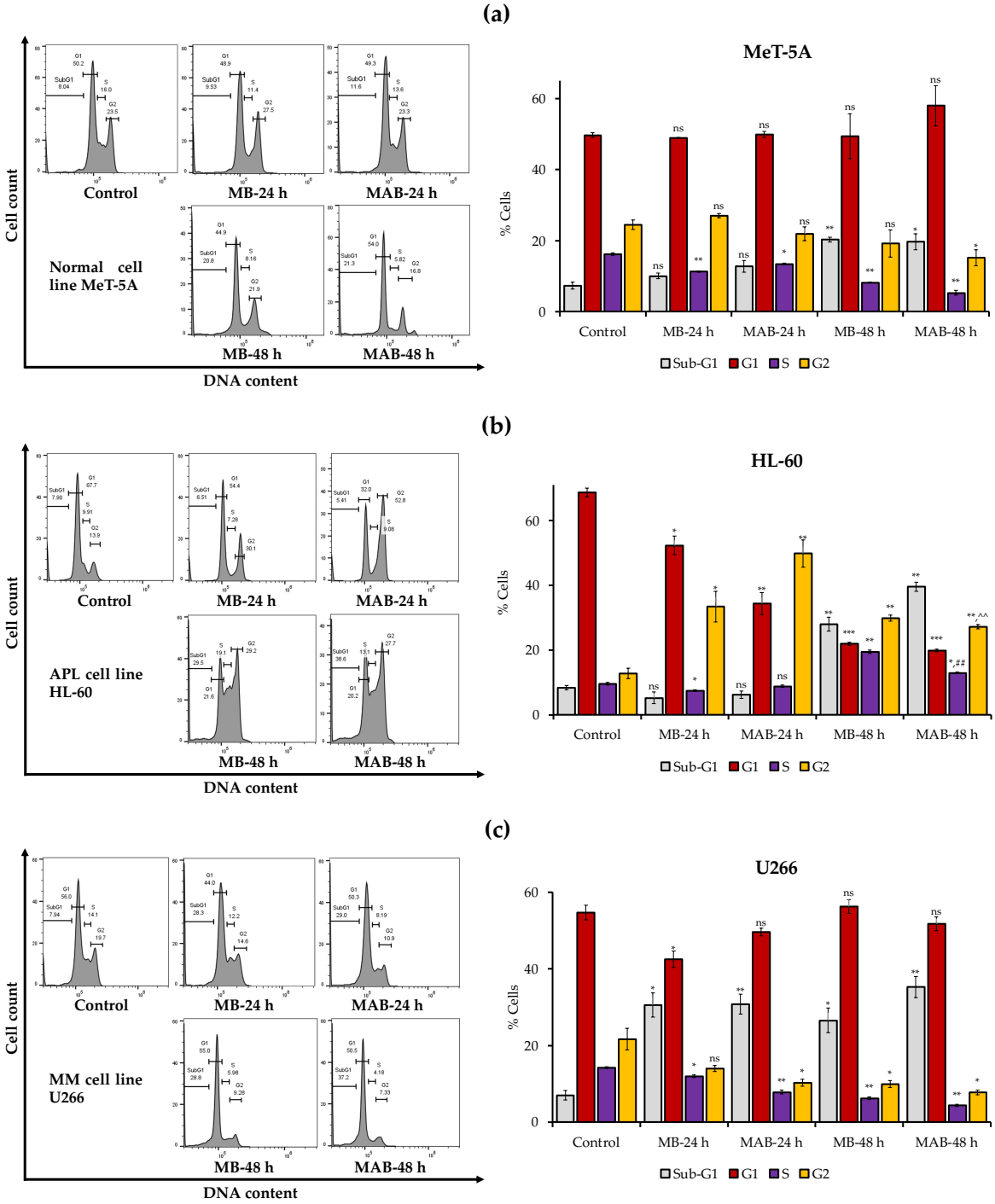

Figure 22. Effects of momilactone B (MB) and the mixture of momilactone A and B (MAB) (1:1, w/w) at 5 μM on the cell cycle of **(a)** non-cancerous (MeT-5A), **(b)** acute promyelocytic leukemia (HL-60), and **(c)** multiple myeloma (U266) cell lines after 24 h and 48 h. Statistical significance was determined by *t*-test. $^{*}p < 0.05$ versus control; $^{**}p < 0.01$ versus control; $^{***}p < 0.01$ versus control; $^{\wedge\wedge}p < 0.01$ versus MAB-24 h; $^{\#\#}p < 0.01$ versus MB-48 h; ns, not significant versus control.

In Figure 22a, MB and MAB reveal a negligible impact on sub-G1 phase of normal cell (MeT-5A) after 24 h. After 48 h, the cell percentages of sub-G1 are increased by 2.59 and 2.65 times under the effects of MB and MAB, respectively after 48 h, compared to the untreated control. The outcomes reveal that MeT-5A cell death is slightly elevated in the treatment with MB and MAB for 48 h which is consistent with the apoptosis (annexin V) results. Whereas the cell counts have insignificant changes in G1 and G2 phases after 24 h and 48 h. While the decreased cell numbers are recorded in S phase of the cells affected by MB and MAB. This finding implies that MB and MAB have an insignificant effect on the cell cycle of MeT-5A (Figure 22a).

For HL-60, MB- and MAB-treated cells are significantly accumulated in G2 phase of the cell cycle. Particularly, the cell counts are increased from 13.9% in G2 phase of the control cells to 30.1% and 52.8%, respectively in the cells affected by MB and MAB after 24 h (Figure 22b). After 48 h, the percentages of HL-60 cells in G2 phase are 29.2% and 27.7% under the effects of MB and MAB, respectively (Figure 22b). The results indicate that MB and MAB remarkably arrest the cell cycle of HL-60 at G2 phase, accompanied by the reduced percentages of cells in G1 and S phases.

In the case of U266 cells, there is no remarkable difference in the cell number of G1 phase among the control and the treatments with MB and MAB (Figure 22c). Meanwhile the cell counts are reduced in S and G2 phases which may be caused by the increased cell

deaths in sub-G1 phase under the effects of MB and MAB after 24 h and 48 h (Figure 22c). Generally, MB and MAB have negligible impacts on U266 cell cycle (Figure 22c).

Generally, MB and MAB show a negligible effect on the cell cycle of normal cells (MeT-5A) and MM cells (U266). Whereas these compounds activate G2 arrest in the cell cycle of APL cells (HL-60).

4.3.4. Effects of momilactones on expressions of proteins related to apoptosis induction and cell cycle arrest of acute promyelocytic leukemia (HL-60), and multiple myeloma (U266) cell lines

Based on the results of apoptosis induction and G2 phase arrest in the cell cycle of HL-60 treated with MB and MAB, the expressions of relevant proteins to apoptosis (total p-38, phosphorylated p-38, BCL-2, procaspase-3, and cleaved caspase-3) and G2 phase (total p-38, phosphorylated p-38, CDK1, and cyclin B1) were evaluated (Figure 23). Meanwhile, MB and MAB promote the apoptotic process in U266, but fail to activate cell cycle arrest. Therefore, the expressions of regulatory proteins in the apoptotic pathways comprising total p-38, phosphorylated p-38, BCL-2, procaspase-3, and cleaved caspase-3 were examined (Figure 23).

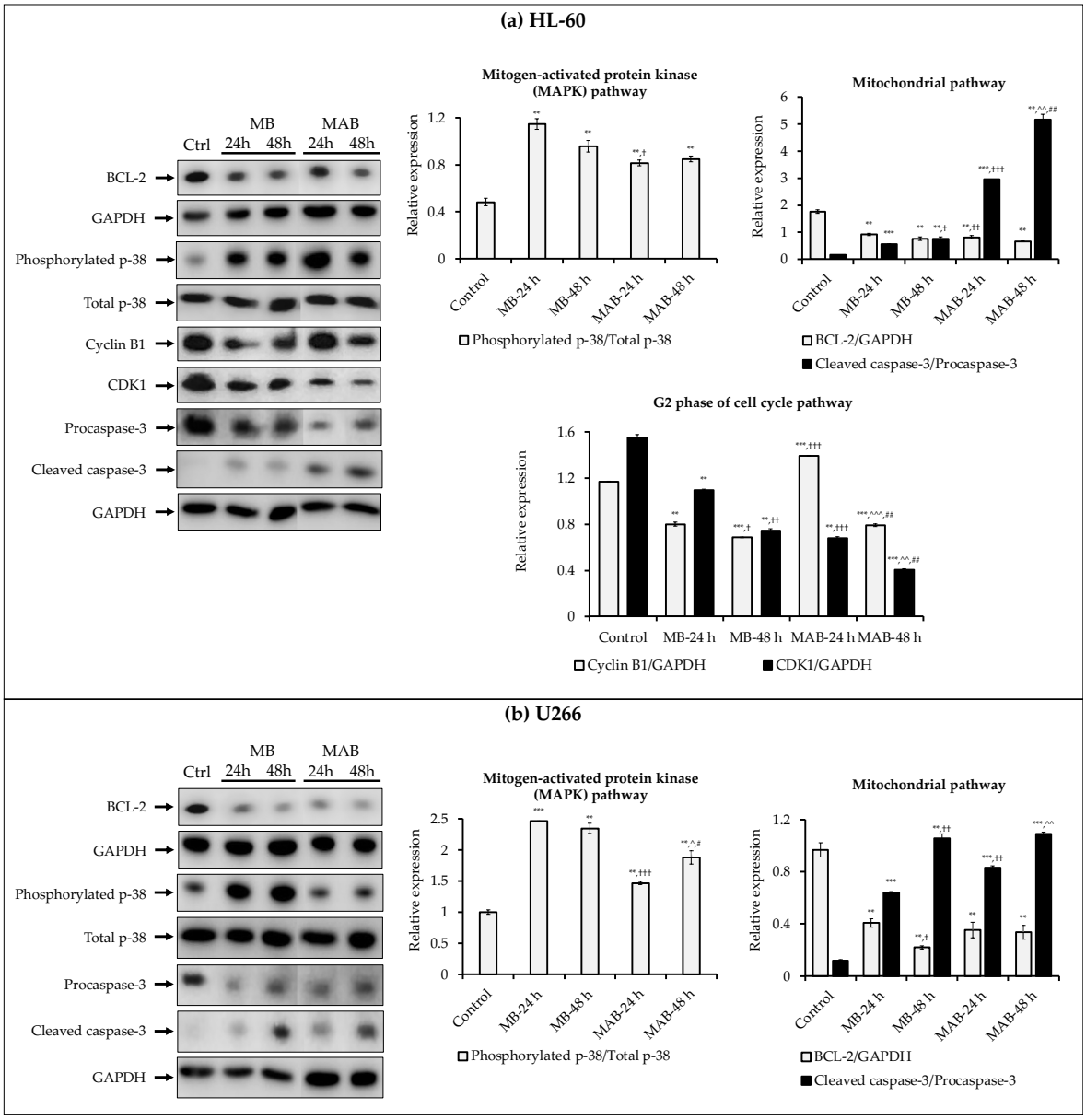

Figure 23. Effects of momilactone B (MB) and the mixture of momilactones A and B (MAB) (1:1, w/w) on the expressions of proteins related to apoptosis induction and cell cycle arrest of **(a)** acute promyelocytic leukemia (APL) HL-60, and **(b)** multiple myeloma (MM) U266 cell lines after 24 h and 48 h. Statistical significance was determined by *t*-test. $^{*}p < 0.05$ versus control; $^{**}p < 0.01$ versus control; $^{***}p < 0.001$ versus control; $^{\dagger}p < 0.05$ versus MB-24 h; $^{\dagger\dagger}p < 0.01$ versus MB-24 h; $^{\dagger\dagger\dagger}p < 0.01$ versus MB-24 h; $^{\wedge}p < 0.05$ versus MAB-24 h; $^{\wedge\wedge}p < 0.01$ versus MAB-24 h; $^{\wedge\wedge\wedge}p < 0.001$ versus MAB-24 h; $^{\#}p < 0.05$ versus MB-48 h; $^{\#\#}p < 0.01$ versus MB-48 h.

According to Figure 23a, expression of phosphorylated p-38/total p-38 is increased in APL (HL-60) cells affected by MB and MAB with the relative expression (RE) values in the control and the treatments including MB-24 h, MB-48 h, MAB-24 h, and MAB-48 h are 0.48, 1.15, 0.96, 0.82, and 0.85, respectively. Meanwhile, the protein bands of BCL-2 are dramatically degraded under the effects of MB (the RE values in 24 h- and 48 h-treatment are 1.92- and 2.32-fold, respectively, lower than the control) and MAB (the RE values in 24 h- and 48 h-treatment are 2.16- and 2.67-fold, respectively, lower than the control) (Figure 23a). Besides, the RE values of cleaved caspase-3/procaspase-3 are substantially enhanced in HL-60 treated with MB (RE = 0.56 and 0.77 after 24 h and 48 h, respectively) and MAB (RE = 2.97 and 5.17 after 24 h and 48 h, respectively), while the value in the untreated control is 0.17 (Figure 23a). In the cell cycle pathway, cyclin B1 and CDK1 expressions are remarkably impeded in HL-60 affected by MB and MAB. The RE values in the control and the treatments comprising MB-24 h, MB-48 h, MAB-24 h, and MAB-48 h are 1.17, 0.80, 0.69, 1.39, 0.79, respectively, for cyclin B1. While the values are 1.55, 1.10, 0.75, 0.68, 0.40, respectively, for CDK1 (Figure 23a).

For MM cell line U266, MB and MAB remarkably elevate the expression of phosphorylated p-38/total p-38 (RE = 1.00, 2.47, 2.35, 1.47, and 1.88 in the control and the treatments of MB-24 h, MB-48 h, MAB-24 h, and MAB-48 h, respectively) (Figure 23b). Besides, MB and MAB inhibit BCL-2 expression after 24 h by 2.37 and 2.74 times, respectively, compared to the control. Meanwhile, after 48 h, MB and MAB decrease the expression of BCL-2 by 4.41- and 2.88-fold, respectively, over the control (Figure 23b). The expression of cleaved caspase-3/procaspase-3 in U266 treated with MB after 24 h and 48 h is increased by 5.33 and 8.83 times, respectively, over the control. While in the treatment with MAB, the RE values of caspase-3/procaspase-3 after 24 h and 48 h are 6.92 and 9.08 times, respectively, higher than the control (Figure 23b).

4.4. Discussion

In anticancer research, the cell viability (MTT) assay is an indispensable initial step in exploring antitumor candidates (Anh et al., 2020; Lam et al., 2022; Quan et al., 2022; Un et al., 2022). Principally, the cytotoxicity of natural compounds is dose-dependent (Anh et al., 2020; Lam et al., 2022; Quan et al., 2022; Un et al., 2022). Therefore, we examined the activities of momilactones in increased concentrations against APL (HL-60) and MM (U266) cell lines, compared with non-cancerous (MeT-5A) cell lines. The drugs including Bortezomib, all-trans retinoic acid (ATRA), arsenic trioxide (ATO), Doxorubicin, and Ibrutinib were tested as reference suppressors (Table 1, Figure 1, and Supplementary Materials, Figure S1). In which, Bortezomib is a famous medicine for MM treatment (Rajkumar, 2022). ATRA and ATO show their effectiveness in APL therapies. (Sanz et a., 2019). Doxorubicin is commonly used to treat lymphoma and MM (Thorn et al., 2011). Besides, Doxorubicin is commonly used to treat lymphoma and MM (Thorn et al., 2011). Especially, Doxorubicin was widely applied as a positive control in the research on cytotoxic activity against HL-60 cell line (Rodrigues et al., 2021). Ibrutinib has been announced as anti-MM agent via *in vitro*, *in vivo*, and clinical tests (Li, 2021; Richardson et al., 2018). However, Ibrutinib was proven that selectively inhibits FLT3-ITD mutant cell lines among acute myeloid leukemia types, which do not include HL-60 (Wu et al., 2016). In fact, Ibrutinib revealed mild cytotoxicity on HL-60 in preceding study (IC_{50} = 41.94 μM) (Li et al., 2017). Therefore, the drug is not considered a standard inhibitor against this cell line. Following the results shown in Figure 20, MB and MAB may be ideal candidates for developing novel anticancer drugs since their cytotoxic abilities (IC_{50} of around 5 μM) are stronger than Doxorubicin in preventing HL-60 cells and Ibrutinib in inhibiting U266 cells (Figure 20). Moreover, the candidate must have a high cytotoxic selectivity against tumors without damaging normal cells (Indrayanto et al., 2021). Interestingly, these compounds are

less toxic to non-cancerous cell MeT-5A than Doxorubicin (Figure 20). Based on that, we selected MB and MAB to clarify their cytotoxic mechanism in suppressing HL-60 and U266 cancer cells.

Via apoptosis, cell cycle, and western blotting analyses (Figures 21, 22, and 23), MB and MAB may inhibit tested cancer cells through apoptosis induction and cell cycle arrest by regulating relevant protein expressions. Among targeted proteins, p-38 group serves as an important signaling mediator in the mitogen-activated protein kinase (MAPK) pathway, which contributes to many biological processes including inflammation, cell cycle, apoptosis, development, differentiation, senescence, and tumor formation in specific cells (Zarubin & Han, 2005). Remarkably, previous studies focusing on the regulation of p-38 were conducted to overcome the drug resistance and improve the suppressive effects on MM cell lines consisting of MM.1S, RPMI8226, and U266 (Hideshima et al., 2003). The activation of p-38 can be determined by the fold increase in the expression of phosphorylated p-38/total p-38 (Rodrigues et al., 2021). Accordingly, the upregulated phosphorylation of p-38 observed from western blotting outcomes may cause apoptosis enhancement of HL-60 and U266 treated with MB and MAB (Figure 23). On the other hand, the elevated expression of p-38 can destabilize cdc25b and cdc25c which subsequently disrupt CDK1/cyclin B1 complex (Ferenbach & Bonventre, 2016). This disruption may lead to HL-60 cell cycle arrest at G2 phase in this study. Regarding apoptosis, an anti-apoptotic member, namely BCL-2, suppresses apoptotic process by sequestering the preforms of fatal cysteine proteases or blocking the release of mitochondrial cell death factors into the cytoplasm (Tsujimoto, 1998). Significantly, elevated expression of BCL-2 has been detected in more than half of all cancer cases (Pfeffer & Singh, 2018). Thus, apoptosis promotion by inhibiting BCL-2 activities could be a promising approach to eliminating tumors. Interestingly, numerous plant-based products have shown their role in activating cancer cell apoptosis through BCL-

2 pathway, for example, curcumin from *Curcuma longa* or graviola from *Annona muricata* (Pfeffer & Singh, 2018), suggesting a great potential in the development of anticancer medicines. In this study, MB and MAB extremely impede the expression of BCL-2 in HL-60 and U266 cell lines after 48 h (Figure 23) which may motivate the apoptotic process in these cell lines. In another concern, many traditional medicines suppress cancer cells primarily depending on the BCL-2/BAX mechanism (Yip & Reed, 2008). Disruption of this signaling pathway can cause intrinsic resistance to drugs (Pfeffer & Singh, 2018). Therefore, substances targeting multiple factors can enhance the effectiveness of cancer treatment. In the present study, the effects of MB and MAB on the activation of a pro-apoptotic factor, namely caspase-3, were also determined (Figure 23). During the apoptotic process, procaspase-3 is converted to the active form caspase-3, which decomposes proteins, resulting in cell death (Pfeffer & Singh, 2018). Importantly, elevated procaspase-3 has been observed in various cancer cases (e.g., acute myeloid leukemia), involving in poor prognosis (Boudreau et al., 2019; Testa & Riccioni, 2007). Through the regulations of procaspse-3 and cleaved caspase-3 expressions (Figure 23), it may be conjectured that MB and MAB stimulate the conversion of procaspase-3 to caspase-3 in both tested cancer cell lines HL-60 and U266. This may cause the promotion of proteolysis in these cancer cells which subsequently kills them. In the cell cycle pathway, the activation of the CDK1/cyclin B1 complex plays a major role in the transition from G2- to M-phase. Thereby, inhibited CDK1/cyclin B1 activity leads to G2 phase arrest (Wang et al., 2000). Several anticancer studies were conducted focusing on G2/M phase arrest through this mechanism. For example, genistein arrested G2/M phase in the cell cycle of colon cancer cells (Zhang et al., 2013) and breast cancer (Choi et al., 1998). In our study, the expressions of CDK1 and cyclin B1 in HL-60 are significantly impeded by MB and MAB (Figure 23a). The finding indicates that MB and MAB may disrupt the interaction of CDK1/cyclin B1 complex, causing HL-60

cell cycle arrest at G2 phase, followed by mitosis inhibition. In other studies, the potential of MB in inhibiting colon cancer cells (HT-29 and SW620) was shown via MTT, lactate dehydrogenase (LDH), and colony-forming ability assays (Kim et al., 2007). Besides, MB suppressed human monocytic leukemia cell line U937 by stimulating apoptosis and the cell cycle arrest at G1 phase via the decrease in pRB phosphorylation and the upregulation of a CDK inhibitor $p21^{Waf1/Cip1}$ (Park et al., 2014). Lee et al. (2008) announced that MB prevented human leukemic T cells (Jurkat) by inducing apoptosis through the mitochondrial pathways. In addition, the inhibitory effect of MB on HL-60 cell viability was previously demonstrated (Lee et al., 2008), but the cytotoxic mechanism has not been elucidated. Furthermore, to the best of our knowledge, the present study is the first to clarify the induction of MB and MAB on apoptotic and cell cycle arrest pathways of HL-60 and U266 cells through the regulation of relevant proteins (Figure 24). Additionally, the cytotoxic potential of momilactones is highlighted by comparing with that of acknowledged standard suppressors in our study which has not been reported elsewhere. Forthcoming trials to develop momilactones as novel anti-APL and anti-MM drugs should also include the comparison between momilactones and well-known medicines. For example, in the case of APL therapies, all-trans retinoic acid (ATRA) and arsenic trioxide (ATO) are widely used (Sanz et al., 2019). While for MM treatments, proteasome inhibitors (PI) (e.g., Bortezomib, Carfilzomib, and Ixazomib), immunomodulatory agents (IMiD) (e.g., Lenalidomide, Pomalidomide, and Thalidomide), monoclonal antibodies (e.g., Daratumumab and Elotuzumab), and targeted B cell maturation agent (BCMA) therapies are commonly applied (Rajkumar, 2022). Moreover, the combination use of momilactones and these drugs should be investigated aiming to enhance the efficiency of targeted therapies, reduce the negative side effects, and overcome drug resistance (Jaaks et al., 2022; Quan et al., 2020; Rajkumar, 2022; Sanz et al., 2019). On the other hand, the impacts of momilactones on normal cells should be comprehensively

interpreted since they might be affected by the same course of event with tumors (Taşkın-Tok & Gowder, 2014). In this study, momilactones slightly promote cell apoptosis of normal mesothelial cell line (MeT-5A) but exhibit no effects on the cell cycle. Forthcoming studies should focus on the alterations of relevant proteins to the apoptotic process in MeT-5A cells treated with momilactones. Additionally, other sensitive cells to drugs including bone marrow, gonads (sex organs), gastrointestinal tract, and skin (hair follicle cells) should be also included to clearly understand the toxicity or adverse effects of momilactones (Taşkın-Tok & Gowder, 2014). This is an integral requirement to minimize failure in later stages of drug development. Furthermore, this may help establish potential drug combinations as well as effective therapies (Taşkın-Tok & Gowder, 2014).

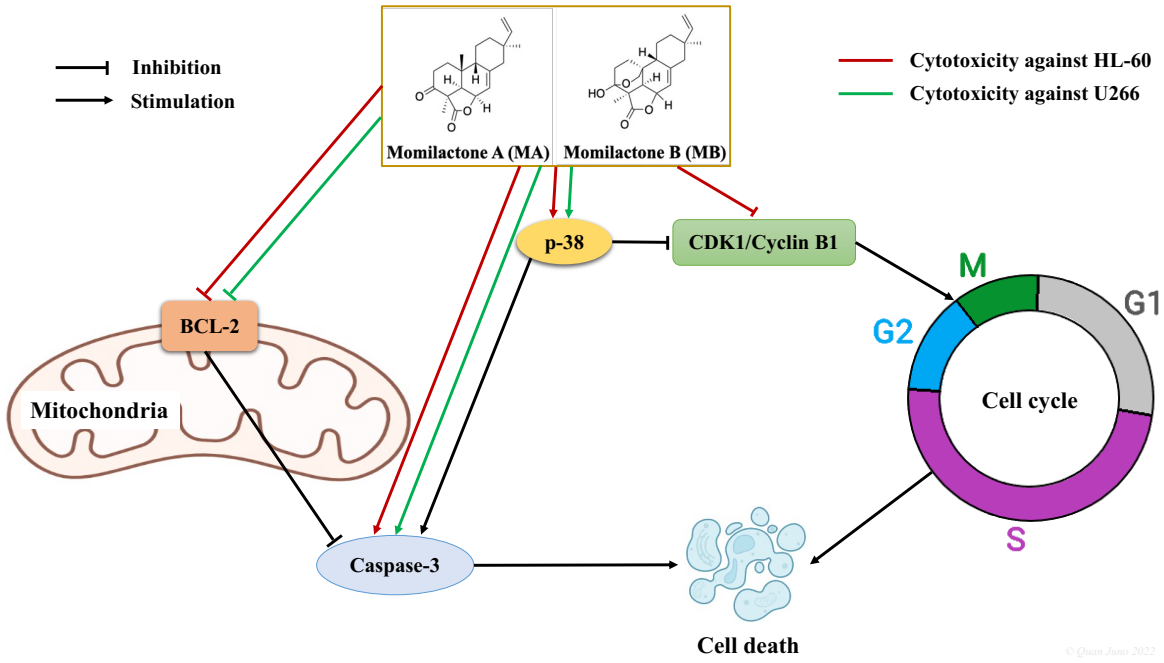

Figure 24. Cytotoxic mechanism of momilactones against acute promyelocytic leukemia (HL-60) and multiple myeloma (U266) cell lines.

In addition to the above-mentioned anticancer potentials, the antioxidant capacity of momilactones was previously reported. It was noteworthy that the synergistic effect of MA and MB revealed stronger antioxidant capacity than individual compounds (Quan et al., 2019a). This may address the complications in cancer progression and treatment due to the

side effects of drugs associated with oxidative stress (Thorn et al., 2011). Thus, substances simultaneously revealing antioxidant and cytotoxic properties may be excellent candidates for the development of effective cancer therapies. Moreover, a correlation between chronic disorders including diabetes, obesity, aging, and cancer through the central role of inflammation and oxidative stress has been acknowledged (Collins, 1999). Interestingly, momilactones have recently exhibited potential for anti-diabetes, anti-obesity, and anti-skin aging activities (Quan et al., 2019a, 2019b, Quan, 2019d). Thereby, these compounds can be considered a promising source for improving blood cancer treatments, especially for patients complicated with oxidative stress and chronic diseases.

MA and MB were principally found in rice husk (Kato-Noguchi et al., 2010), leaf (Xuan et al., 2016), and root (Kato-Noguchi et al., 2010). Recently, a specific sample preparation technique and advanced ultra-performance liquid chromatography-electrospray ionization-mass spectrometry (UPLC-ESI-MS) method were improved to increase the detection sensitivity that help quantify MA and MB in different rice organs with a minor amount (e.g., in rice bran) (Quan et al., 2019b). Those outstanding achievements may support prospective strategies to take the advantages of momilactones from rice and rice by-products for pharmaceutical purposes. Notably, rice is monocot plant, which adapt to a wide range of environmental conditions (Simpson, 2010). Thus, rice organs can be feasibly exploited for medicinal production and therapeutics with an abundant biomass availability. In addition to momilactones, a number of 47 momilactone-like molecules have acknowledged (Zhao et al., 2018), suggesting an abundant source for further investigations of their cytotoxic potentials against blood cancer cells. In another concern, the biological activity and bioaccessibility of substances can be affected by human digestion (Un et al., 2022). Accordingly, next studies should be conducted to investigate the bioaccessibility and bioavailability of momilactones during the digestive stages. Moreover, a natural-based

product must satisfy the requirements of benefits outweighing risks (Teschke & Xuan, 2020c). Therefore, the effective concentration of momilactones should be established to exhibit the strongest cytotoxicity against tumors without harmful effects on normal cells. On the other hand, the potential risks such as neurotoxicity and hepatotoxicity by using herbal products should be seriously considered and thoroughly evaluated (Quan et al., 2020).

Overall, MB and MAB are promising candidates, which are highly recommended for the next steps of developing novel anti-APL and anti-MM medicines. *In vivo* tests are required to confirm their possibilities for proposing prospective and appropriate clinical trials.

4.5. Conclusions

In this report, we interpret, for the first time, the cytotoxic mechanism of momilactones A (MA) and B (MB) and their mixture (MAB) against acute promyelocytic leukemia (APL) HL-60 and multiple myeloma (MM) U266 cell lines. Remarkably, the cytotoxicity of MB and MAB is more potent than that of Doxorubicin and Ibrutinib in preventing HL-60 and U266. MB and MAB may induce HL-60 and U266 cell apoptosis via the mitogen-activated protein kinase (p-38) and mitochondrial (BCL-2 and caspase-3) signaling pathways. In addition, HL-60 cell cycle is arrested at G2 phase by MB and MAB through the regulations of related protein (p-38, CDK1, and cyclin B1) expressions. Significantly, momilactones reveal an insignificant effect on the normal cell line MeT-5A. It can be concluded that momilactones are promising candidates for developing novel anti-APL and anti-MM medicines. Moreover, momilactones and momilactone-like compounds are expected as prospective natural sources for future production. However, the dose-effectiveness, bioaccessibility, and bioavailability of these analytes need validation via *in vivo* tests before considering further clinical trials.

CHAPTER 5: EFFECTS OF *IN VITRO* DIGESTION ON ANTI-BLOOD CANCER PROPERTIES OF MOMILACTONES

5.1. Introduction

Blood cancer is a dangerous human disease, causing about 1.2 million cases annually (Sung et al., 2021). In which, lymphoma accounting for more than half million cases per year is the most common type with 48% of death (Sung et al., 2021). Mantle cell lymphoma is a subtype of lymphoma, resulting in a short survival time of 3 to 5 years for patient (Cheah et al., 2016). On the other hand, leukemia comprising chronic and acute conditions is the second most common blood cancer type with over 400,000 new cases every year. However, leukemia results a high mortality rate of 66% (Sung et al., 2021). In leukemia, the disruption of white blood cell's functional activities and their overgrowth are occurred, causing adverse problems for human health (Sung et al., 2021). Another blood cancer type is multiple myeloma with the fewest new cases of 176,404 annually. However, this disorder results in 66% of deaths (Sung et al., 2021). Additionally, patients suffering from multiple myeloma can go through with the loss of bone structure and function (Hanamura, 2021). Recently, blood cancer has been causing serious and complicated problems for patients. Therefore, novel anti-blood cancer agents are urgently needed, considering the potential of plant-based products for therapeutic use, an attractive field of current research.

In the development of anticancer therapy, numerous oral anticancer substances have been registered as drugs, and many others are under improvement. Orally administered medications have been attracted much attention because of its convenience and simple application, especially in palliative conditions (Liu et al., 1997; Payne, 1992). Regarding oral administration, numerous phytocompounds exhibited potential biological activities, however they severe conditions of gastrointestinal digestion, leading to the reduction in their bioaccessibility and bioavailability (Krzyzanowska et al., 2010; Un et al., 2022; Choonara

et al., 2014). Therefore, a thorough understanding of the effects of human digestion on bioaccessibility and bioavailability of interested candidates is required to develop them for pharmaceutical purposes (Krzyzanowska et al., 2010). However, *in vivo* and clinical studies are expensive, challenging, and required ethical constraints (Kong & Singh, 2008a, 2008b). Notably, an effective protocol of *in vitro* digestion (oral, gastric, and intestinal stages) has been widely developed to simulate human digestive process (Kong & Singh, 2008a, 2008b). The models are low-priced, useful, flexible, and no ethical concerns regarding clinical trials (Kong & Singh, 2008a, 2008b). Accordingly, *in vitro* simulated digestion method is simple and convenient to investigate structural modifications, digestibility, and the release of target products.

Based on the above-mentioned rationales, the objectives of this study were (1) to elucidate the cytotoxic potentials of momilactones against chronic myeloid leukemia (CML) Meg-01, acute promyelocytic leukemia (APL) HL-60, mantle cell lymphoma (MCL) Mino, and multiple myeloma (U266) cell lines; and (2) to clarify the effects of *in vitro* simulated digestion (oral, gastric, and intestinal stages) on cytotoxic activity and bioaccessibility of momilactones.

5.2. Materials and methods

5.2.1. Materials

Momilactones were purified and confirmed from the previous study conducted in our laboratory of Plant Physiology and Biochemistry, Hiroshima University, Japan (Quan et al., 2019b).

The tested blood cancer cell lines in this study were obtained from American Type Culture Collection (ATCC) and presented in Table 8.

Table 8. List of blood cancer cell lines

No.	Cell line	ATCC number	Cell type

1	Meg-01	(CRL-2021™)	Chronic myeloid leukemia (CML)
2	HL-60	(CCL-240™)	Acute promyelocytic leukemia (APL)
3	Mino	(CRL-3000™)	Mantle cell lymphoma (MCL)
4	U266	(TIB-196™)	Multiple myeloma (MM)

5.2.2. In vitro digestion model

The model was conducted following the protocol described by Un et al. (2022). Accordingly, the artificial saliva, gastric, and intestinal juices were prepared with the major components and enzymes which are presented in Table 9.

Table 9. Components of artificial digestion juices (Un et al., 2022)

	Major components	**Volume/amount**	**pH**
Artificial saliva	KCl (89.6 mg/mL)	10.0 mL	6.5 ± 0.1
	KSCN (20 mg/mL)	10.0 mL	
	NaH_2PO_4 (88.8 mg/mL)	10.0 mL	
	Na_2PO_4 (57 mg/mL)	10.0 mL	
	NaCl (175.3 mg/mL)	1.7 mL	
	urea (25 mg/mL)	8.0 mL	
	α-Amylase	145.0 mg	
	Uric acid	15.0 mg	
	Mucin	50.0 mg	
Gastric juice	NaCl (175.3 mg/mL)	15.7 mL	1.0 ± 0.1
	NaH_2PO_4 (88.8 mg/mL)	3.0 mL	
	KCl (89.6 mg/mL)	9.2 mL	
	$CaCl_2.2H_2O$ (22.2 mg/mL)	18.0 mL	
	NH_4Cl (30.6 mg/mL)	10.0 mL	

	HCl (37%, g/g)	8.3 mL	
	Glucose (65 mg/mL)	10.0 mL	
	Glucuronic acid (2 mg/mL)	10.0 mL	
	Urea (25 mg/mL)	3.4 mL	
	BSA	1.0 g	
	Pepsin	1.0 g	
	Mucin	3.0 g	
Intestinal juice	NaCl (175.3 mg/mL)	40.0 mL	7.8 ± 0.2
	$NaHCO_3$ (84.7 mg/mL)	40.0 mL	
	KH_2PO_4 (8 mg/mL)	10.0 mL	
	KCl (89.6 mg/mL)	6.3 mL	
	$MgCl_2$ (5 mg/mL)	10.0 mL	
	HCl (37%, g/g)	0.18 mL	
	Urea (25 mg/mL)	4.0 mL	
	$CaCl_2.2H_2O$ (22.2 mg/mL)	9.0 mL	
	BSA	1.0 g	
	Pancreatin	3.0 g	
	Lipase	0.5 g	

In the first step, 1 mL of sample (1.0 mg/mL) was added to 3 mL of artificial saliva. The combination was incubated for 5 min at 37 °C under shaking. After that, an equivalent volume of ethyl acetate to samples was supplied for stopping enzymatic reaction and extracting oral digested samples in upper layer. The extraction was repeated for five times. The simulated digestion in stomach was carried out by providing 4 mL of gastric juice to oral digested samples. The mixture was then incubated under shaking for 1 hour at 37 °C. The gastric digested samples were obtained by the same method of extracting oral digested

samples. For intestinal phase, 4 mL of intestinal juice was mixed with gastric digested samples before incubating under the same condition for 1 hour. The intestinal digested samples were achieved by the same extraction method with ethyl acetate as above description. The schematic representation of *in vitro* digestion is summarized in Figure 25.

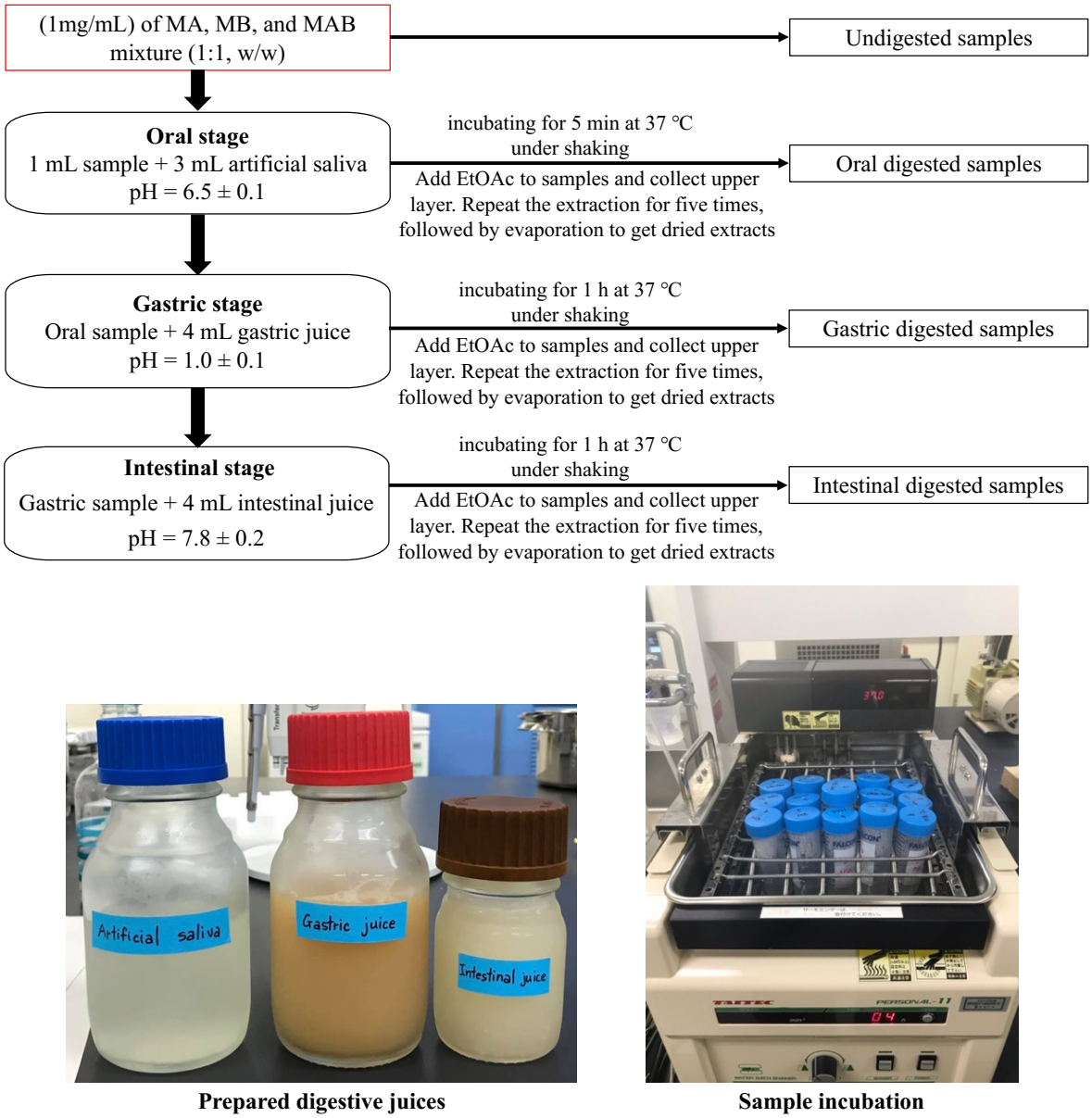

Figure 25. Procedure for *in vitro* simulated digestive model

5.2.3. Cell viability (MTT) assay

In this assay, culture media was prepared by adding fetal bovine serum (10%), L-glutamine (5 mM), penicillin (100 IU/mL), and streptomycin (100 µg/mL) to IMDM

(Sigma-Aldrich, Missouri, United States). The cells (10 µL) were seeded into a 96-well plate filled with culture media (90 µL) and placed in a CO_2 incubator at 37 °C. After 24 h, the cells were treated with undigested and digested (oral, gastric, and intestinal phases) samples (10 µL) with different concentrations (0.5, 1, 5, and 10 µM) for 48 h. Subsequently, 10 µL of the MTT solution (5 mg/mL, Sigma-Aldrich) was pipetted into each well. The cells were continuously incubated for 4 h. Finally, 100 µL of cell lysis buffer (10% SDS in 0.01 M HCl) was applied to dissolve the colored formazan crystals. Culture media instead of momilactones was used as the negative control. Meanwhile the well-known medicines comprising Doxorubicin, Imatinib, and Ibrutinib were tested as the standard inhibitors. The absorbance at 595 nm was scanned to determine the cell growth rate in value using a spectrophotometer (SpectraMAX M5, Molecular Devices, Sunnyvale, CA, USA) (Anh et al., 2020). The cytotoxic activity (% inhibition) of samples/or inhibitors on the tested cell lines was as follows:

$$\text{Inhibition (\%)} = (A_{NC} - A_S)/A_{NC} \times 100$$

A_{NC}: Absorbance of reaction with negative control, A_S: Absorbance of reaction with sample/or inhibitor.

Dose-responding curves and IC_{50} values of the momilactones and standard inhibitors for cytotoxicity against tested cell lines were established. A lower IC_{50} indicates a stronger cytotoxicity activity.

5.2.4. Quantification of momilactones

Momilactones A and B in rice extract were quantified based on the method described by Quan et al. (2019b). In particular, the UPLC-ESI-MS system included LTQ Orbitrap XL mass spectrometers (Thermo Fisher Scientific, Waltham, United States) and an electrospray ionization (ESI) source. For analysis, a methanolic sample (10 µg/ml) with a volume of 3.0 µL was injected into the ZORBAX Eclipse Plus C18 (1.8 µm, 2.1 × 50 mm) column (Agilent

Technologies, Santa Clara, California, United States). The column temperature was maintained at 25 °C. The gradient model with 2 solvents was set up as follows: solvent A was 0.1% trifluoroacetic acid in water, solvent B was 0.1% trifluoroacetic acid in acetonitrile. The gradient program was: 50% B during 0–5 min, then adjusted to 100% B during 5–10 min, subsequently maintained for 0.1 min, and another 5 min for equilibration. The flow rate was 300 μL/min. The operation was run in 15.1 min. A positive FTMS mode with a range of 100 to 800 m/z was applied for mass scanning. The presence of MA and MB in rice samples was confirmed by comparing their extracted ion chromatograms (EIC) and mass spectra of samples with those of standard momilactones. The calibration curves of MA and MB were established by applying different concentrations of momilactone standards (0.5, 1, 5, 10 μg/ml) to determine the momilactone content in rice seedlings. The peak areas of MA and MB detected in samples were used to calculate the amount of each compound by standard curves. The result was expressed as micrograms per gram of sample dry weight (μg/g DW). The bioaccessibility of momilactones during digestion was calculated following the below formula:

$$\text{Bioaccessibility} = (A - B)/A \times 100$$

A: quantified amount before digestion; B: quantified amount after digestion.

5.3. Results

5.3.1. Effects of in vitro digestion on cytotoxic activity of momilactones against acute promyelocytic leukemia (HL-60) cell line

The cytotoxic activity of momilactones A and B and their mixture (1:1, w/w) before and after digestion against acute promyelocytic leukemia (APL) HL-60 cell line is presented in Table 10. Accordingly, undigested MA and digested MA present insignificant effects on this cell line. In contrast, the cytotoxicity of MB and MAB before digestion against HL-60 (IC_{50} = 4.30 and 3.22 μM, respectively) is stronger than that of the well-known drug

Doxorubicin (IC_{50} = 5.22 μM). However, after digestion, the inhibitory effects of MB and MAB are significantly reduced. Particularly, the IC_{50} values of MB and MAB in oral phase are 28.94 and 47.82 μM, respectively. In gastric phase, the IC_{50} values of MB and MAB are 12.94 and 34.63 μM, respectively. Meanwhile, these values are 10.36 and 39.84 μM, respectively in intestinal phase Table 10.

Table 10. Effect of *in vitro* digestion on cytotoxic activity against HL-60 cell line of momilactones (IC_{50}, μM)

Compound	U	O	G	I
MA	ne	ne	ne	ne
MB	4.30 ± 0.33^{g}	28.94 ± 1.40^{d}	12.94 ± 0.87^{e}	10.36 ± 1.44^{e}
MAB	3.22 ± 0.02^{g}	47.82 ± 0.47^{a}	34.63 ± 0.73^{c}	39.84 ± 2.00^{b}
Doxorubicin	5.22 ± 0.15^{f}	-	-	-

U, undigested sample; O, oral digestion; G, gastric digestion; I, intestinal digestion; MA, momilactone A; MB, momilactone B; MAB, the mixture of momilactones A and B (1:1, w/w); ne, negligible effect; -, not determined. Data are expressed as mean ± SD (n = 3). Different superscript letters indicate significant differences by Tukey's test ($p < 0.05$).

5.3.2. Effects of in vitro digestion on cytotoxic activity of momilactones against chronic myeloid leukemia (Meg-01) cell line

The cytotoxic activity of momilactones against chronic myeloid leukemia (CML) Meg-01 cell line under the effects of digestion including oral, gastric, and intestinal stages is described in Table 11. The results show that MA before and after digestion reveals negligible impacts on Meg-01. In undigested samples, MB exhibits the most potent suppression against Meg-01 (IC_{50} = 6.87 μM), followed by MAB (IC_{50} = 18.19 μM). During oral and gastric stages, the cytotoxic activity of MB is remarkably decreased (IC_{50} = 69.35 and 80.73 μM in oral and gastric phases, respectively). Notably, MB reveals negligible

effects on Meg-01 in intestinal stage. On the other hand, MAB show no impact on Meg-01 after digestion (Table 11).

Table 11. Effect of *in vitro* digestion on cytotoxic activity against Meg-01 cell line of momilactones (IC_{50}, μM)

Compound	U	O	G	I
MA	ne	ne	ne	ne
MB	6.87 ± 0.42^{d}	69.35 ± 1.40^{b}	80.73 ± 5.96^{a}	-
MAB	18.19 ± 0.97^{c}	-	-	-
Doxorubicin	3.34 ± 0.42^{e}	-	-	-
Imatinib	0.61 ± 0.01^{f}	-	-	-

U, undigested sample; O, oral digestion; G, gastric digestion; I, intestinal digestion; MA, momilactone A; MB, momilactone B, MAB, the mixture of momilactones A and B (1:1, w/w); ne, negligible effect; -, not determined. Data are expressed as mean ± SD (n = 3). Different superscript letters indicate significant differences by Tukey's test ($p < 0.05$).

5.3.3. Effects of in vitro digestion on cytotoxic activity of momilactones against mantle cell lymphoma (Mino) cell line

In the case of multiple cell lymphoma (MCL), MB shows the most substantial inhibition on Mino cell viability (IC_{50} = 1.07 μM) which is close to the widely applied drugs including Doxorubicin (IC_{50} = 0.64 μM) and Ibrutinib (IC_{50} = 0.85 μM) (Table 12). The second most potent sample in suppressing Mino is MAB (IC_{50} = 7.31 μM), followed by MA (IC_{50} = 23.85) (Table 12). However, the activity of MA, MB and MAB is substantially reduced during digestion. In which, MA displays insignificant effects on Mino cell expansion. On the other hand, the cytotoxicity of MB decreased by 15.14, 16.52, and 33.78 times through the oral, gastric, and intestinal stages, respectively, compared to the undigested stage (Table 12). Meanwhile, the cytotoxicity of MAB reduced by 3.94, 2.21,

5.37 times via the oral, gastric, and intestinal phases, respectively, compared to undigested MAB (Table 12).

Table 12. Effect of *in vitro* digestion on cytotoxic activity against Mino cell line of momilactones (IC_{50}, μM)

Compound	U	O	G	I
MA	23.85 ± 0.75^{c}	ne	ne	ne
MB	1.07 ± 0.03^{f}	16.20 ± 1.32^{d}	17.68 ± 0.15^{d}	36.14 ± 0.76^{a}
MAB	7.31 ± 0.12^{e}	28.77 ± 1.63^{b}	16.16 ± 1.84^{d}	39.22 ± 2.38^{a}
Doxorubicin	0.64 ± 0.03^{h}	-	-	-
Ibrutinib	0.85 ± 0.03^{g}	-	-	-

U, undigested sample; O, oral digestion; G, gastric digestion; I, intestinal digestion; MA, momilactone A; MB, momilactone B; MAB, the mixture of momilactones A and B (1:1, w/w); ne, negligible effect; -, not determined. Data are expressed as mean ± SD (n = 3). Different superscript letters indicate significant differences by Tukey's test ($p < 0.05$).

5.3.4. Effects of in vitro digestion on cytotoxic activity of momilactones against multiple myeloma (U266) cell line

The cytotoxic activity of MA, MB, and MAB before and after digestion against multiple myeloma (MM) U266 cell line is presented in Table 13. The outcomes show that MB and MAB reveal potent suppression against U266 cell proliferation (IC_{50} = 3.42 and 3.70 μM, respectively) which is over twice stronger than Ibrutinib (IC_{50} = 7.97 μM) (Table 13). Doxorubicin is the strongest sample inhibiting U266 with IC_{50} value of 0.24 μM, whereas MA is the weakest sample with IC_{50} value of 20.09 μM (Table 13). However, digestion significantly diminished the activity of MA. Besides, the cytotoxicity of MB is dramatically impeded under the effects of oral, gastric, and intestinal phases with IC_{50} values of 23.41, 7.60, 16.30 μM, respectively (Table 13). Meanwhile, the activity of MAB during

oral, gastric, and intestinal stages is reduced by 5.30, 3.65, and 7.68, respectively, compared to undigested sample (Table 13).

Table 13. Effect of *in vitro* digestion on cytotoxic activity against U266 cell line of momilactones (IC_{50}, μM)

Compound	U	O	G	I
MA	20.09 ± 1.28^{c}	ne	ne	ne
MB	3.42 ± 0.34^{g}	23.41 ± 1.31^{b}	7.60 ± 0.57^{f}	16.30 ± 0.86^{d}
MAB	3.70 ± 0.10^{g}	19.62 ± 0.26^{c}	13.50 ± 0.78^{e}	28.42 ± 1.63^{a}
Doxorubicin	0.24 ± 0.01^{h}	-	-	-
Ibrutinib	7.97 ± 0.34^{f}	-	-	-

U, undigested sample; O, oral digestion; G, gastric digestion; I, intestinal digestion; MA, momilactone A; MB, momilactone B; MAB, the mixture of momilactones A and B (1:1, w/w); ne, negligible effect; -, not determined. Data are expressed as mean ± SD (n = 3). Different superscript letters indicate significant differences by Tukey's test ($p < 0.05$).

5.3.5. Bioaccessibility of momilactones during in vitro digestion

The digestive stages including oral, gastric, and intestinal phases dramatically decreased the bioaccessibility of MA, MB, and MAB (Figure 26).

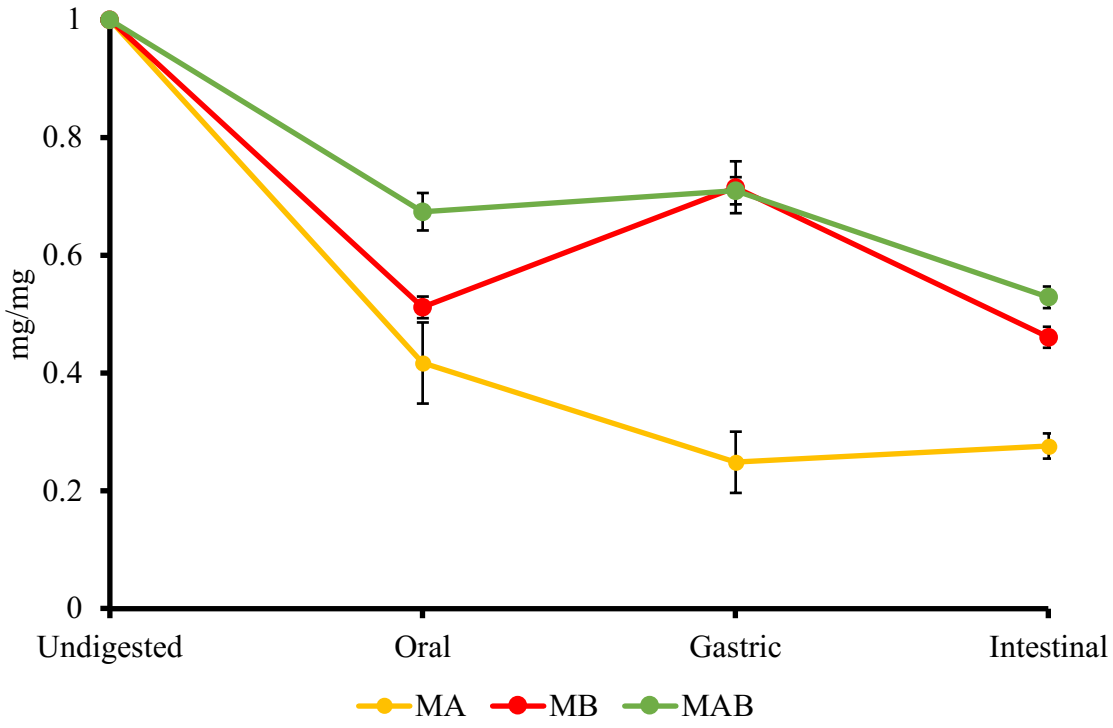

Figure 26. Bioaccessibility of momilactones under digestion. MA, momilactone A; MB, momilactone B; MAB, the mixture of momilactones A and B (1:1, w/w).

According to the results shown in Figure 26 and Table 14, the bioaccessibility of MA, MB, and MAB is decreased by 58.28%, 48.83%, and 32.59%, respectively, under the effects of oral digestive stage, compared to undigested samples. Meanwhile, in gastric phase, the quantities of MA, MB, and MAB is reduced by 75.14%, 28.44%, and 29.03%, respectively, over undigested samples (Figure 26 and Table 14). Through intestinal digestion, the contents of MA, MB, and MAB are impeded by 72.37%, 53.91%, and 47.13%, respectively, compared to undigested samples (Figure 26 and Table 14).

Table 14. Variation percentages of momilactones under digestion

Compound	**Variation (%)**		
	O	**G**	**I**
MA	-58.28	-75.14	-72.37

MB	-48.83	-28.44	-53.91
MAB	-32.59	-29.03	-47.13

MA, momilactone A; MB, momilactone B; MAB, the mixture of momilactones A and B (1:1, w/w); O, oral phase; G, gastric phase; I, intestinal phase.

5.3.6. Correlation coefficients between quantities of momilactones and their cytotoxic activities during in vitro digestion

Based on the correlation coefficient results, the reduced cytotoxic activities of momilactones strongly correlated with their decreased quantities under the effects of digestion. Concretely, the correlation value between MA content and inhibitory activities against Mino and U266 is 0.97 (Table 15). On the other hand, the reduced amounts of MB during digestion closely associate with the decreased cytotoxic activity of this compounds against HL-60, Meg-01, Mino, and U266 cell lines with the correlation levels of 0.85, 0.91, 0.90, and 0.97, respectively (Table 15). Besides, the impeded content of MAB may cause the weakened cytotoxicity of this sample under the effects of digestion (Correlation levels = 0.91, 0.91, 0.97, and 0.95 for HL-60, Meg-01, Mino, and U266, respectively) (Table 15).

Table 15. Correlation coefficients between quantities of momilactones and their cytotoxicity during digestion

Cytotoxicity	**Quantity during digestion**		
	MA	**MB**	**MAB**
HL-60	-	0.845	0.914
Meg-01	-	0.907	0.912
Mino	0.970	0.896	0.965
U266	0.969	0.971	0.953

-, not determined; MA, momilactone A; MB, momilactone B; MAB, the mixture of momilactones A and B (1:1, w/w).

5.4. Discussion

In earlier research, momilactone B was reported to suppress colon cancer (Kim et al., 2007), monocytic leukemia (Park et al., 2014), leukemic T cell lines (Lee et al., 2008). However, the cytotoxic potentials of momilactones were not previously compared to that of anticancer medicines. In the present study, we indicate, for the first time, that momilactone B (MB) and the mixture of momilactones A and B (MAB) (1:1, w/w) may prevent the cell proliferation of acute promyelocytic leukemia (APL) HL-60, chronic myeloid leukemia (CML) Meg-01, mantle cell lymphoma (MCL) Mino, and multiple myeloma (MM) U266 cell lines. Besides, the well-known drugs of Doxorubicin, Imatinib, and Ibrutinib were tested as standard inhibitors. Doxorubicin is commonly used to treat lymphoma and MM (Thorn et al., 2011). Especially, Doxorubicin was widely applied as a positive control in the research on cytotoxic activity against HL-60 cell line (Rodrigues et al., 2021). Ibrutinib has been announced as anti-MM agent via *in vitro*, *in vivo*, and clinical tests (Li, 2021; Richardson et al., 2018). The findings from our research imply that the cytotoxic activity of MB and MAB is close to that of Doxorubicin against Meg-01 and Mino. Notably, MB and MAB are stronger than Doxorubicin and Ibrutinib in suppressing HL-60 and U266, respectively. Besides, the applicability of momilactones for the development of novel anti-blood cancer drugs, considering oral application was investigated in the current research. Particularly, the effects of digestive processes including oral, gastric, and intestinal phases on bioaccessibility and cytotoxic activities of momilactones against selected blood cancer cell lines are indicated in our research which has not been reported in any other studies.

Under digestion, the stability of compound structures and functional groups can be affected that may involve in the regulations of associated biological properties. In which, pH level may play an important role in altering the bioaccessibility of bioactivity of target compounds (Hodgkinson et al., 2018; Pérez-Vicente et al., 2002; Un et al., 2022; Wootton-

Beard et al., 2011). For example, anthocyanin compounds are mostly converted to non-red forms and/or degraded from the pomegranate juice due to pH shift during digestion. Vitamin C in the pomegranate juice was also significantly degraded under the changes in pH of each digestive stages (Pérez-Vicente et al., 2002). In the research of (Un et al., 2022), the changes in pH conditions in simulated digestive model may cause the possible formation or degradation of bioactive compounds isolated from *Sargassum* spp., leading to the variation in their associated biological activities (Un et al., 2022). In line with that research, the cytotoxicity of momilactones reduce through digestion which is consistent with the reduction of momilactone contents in digested samples. The variations of momilactone contents and associated cytotoxic activities may be affected by different pH and enzyme constituents. Notably, MB content significantly reduces after the oral phase, which may be due to α-amylase activity. MB amount increases during the gastric phase compared to the previous phase, suggesting that acidic environment (pH = 1.0) together with pepsin activity may lead to the re-formation of MB. With the increasing pH in the intestinal phase and lipase effects, the quantity of MB again decreases. Further studies should be conducted to validate this paradigmatic research.

To develop momilactones as novel oral administrated medicines, advanced solutions such as capsule technology and nanotechnology are highly recommended in further anticancer research. In which, capsule method has been revealed positive impacts on bioaccessibility and bioavailability of target bioactive components during digestion. Moreover, this approach can ensure the compounds' targets as well as control their release (Grgić et al., 2020). Besides, capsule can address the undesirable odors, tastes as well as contribute to better organoleptic properties (Grgić et al., 2020). Nanotechnology is another promising approach that can increase the effectiveness of orally administrated medicines. Particularly, nanocarriers can help enhance solubility, stability, and epithelium permeability

of target products, since then increase their bioaccessibility and bioavailability (Hsu et al., 2019). Furthermore, our study indicates that cytotoxic activities of momilactones are varied among digestive stages against different blood cancer cell lines. The finding may lead to further effective approaches of capsule- or nano-technology to enhance bioaccessibility and bioavailability of momilactones under digestion effect against specific targeted blood cancer cell line.

In another concern, a natural-based drug must satisfy many strict requirements including benefits over risks to be acknowledged as novel drugs (Teschke & Xuan, 2020c). Therefore, the optimized dose of momilactones should be established to suppress substantially tumors without harmful effects on normal blood cells. On the other hand, the potential risk such as neurotoxicity and hepatotoxicity by using herbal products should be seriously considered and thoroughly evaluated (Quan et al., 2020). Accordingly, *in vivo* tests and clinical trials are required for the development of momilactones as novel anti-blood cancer drugs.

CHAPTER 6: GENERAL DISCUSSION

6.1. Key findings

In this study, we indicated, for the first time, that the problematic invasive weed *A. virginicus*, which was once thought to be of no use, may be a promising source of antioxidant, anti-diabetic, anti-skin aging, and anti-blood cancer agents (Table 16). The findings are expected to support both crop protection and human health concerns.

In addition, momilactone B (MB) and the mixture of momilactones A and B (MAB) (1:1, w/w) isolated from rice (*O. sativa*) significantly inhibit the viability of different blood cancer cell lines including chronic myeloid leukemia (CML), acute promyelocytic leukemia (APL), mantle cell lymphoma (MCL), and multiple myeloma (MM). The cytotoxic activity of MB and MAB against CML cell lines is close to that of the well-known drug Doxorubicin. Meanwhile MB and MAB are more potent than Doxorubicin and Ibrutinib in suppressing APL and MM cell lines, respectively. Besides, MB and MAB prevent the tested blood cancer cell lines by promoting their cell apoptosis. Whereas these compounds reveal insignificant effects on the non-cancerous cell line. The findings were not presented in any other studies.

Another novel finding of this study is to scrutinize that MB and MAB promote MM cell apoptosis by regulating relevant protein expressions (Table 16). While these compounds altering the expressions of regulatory proteins related to apoptosis activation and G2 phase arrest of the cell cycle that cause the inhibition of APL cells (Table 16).

Besides, this is the first study to investigate the cytotoxic activity on blood cancer cell lines and bioaccessibility of momilactones through *in vitro* simulated human digestion. Accordingly, the cytotoxicity of momilactones may reduce under the effects of digestion which is consistent with the reduction of momilactone contents in digested samples. Further studies should be conducted applying advanced methods such as capsule- and nano-

technology to enhance the bioaccessibility and bioavailability of momilactones for developing novel anti-blood cancer drugs.

Table 16. Key findings

Chapter	This study	Previous study
Chapter 2	• This is the first report describing that *A. virginicus* is a potential natural source of antioxidants, tyrosinase and α-amylase inhibitors, and anti-chronic myeloid leukemia (CML) agents	• There has been no conducted research on pharmaceutical properties of *A. virginicus*
Chapter 3	• MB and MAB reveal insignificant effects on non-cancerous cell line (MeT-5A). • MB and MAB inhibit the blood cancer cell lines comprising chronic myelogenous leukemia (Meg-01 and K562), acute promyelocytic leukemia (HL-60), mantle cell lymphoma (Mino); multiple myeloma (U266 and KMS-11) by promoting cell apoptosis. • The cytotoxic activity of MB and MAB against chronic myeloid leukemia (CML) cells is close to	• The cytotoxic activity of momilactones on normal cells was not indicated. • MB inhibits the cell viability of human cancer cell lines including colon cancer (HT-29 and SW620), acute promyelocytic leukemia (HL-60), and leukemic T cells (Jurkat and RBL-2H3) (Kim et al., 2007; Lee et al., 2008). • MB induces apoptosis and G1 phase arrest in the cell cycle of U937 cells (Park et al., 2014).

	that of well-known drug Doxorubicin. While MB and MAB are stronger than the drugs of Doxorubicin and Ibrutinib in preventing acute promyelocytic leukemia (APL) and multiple myeloma (MM) cells, respectively.	• MB promotes Jurkat cell apoptosis (Lee et al., 2008). • The cytotoxicity of momilactones was not compared to that of widely applied anti-blood cancer medicines.
Chapter 4	• MB and MAB show negligible effects on cell apoptosis and cell cycle of non-cancerous cell line MeT-5A. • MB and MAB at 5 μM inhibit HL-60 cells through the regulations of relevant proteins to apoptosis-inducing factors (p-38, BCL-2, and caspase-3) and cell cycle arrest at G2 phase (p-38, CDK1, and cyclin B1). • MB and MAB at 5 μM enhance U266 cell apoptosis by altering p-38, BCL-2, and caspase-3 signaling pathways.	• MB induces apoptosis and G1 arrest of the cell cycle in monocytic leukemia U937 cells through downregulation of pRB phosphorylation and induction of the CDK inhibitor $p21^{Waf1/cip1}$ (Park et al., 2014). • MB promotes Jurkat cell apoptosis via caspase and mitochondria pathways (Lee et al., 2008).

Chapter 5	• The cytotoxicity of momilactones may reduce through the digestive stages, which is in line with the reduction of momilactone contents in digested samples.	• There has been no research on cytotoxic activities against blood cancer cell lines and bioaccessibility of momilactones under the effects of human digestion.

6.2. Comparison between cytotoxic activities of isolated components from rice (*O. sativa* var. Koshihikari) and the invasive weed (*A. virginicus*)

Based on the cytotoxic results against chronic myeloid leukemia (CML) cell lines, momilactones from rice exhibit much stronger inhibitory activities on Meg-01 and K562 cell viability than extracts from *A. virginicus* (Table 17). Therefore, momilactones were selected to investigate their cytotoxic mechanisms and bioaccessibility during digestion in our study. However, further studies should be conducted focusing on the isolation and purification of the responsible compounds for the anti-blood cancer activity of *A. virginicus*, followed by indicating their cytotoxic mechanisms and bioaccessibility under digestive processes.

Table 17. Cytotoxic activities of isolated components from broomsedge bluestem and rice (Achieved results from Chapters 2 and 3)

Original plant	**Sample**	**Meg-01** IC_{50} (μg/mL)	**K562** IC_{50} (μg/mL)
Broomsedge bluestem (*A. virginicus*)	T-Anvi	91.40[c]	247.88[a]
	H-Anvi	198.07[a]	-
	E-Anvi	168.94[b]	112.01[b]
Rice	MA	2.26[d]	2.57[c]

(*O. sativa*)	MB	1.45^{f}	1.66^{d}
	MAB	1.39^{f}	1.33^{e}
Standard inhibitor	Doxorubicin	1.82^{e}	1.70^{d}
	Imatinib	0.33^{g}	0.33^{f}

Different superscript letters indicate significant differences. T-Anvi, total crude extract; H-Anvi, hexane extract; E-Anvi, ethyl acetate extract; MA, momilactone A; MB, momilactone B; MAB, the mixture of momilactones A and B (1:1, w/w).

6.3. Exploitation of products from rice (*O. sativa*) and the invasive weed (*A. virginicus*) for developing blood cancer treatments

In this study, we indicated the potentials of momilactones isolated from rice and extracts from *A. virginicus* for anti-blood cancer properties. In which, momilactones significantly inhibit tested blood cancer cell lines by regulating the related proteins to apoptosis and cell cycle pathways. On the other hand, the impacts of momilactones on normal blood cells including red blood cells (erythrocytes), white blood cells (monocytes, lymphocytes, neutrophils, eosinophils, basophils, and macrophages), and platelets (thrombocytes) should be comprehensively interpreted since they might be affected by the same course of event with tumors (Taşkın-Tok & Gowder, 2014). Forthcoming studies should focus on the effects of momilactones on relevant proteins to cell apoptosis and cell cycle pathway of normal blood cells treated with momilactones. This is an integral requirement to minimize failure in later stages of drug development. Furthermore, this may help establish potential drug combinations as well as effective therapies (Taşkın-Tok & Gowder, 2014).

Through *in vitro* digestion assay, cytotoxic activities of momilactones significantly decrease during digestion. Therefore, forthcoming studies should be conducted to improve

the bioaccessibility of momilactones, followed by *in vivo* and clinical tests to confirm their capacities in the development of novel anti-blood cancer drugs.

In another aspect, the application of anti-cancer medicines (e.g., Doxorubicin) may lead to oxidative stress by increasing free radicals (Thorn et al., 2011) and a high risk of getting other chronic disorders such as diabetes, obesity, and skin diseases (Libby et al., 2009). Moreover, a relationship between oxidative stress, inflammation, cancer, and chronic problems including diabetes, obesity, and skin disorders which may eventually cause an increase in morbidity and mortality (Figure 27). Accordingly, momilactones isolated from rice with potentials for antioxidant (Quan et al., 2019a), anti-diabetes, anti-obesity, and anti-skin aging (Quan et al., 2019a, 2019b, 2019c), and anti-blood cancer activities (Chapters 3 and 4), and products extracted from *A. virginicus* with potentials for antioxidant, anti-diabetes, anti-skin aging, and anti-blood cancer properties (Chapter 2) can be considered a promising source for improving blood cancer treatments, especially for patients complicated with oxidative stress and chronic diseases.

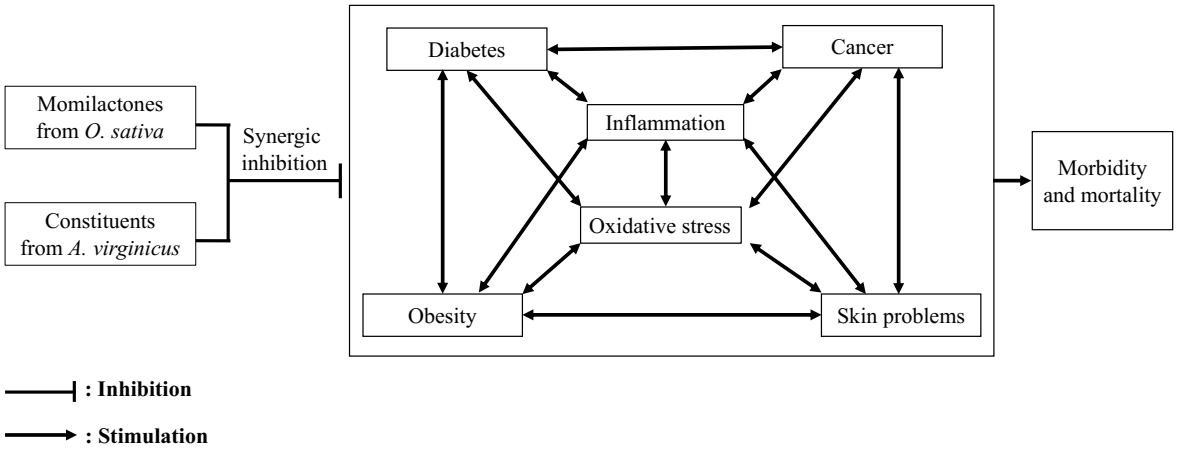

Figure 27. Potential approach for exploiting natural compounds from rice (*O. sativa*) and the invasive weed (*A. virginicus*) for therapeutic purposes

On the other hand, the interactions between compounds may be more important than individual compounds in determining biological activity (Quan et al., 2019f). Therefore, the combination of momilactones from rice and isolated components from *A. virginicus* may be

a promising approach for developing blood cancer treatments avoiding the risks of getting oxidative stress and other chronic disorders. The results from our study may lead to further strategies to take advantage of this problematic invasive weed and rice by-products for pharmaceutical purposes.

Additionally, both *A. virginicus* and rice are monocot plants, which adapt to a wide range of environmental conditions (Simpson, 2010). Thus, they can be feasibly exploited for pharmaceutical purposes with an abundant biomass availability. For momilactones, in addition to rice source, the *Hypnum* moss (*Hypnum plumaeforme*) should be paid more considerations as a promising source of momilactones. On the other hand, research on synthetic momilactones may be an effective approach for the development of medicinal production and therapeutics. Besides, a number of 47 momilactone-like molecules were reported (Zhao et al., 2018), suggesting an abundant source for further investigation of their cytotoxic potentials against blood cancer cells. Moreover, a natural-based product must satisfy the requirements of benefits outweighing risks (Teschke & Xuan, 2020c). Therefore, the effective concentration of isolated momilactones from rice and components from *A. virginicus* should be established to exhibit the strongest cytotoxicity against tumors without harmful effects on normal blood cells. In contrast, the potential risk such as neurotoxicity and hepatotoxicity by using derived products from plants should be seriously considered and thoroughly evaluated (Quan et al., 2020). Thus, *in vivo* tests and clinical trials are highly recommended in forthcoming studies.

Overall, the study is expected to support the sustainable development goals (SDGs) of ensuring healthy lives and life on land, ending poverty and hunger in the world, especially in the rice-producing countries as well as the countries suffering from the problematic invasive *A. virginicus*.

SUPPLEMENTARY DATA

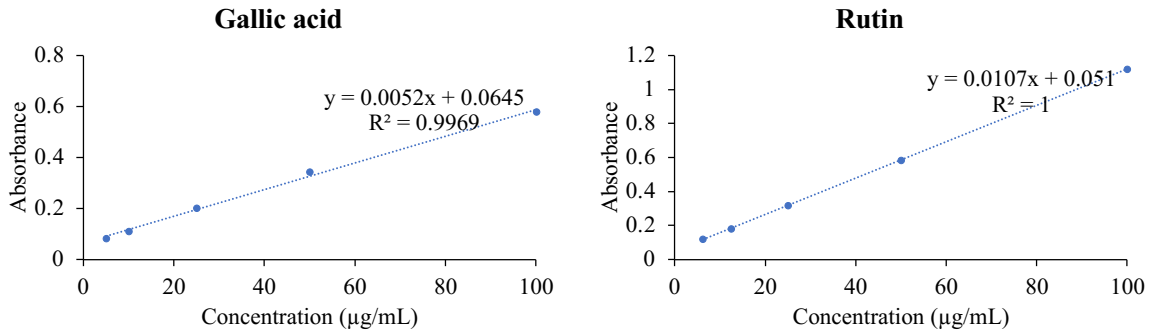

Figure S1. Standard curves of gallic acid and rutin.

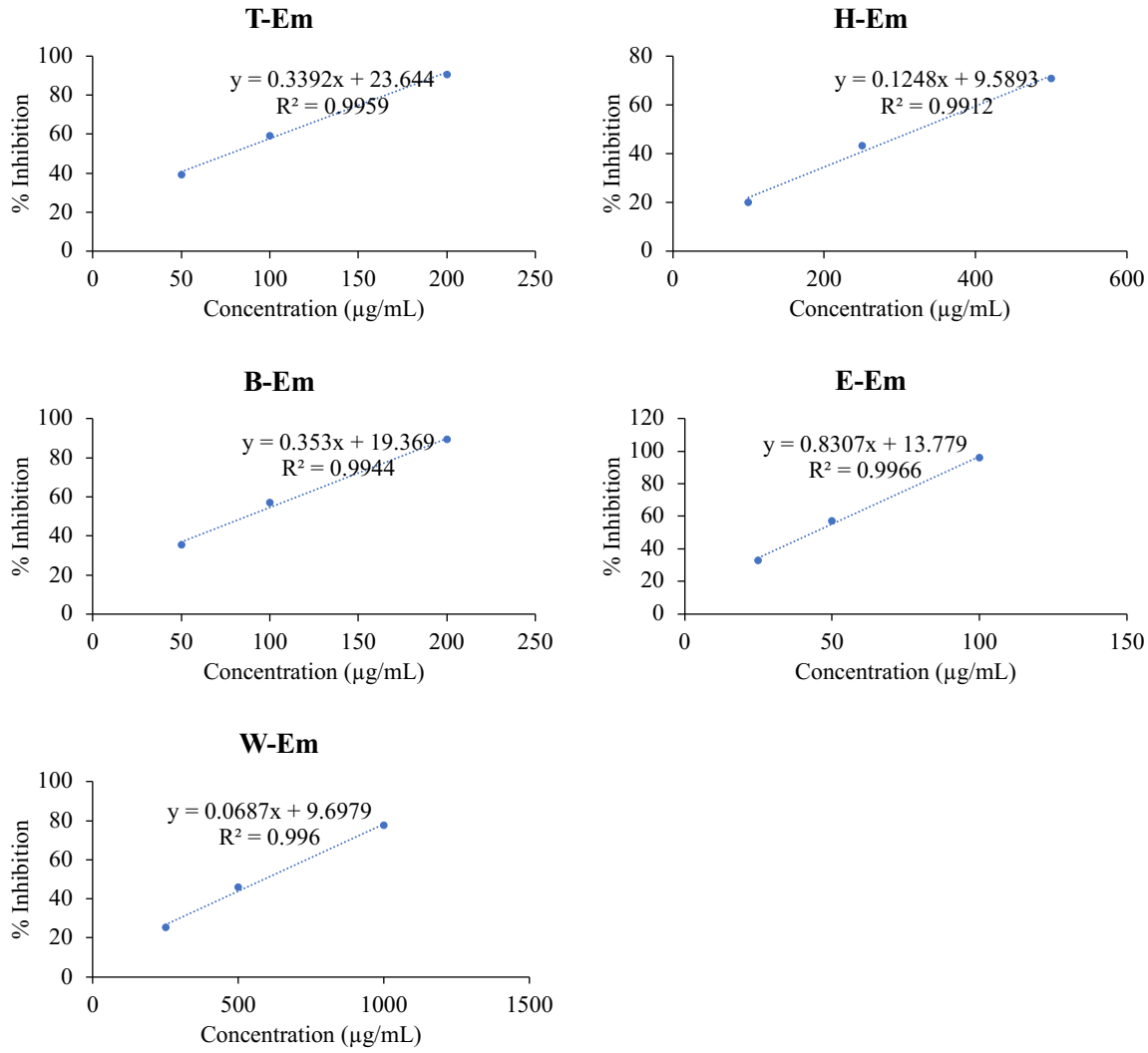

Figure S2. Antiradical activity of *A. virginicus* extracts via 2,2′-azinobis-(3-ethylbenzothiazoline-6-sulfonic acid) (ABTS) assay. T-Anvi, total crude extract; H-Anvi,

hexane extract; E-Anvi, ethyl acetate extract; B-Anvi, butanol extract; W-Anvi, water extract.

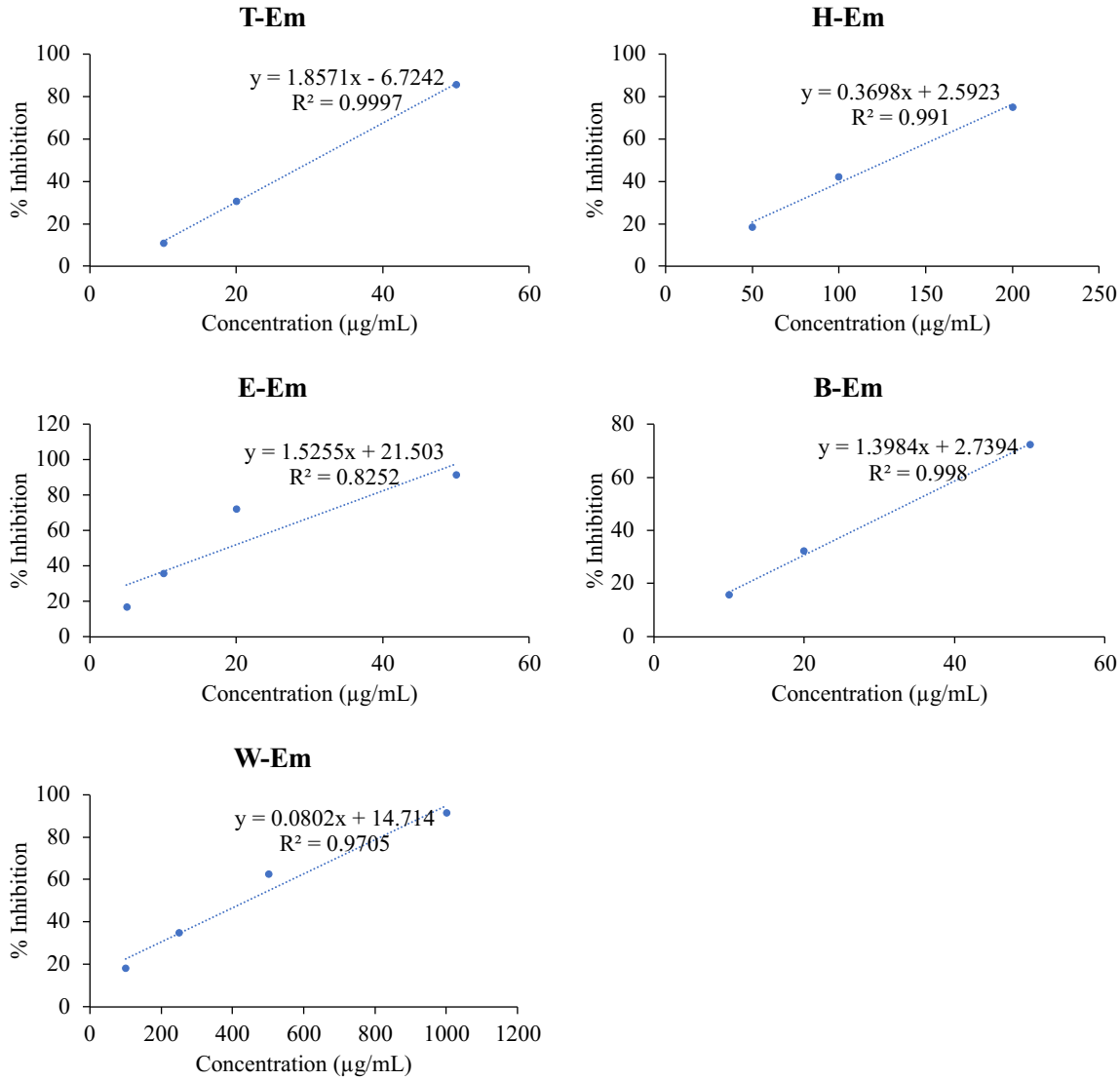

Figure S3. Antiradical activity of *A. virginicus* extracts via 2,2-diphenyl-1-picrylhydrazyl (DPPH) assay. T-Anvi, total crude extract; H-Anvi, hexane extract; E-Anvi, ethyl acetate extract; B-Anvi, butanol extract; W-Anvi, water extract.

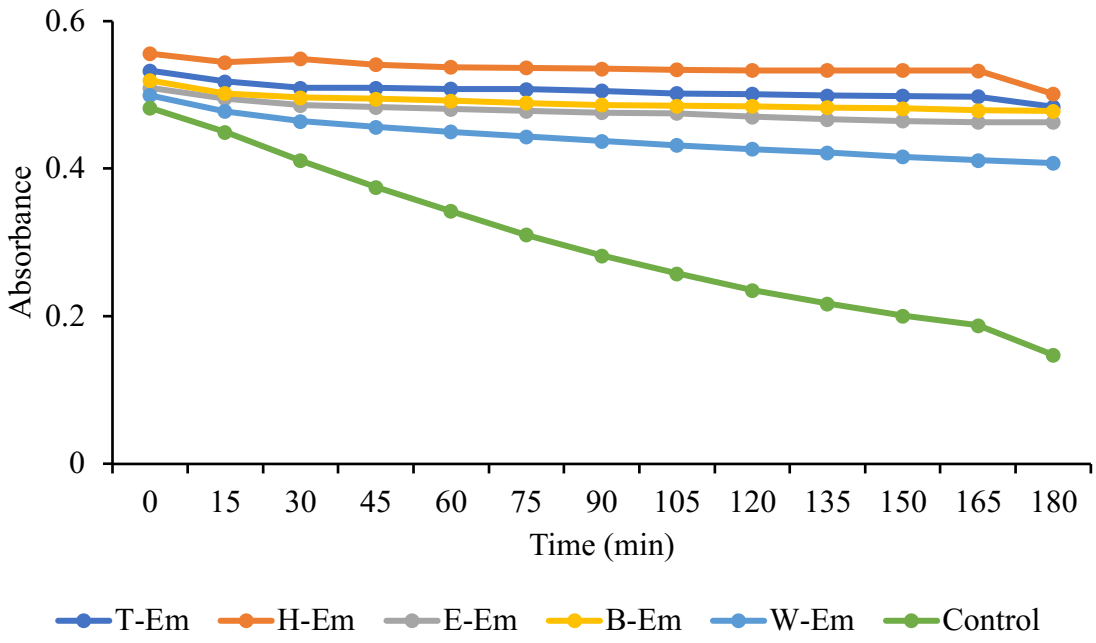

Figure S4. Inhibition on lipid peroxidation of *A. virginicus* extracts. T-Anvi, total crude extract; H-Anvi, hexane extract; E-Anvi, ethyl acetate extract; B-Anvi, butanol extract; W-Anvi, water extract.

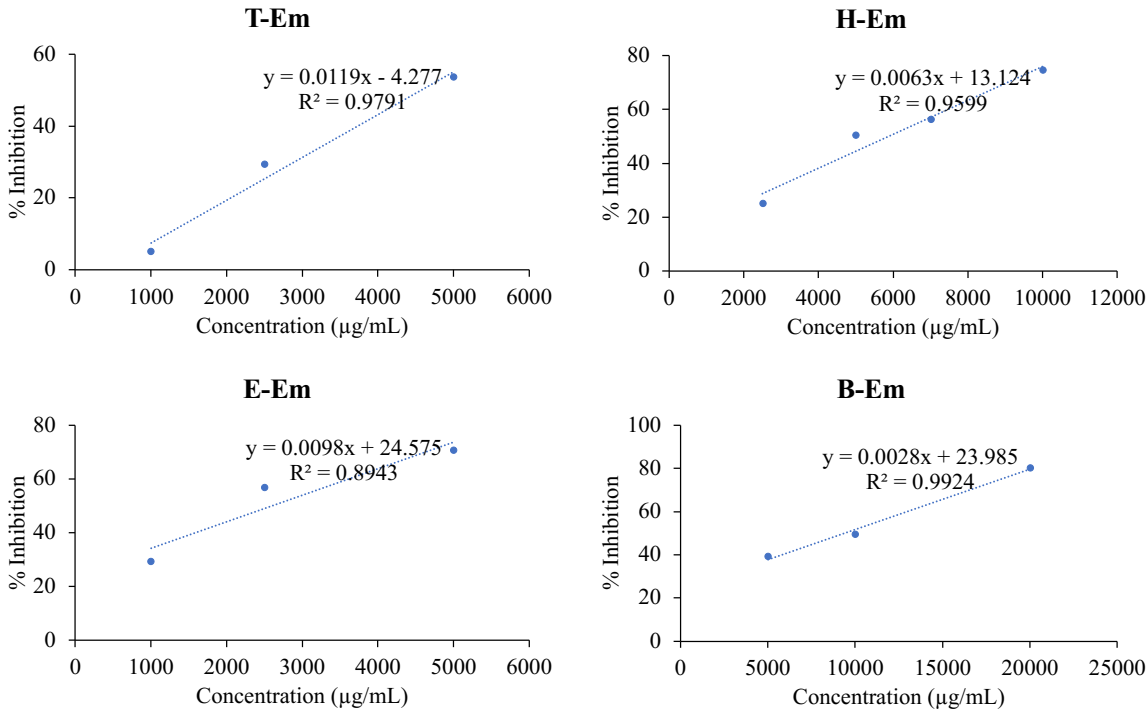

Figure S5. Tyrosinase inhibitory activities of *A. virginicus* extracts. T-Anvi, total crude extract; H-Anvi, hexane extract; E-Anvi, ethyl acetate extract; B-Anvi, butanol extract.

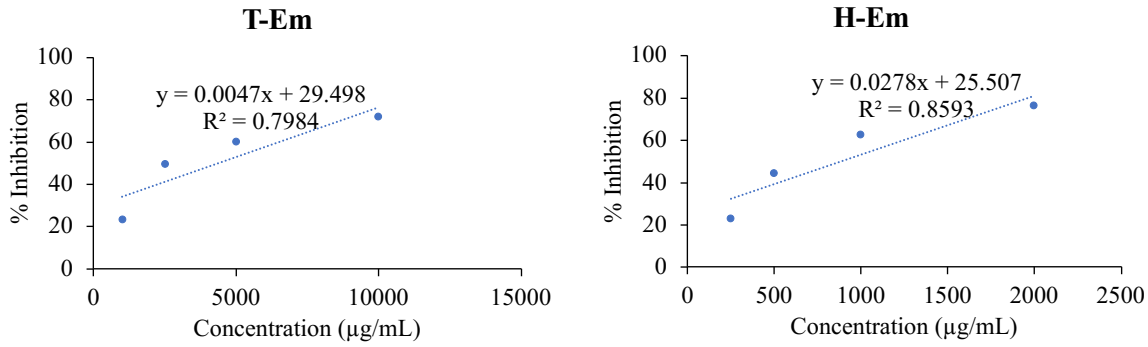

Figure S6. α-Amylase inhibitory activities of *A. virginicus* extracts. T-Anvi, total crude extract; H-Anvi, hexane extract.

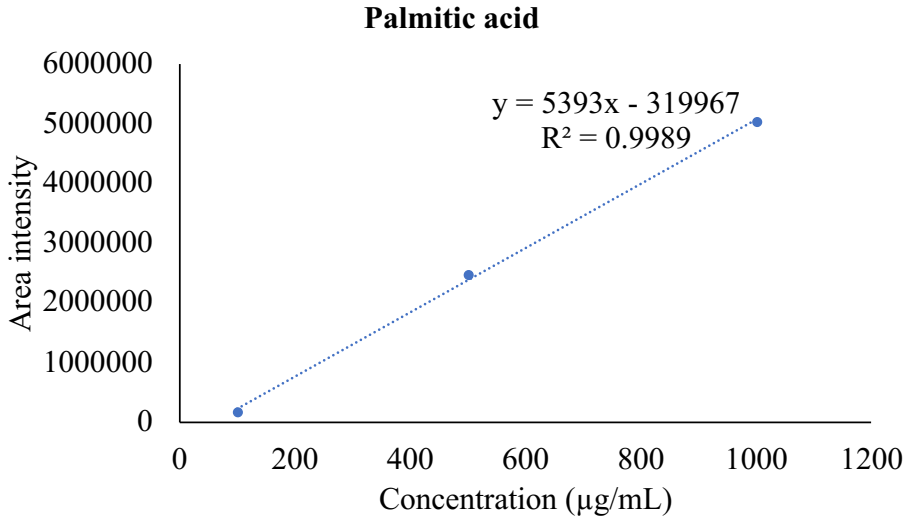

Figure S7. Standard curve of palmitic acid

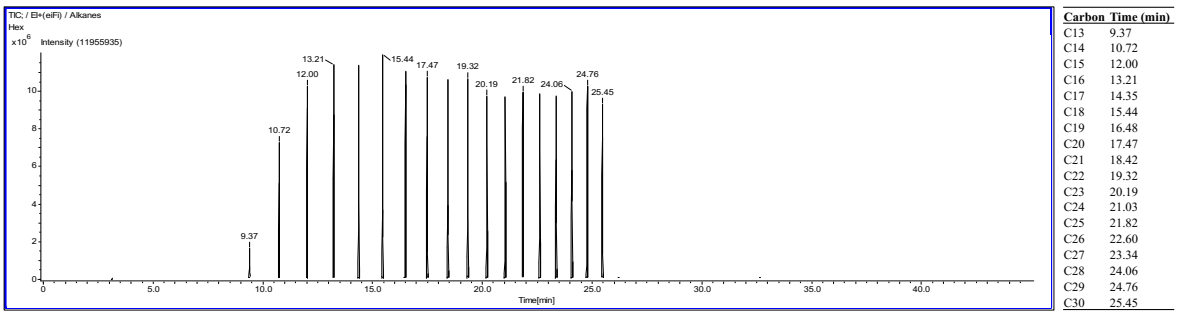

Figure S8. GC chromatogram of n-alkane mixture (C13–C30)

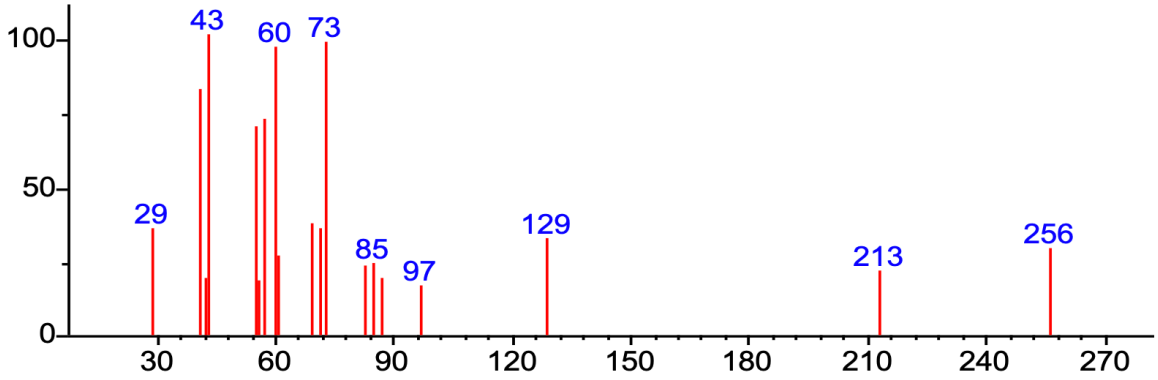

Figure S9. Mass spectra (MS) of palmitic acid found in hexane extracts (H-Anvi) from *A. virginnicus* analyzed by gas chromatography-mass spectrometry (GC-MS).

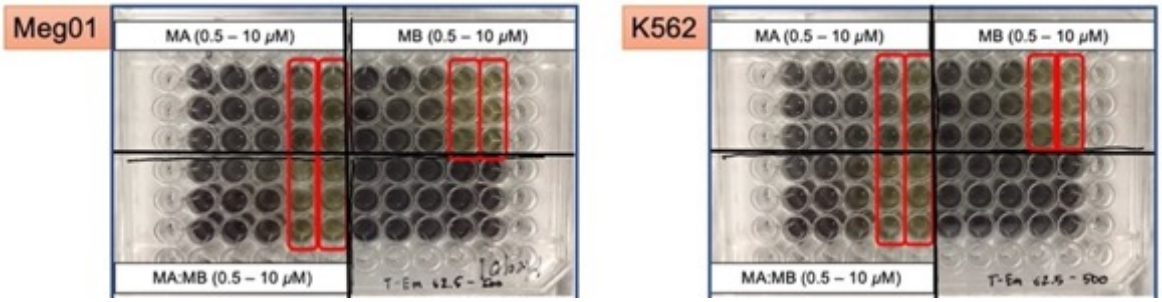

Figure S10. Effects of momilactones A (MA) and B (MB) on cell viability of tested blood cancer cell lines via MTT assay.

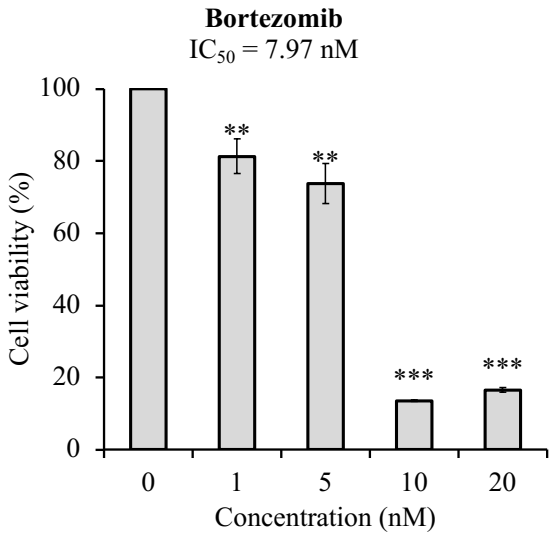

Figure S11. Effects of Bortezomib on cell viability of multiple myeloma (U266) cell lines after 48 h. $^{**}p < 0.01$ versus control (0 nM); $^{***}p < 0.001$ versus control (0 nM).

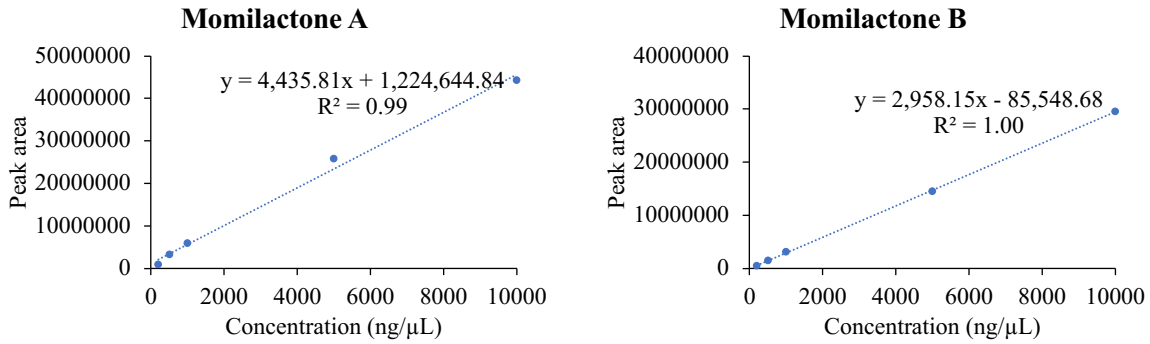

Figure S12. Standard curves of momilactones A and B.

(a)

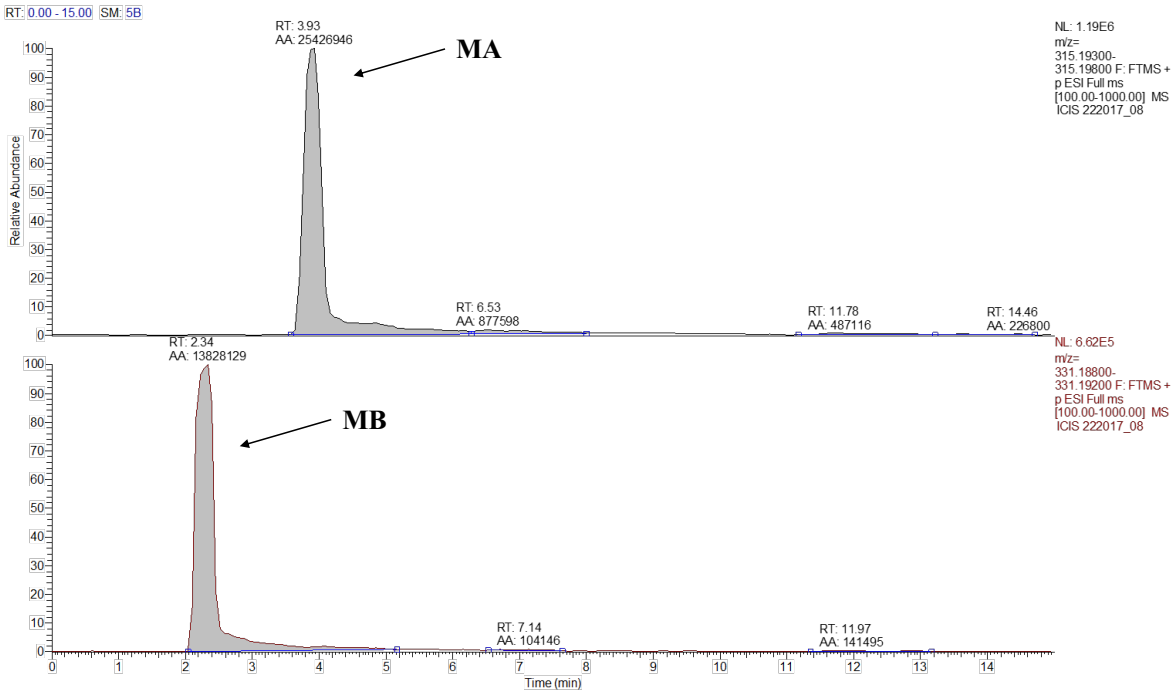

(b)

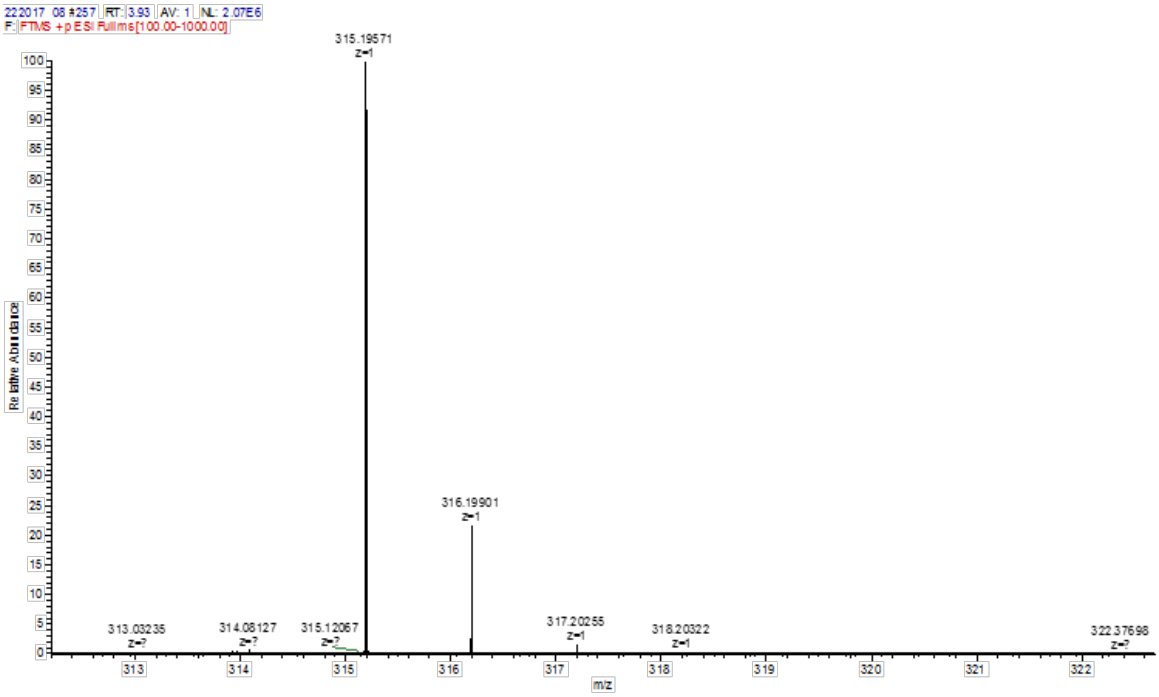

MA

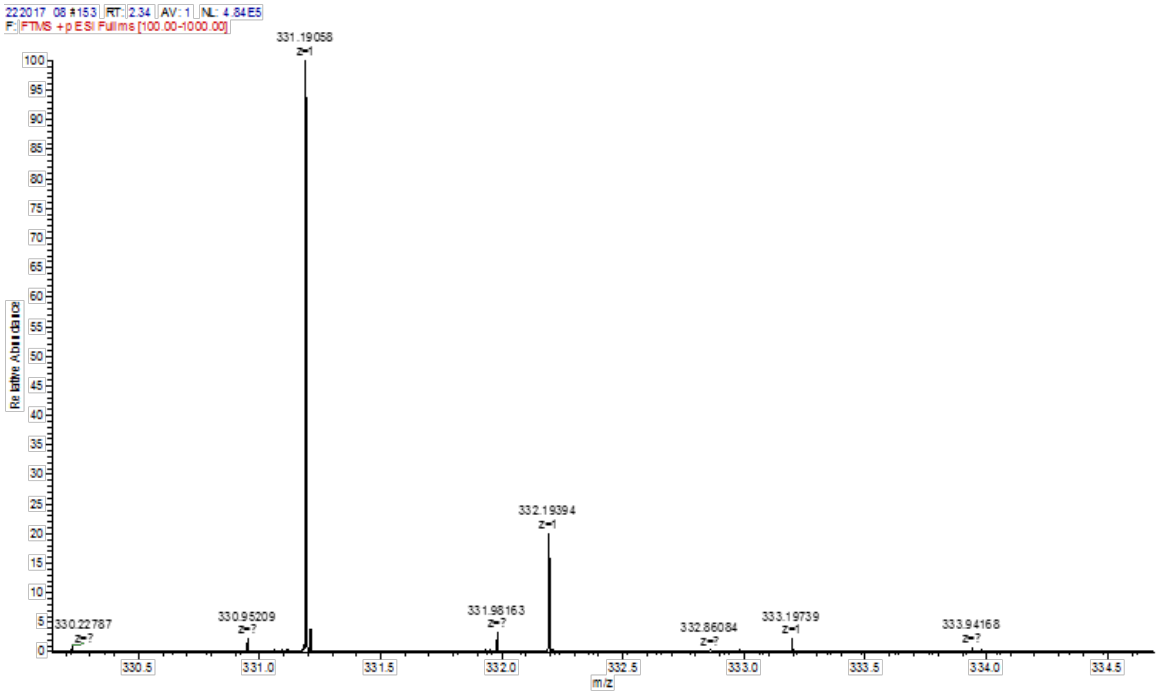

MB

Figure S13. (a) Extracted ion chromatograms (EIC) and **(b)** mass spectra (MS) of the standards of momilactones A (MA) and B (MB) by ultra-performance liquid chromatography-electrospray ionization-mass spectrometry (UPLC-ESI-MS).

(a)

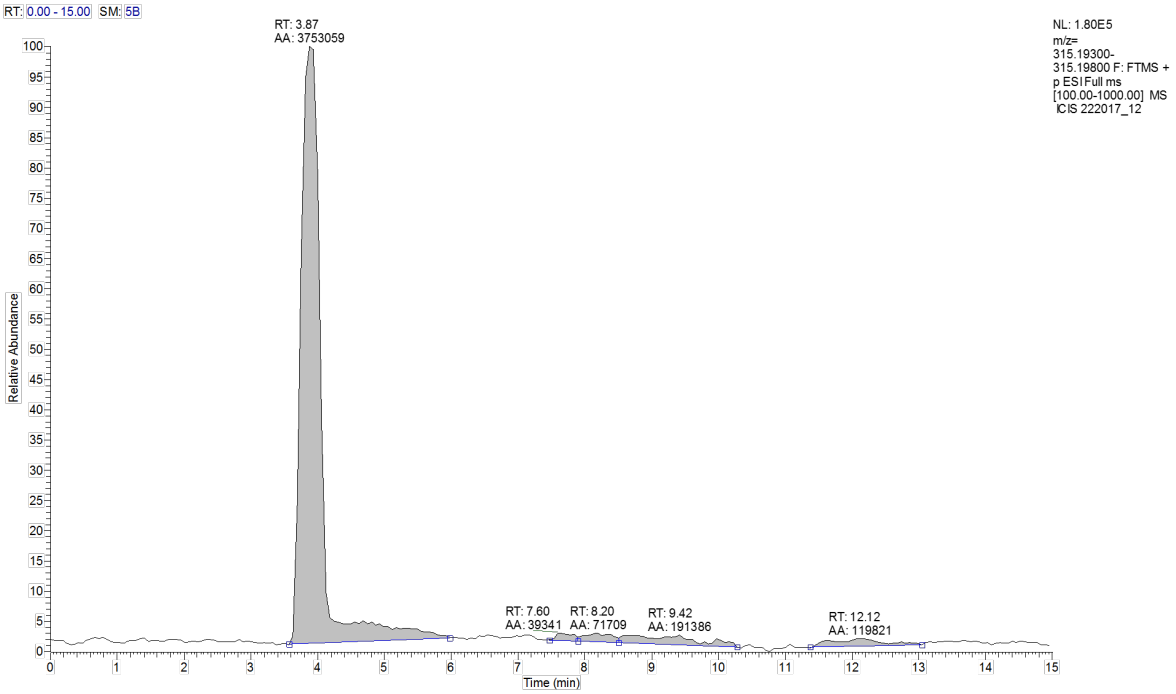

(b)

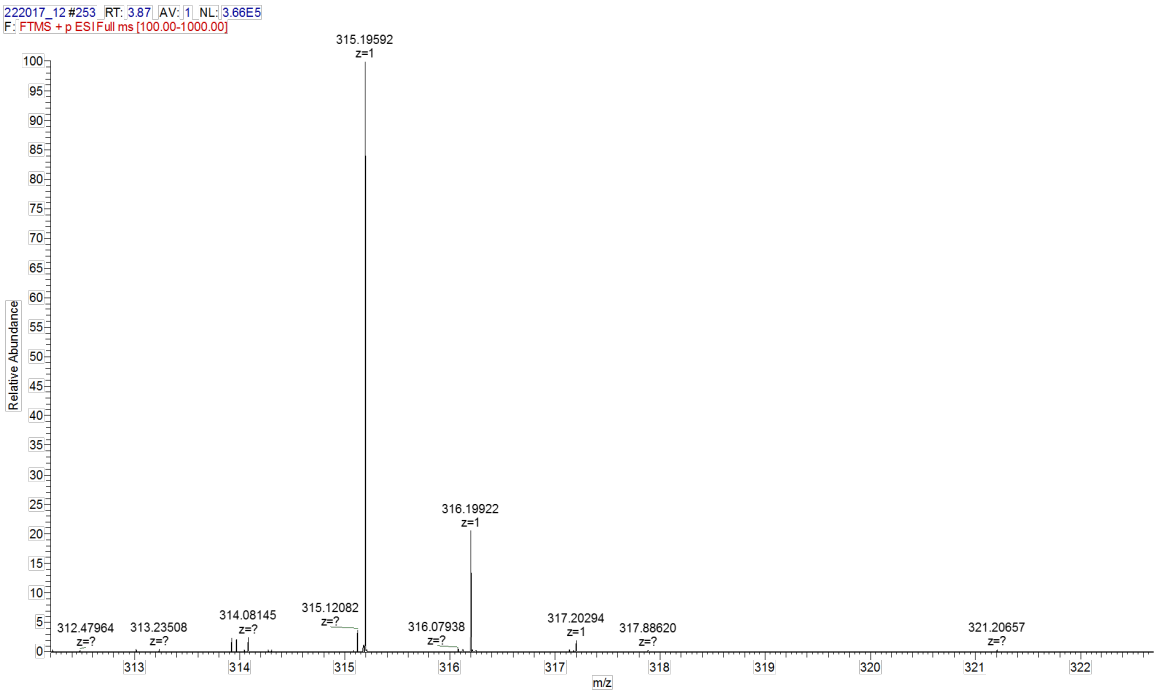

Figure S14. (a) Extracted ion chromatograms (EIC) and **(b)** mass spectra (MS) of momilactone A (MA) in oral digested sample by ultra-performance liquid chromatography-electrospray ionization-mass spectrometry (UPLC-ESI-MS).

(a)

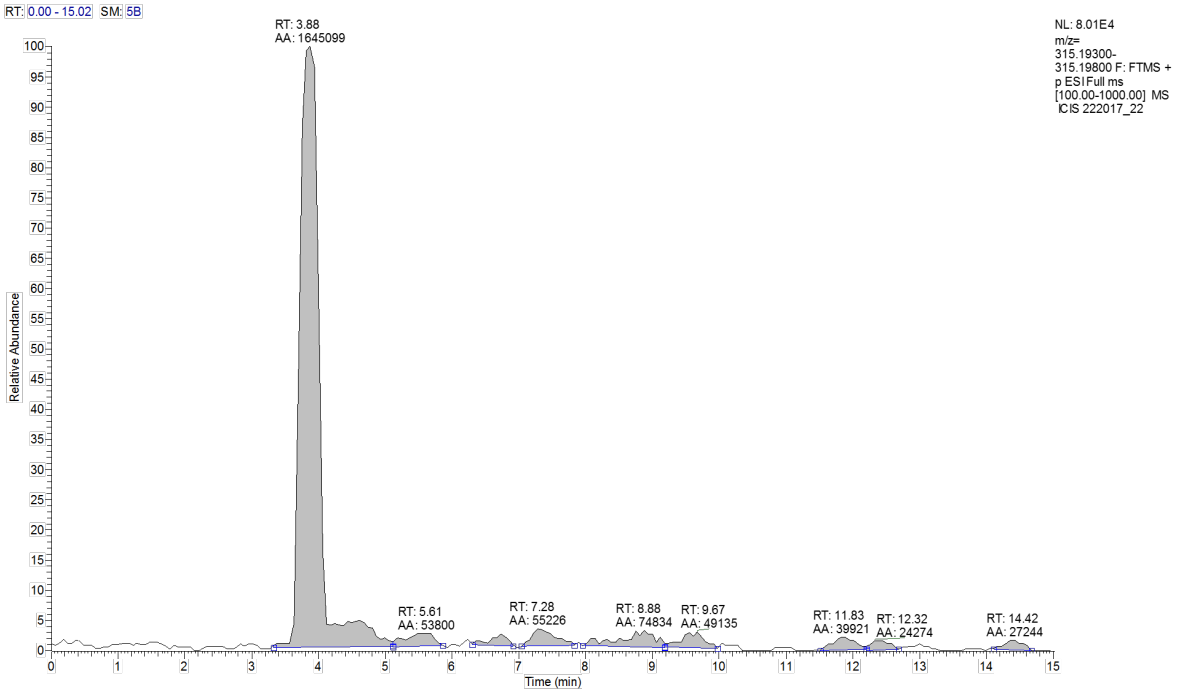

(b)

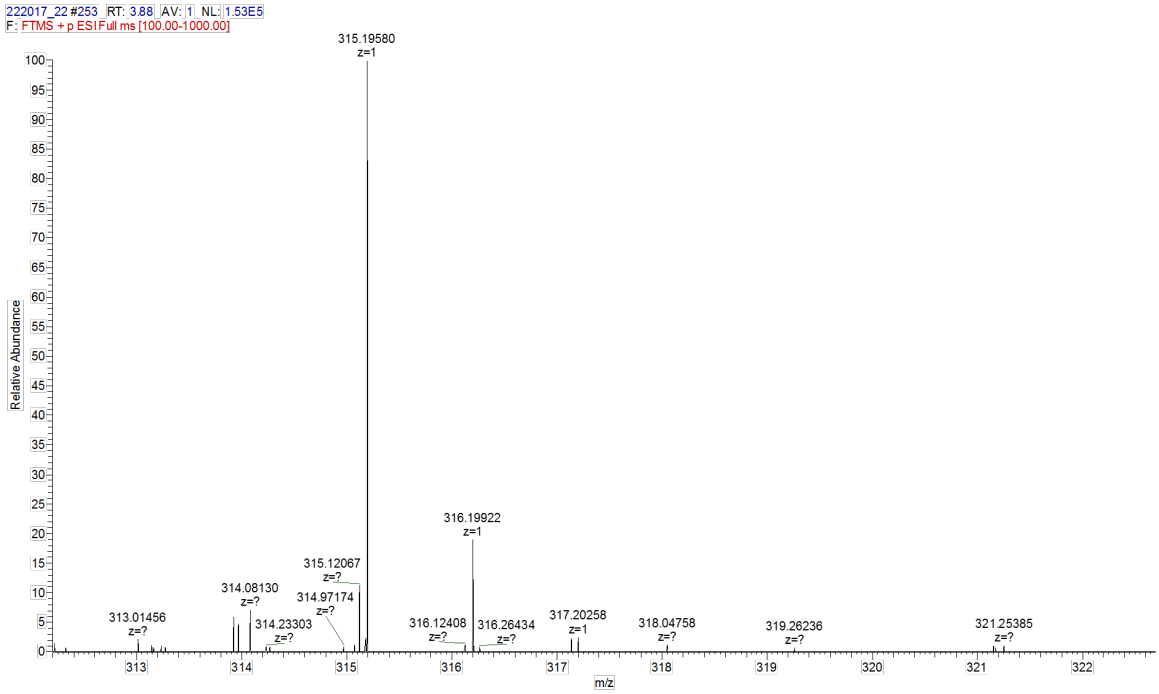

Figure S15. (a) Extracted ion chromatograms (EIC) and **(b)** mass spectra (MS) of momilactone A (MA) in gastric digested sample by ultra-performance liquid chromatography-electrospray ionization-mass spectrometry (UPLC-ESI-MS).

(a)

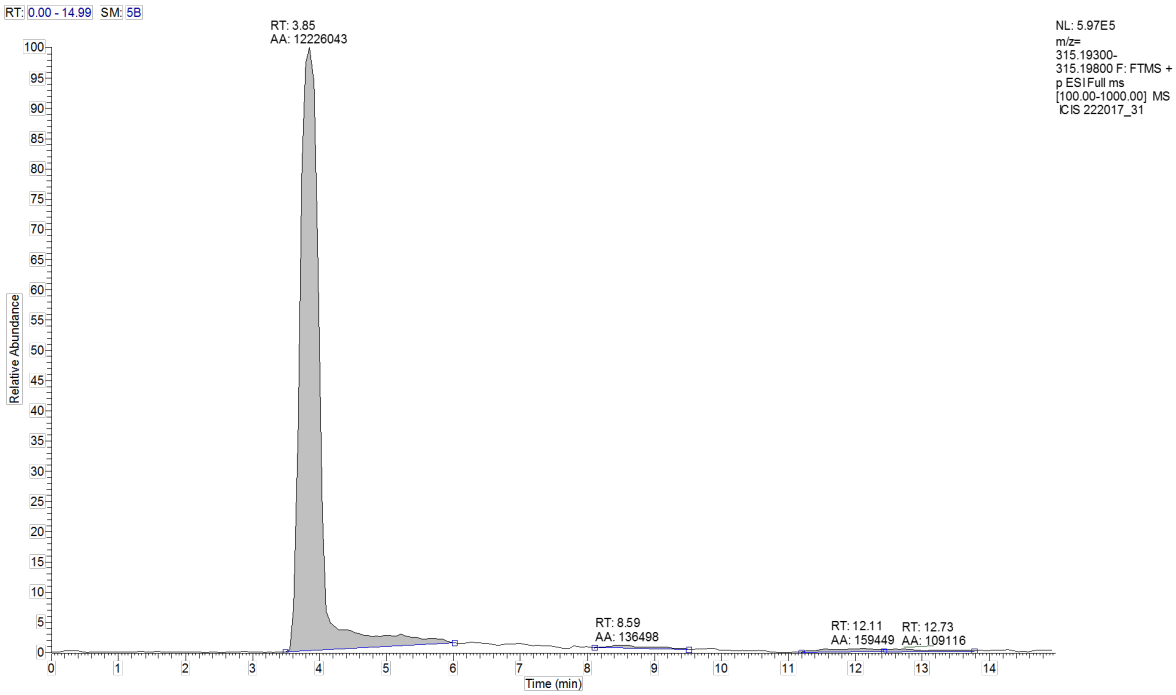

(b)

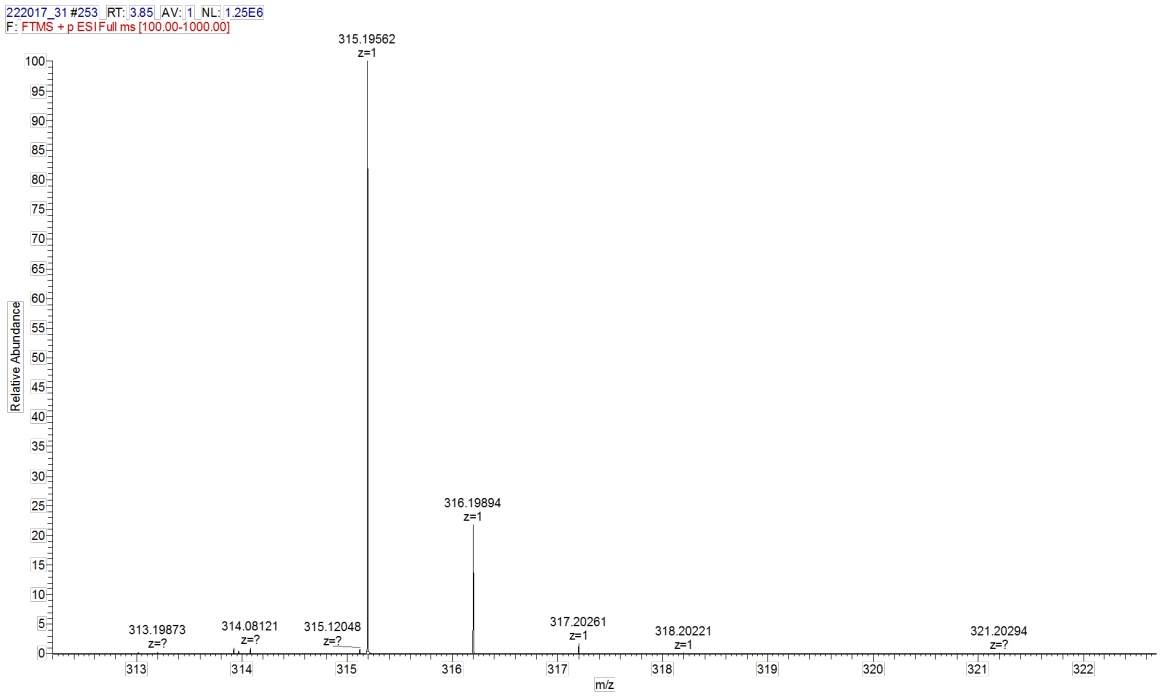

Figure S16. (a) Extracted ion chromatograms (EIC) and **(b)** mass spectra (MS) of momilactone A (MA) in intestinal digested sample by ultra-performance liquid chromatography-electrospray ionization-mass spectrometry (UPLC-ESI-MS).

(a)

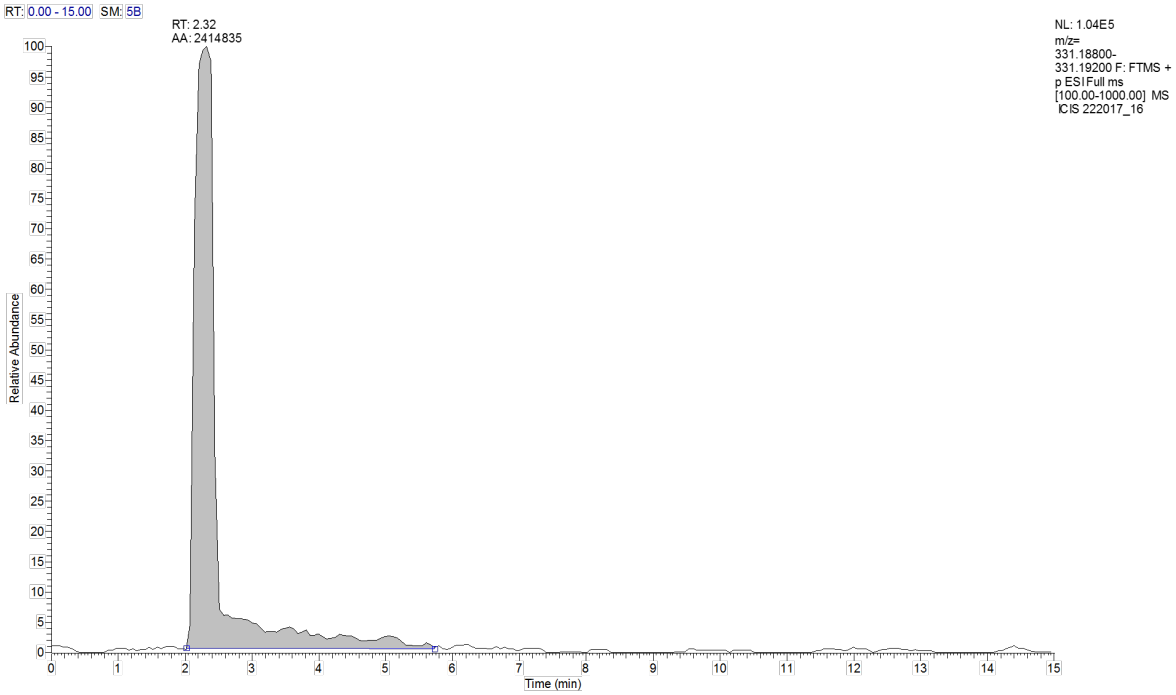

(b)

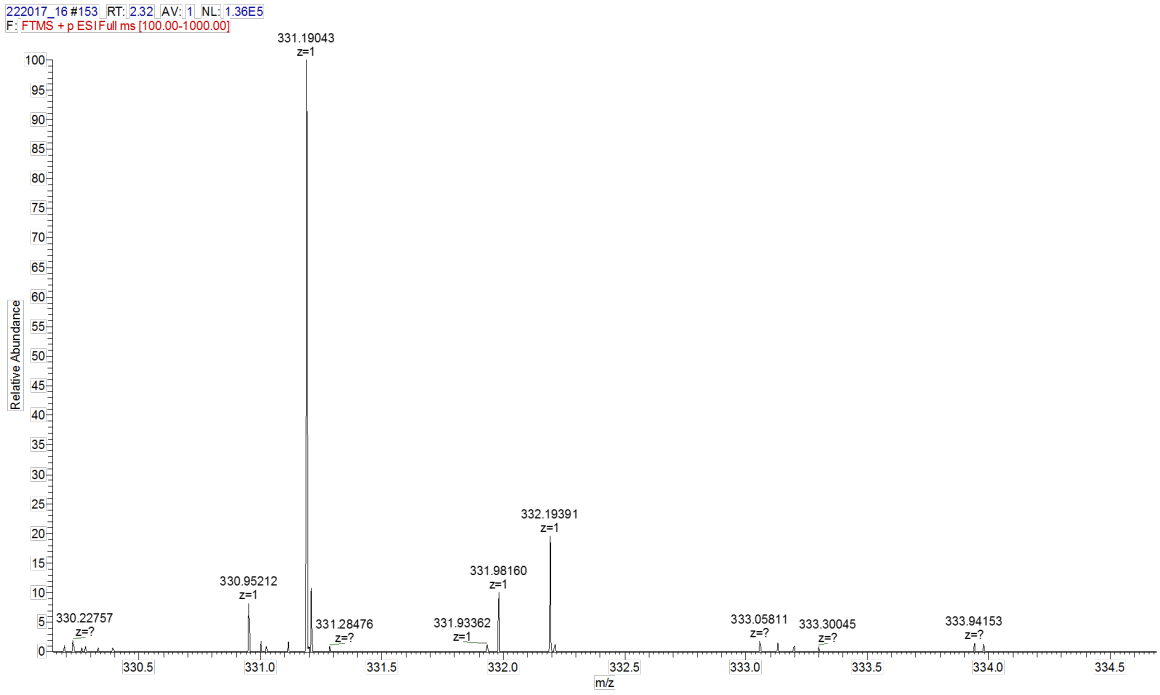

Figure S17. (a) Extracted ion chromatograms (EIC) and **(b)** mass spectra (MS) of momilactone B (MB) in oral digested sample by ultra-performance liquid chromatography-electrospray ionization-mass spectrometry (UPLC-ESI-MS).

(a)

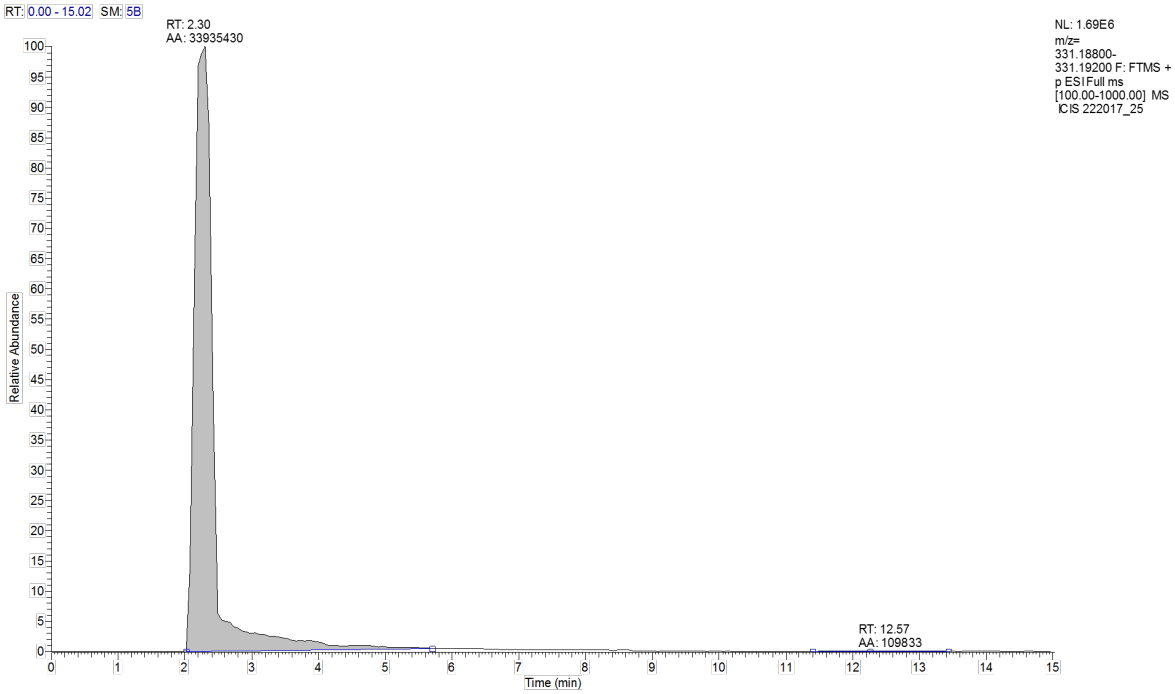

(b)

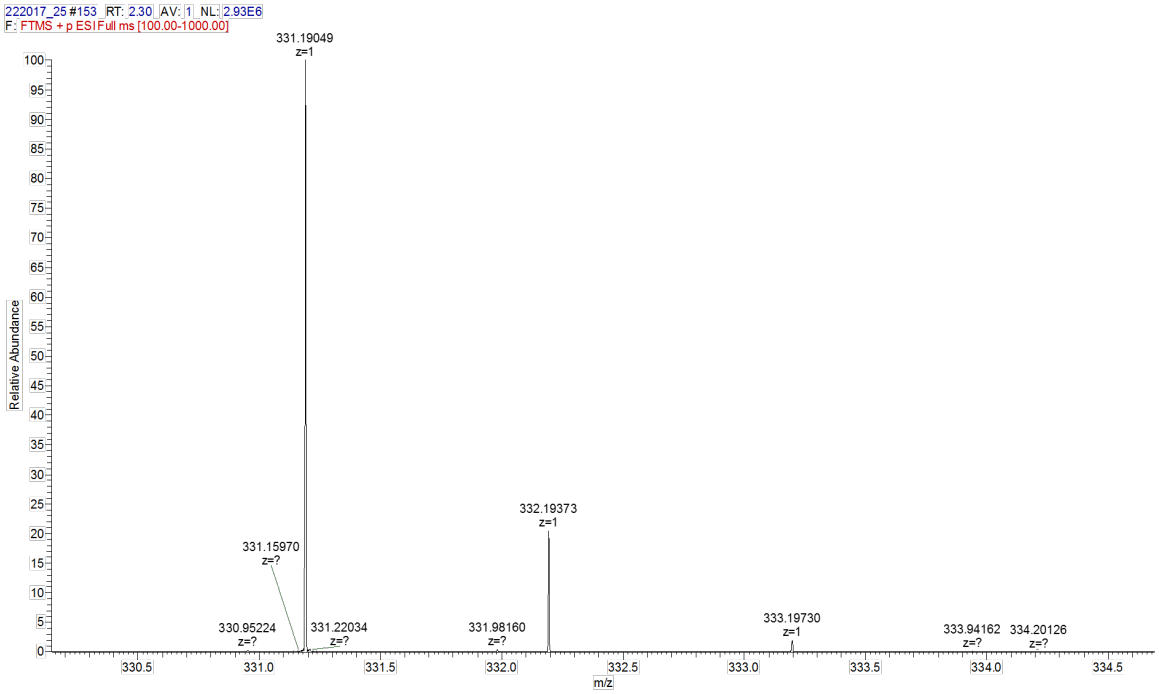

Figure S18. (a) Extracted ion chromatograms (EIC) and **(b)** mass spectra (MS) of momilactone B (MB) in gastric digested sample by ultra-performance liquid chromatography-electrospray ionization-mass spectrometry (UPLC-ESI-MS).

(a)

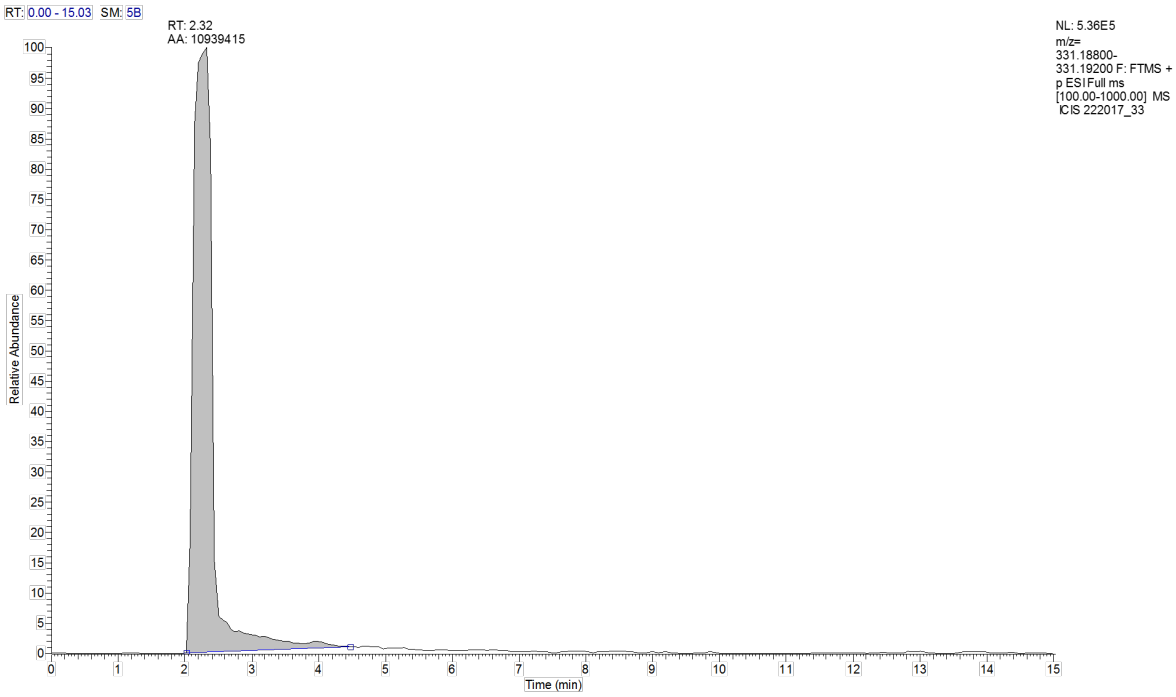

(b)

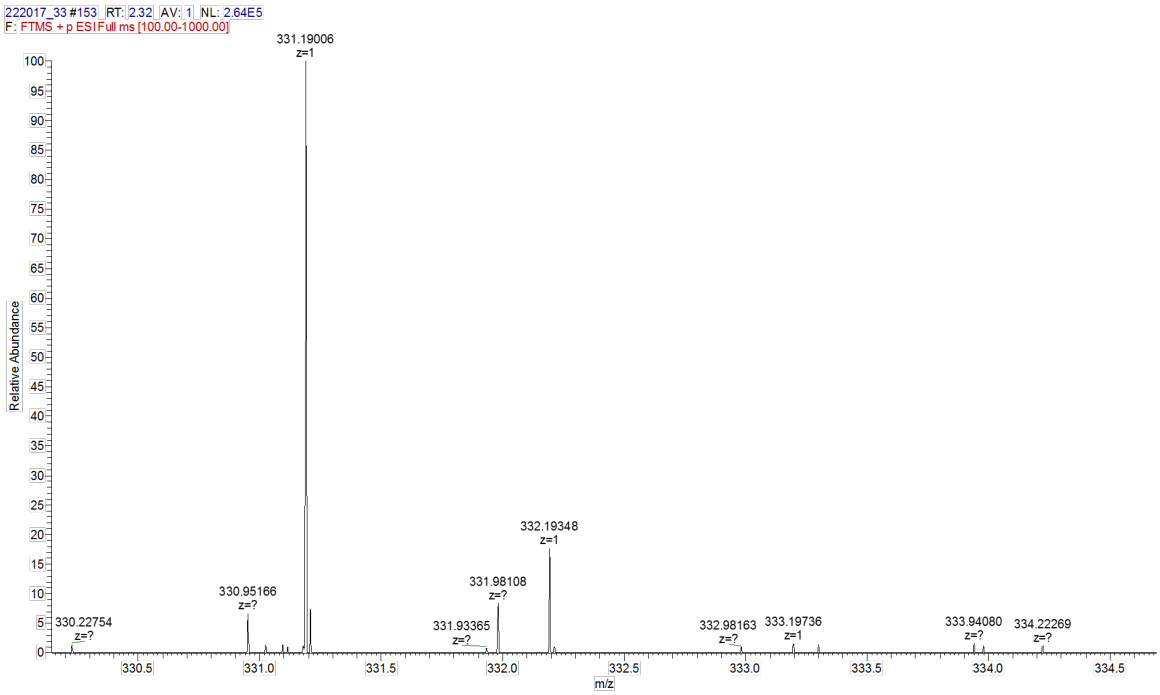

Figure S19. (a) Extracted ion chromatograms (EIC) and **(b)** mass spectra (MS) of momilactone B (MB) in intestinal digested sample by ultra-performance liquid chromatography-electrospray ionization-mass spectrometry (UPLC-ESI-MS).

(a)

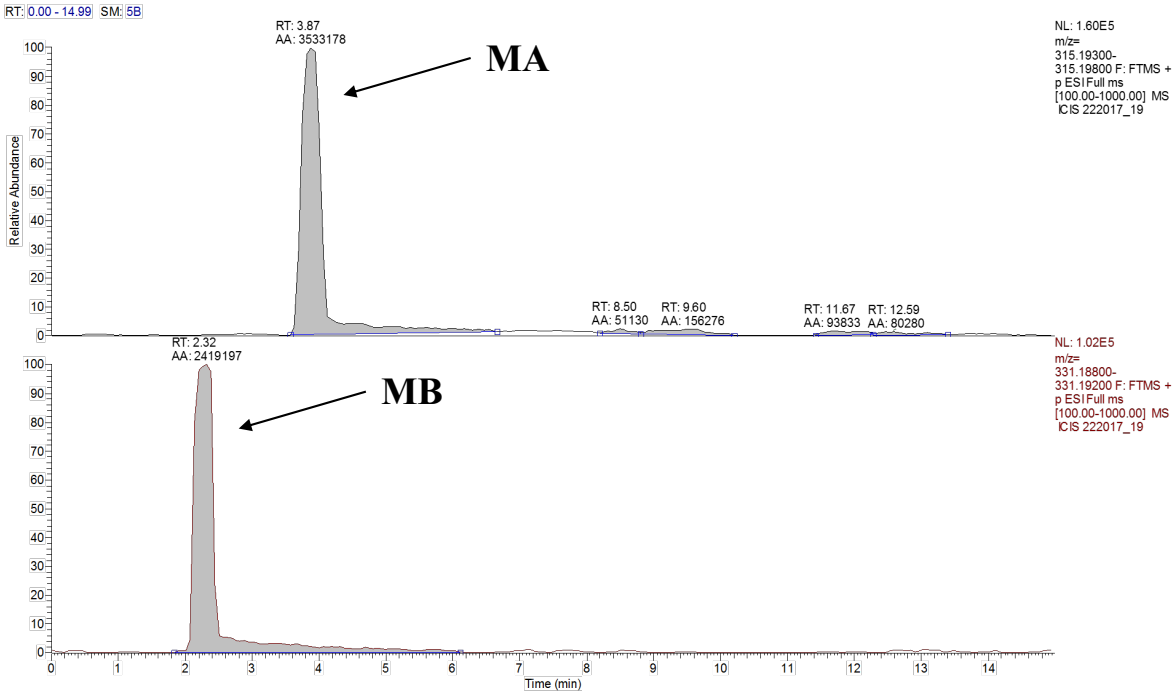
RT: 0.00 - 14.99 SM: 5B
RT: 3.87
AA: 3533178
MA
NL: 1.60E5
m/z=
315.19300-
315.19800 F: FTMS +
p ESI Full ms
[100.00-1000.00] MS
ICIS 222017_19
Relative Abundance
RT: 8.50
AA: 51130
RT: 9.60
AA: 156276
RT: 11.67
AA: 93833
RT: 12.59
AA: 80280
RT: 2.32
AA: 2419197
MB
NL: 1.02E5
m/z=
331.18800-
331.19200 F: FTMS +
p ESI Full ms
[100.00-1000.00] MS
ICIS 222017_19
Time (min)

(b)

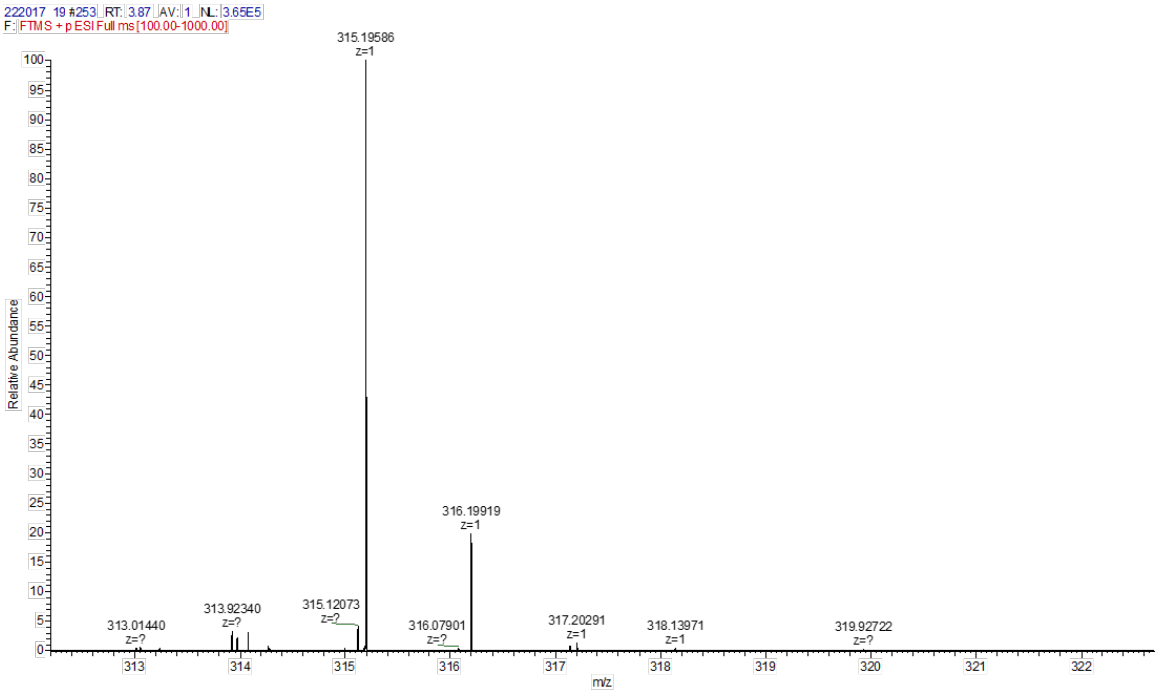
222017 19 #253 RT: 3.87 AV: 1 NL: 3.65E5
F: FTMS + p ESI Full ms [100.00-1000.00]
315.19586
z=1
316.19919
z=1
313.01440
z=?
313.92340
z=?
315.12073
z=?
316.07901
z=?
317.20291
z=1
318.13971
z=1
319.92722
z=?
Relative Abundance
m/z

MA

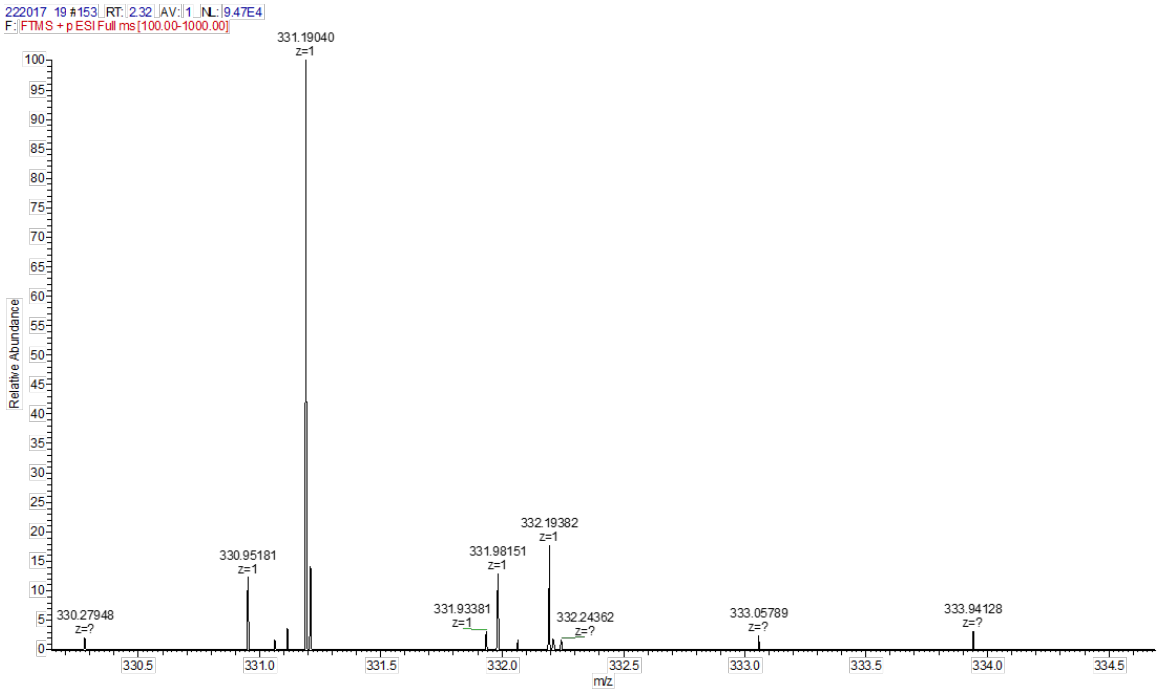

MB

Figure S20. (a) Extracted ion chromatograms (EIC) and **(b)** mass spectra (MS) of momilactone A (MA) and B (MB) in oral digested sample by ultra-performance liquid chromatography-electrospray ionization-mass spectrometry (UPLC-ESI-MS).

(a)

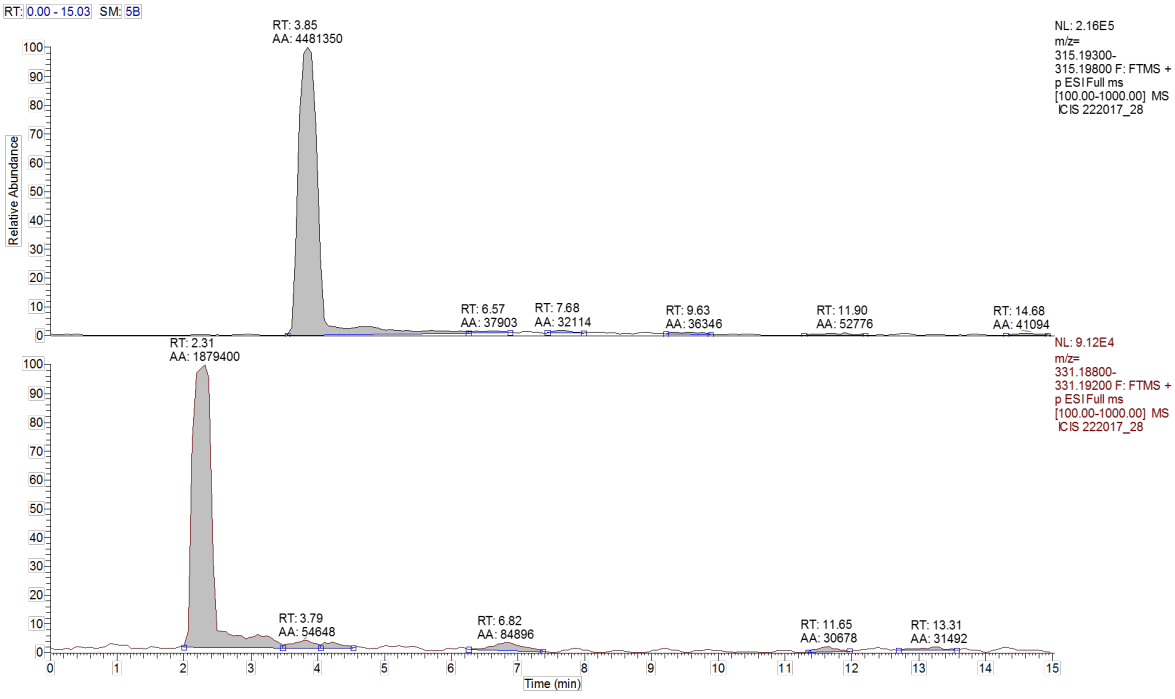

(b)

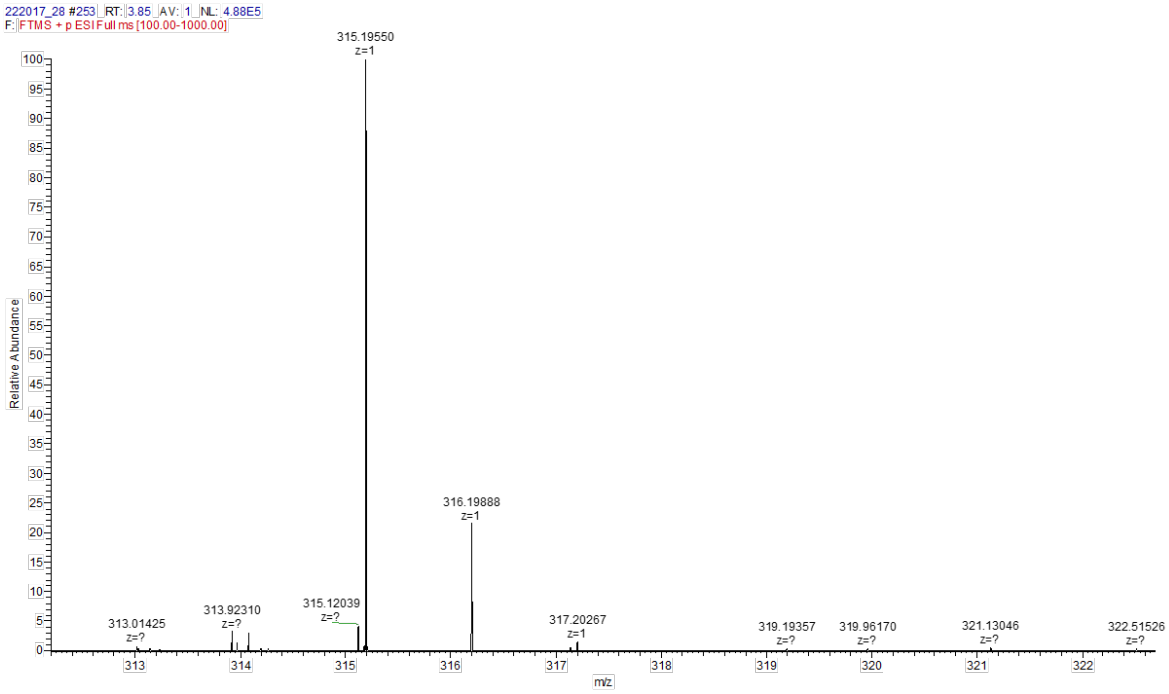
222017_28 #253 RT: 3.85 AV: 1 NL: 4.88E5
F: FTMS + p ESI Full ms [100.00-1000.00]
315.19550
z=1
316.19888
z=1
313.01425
z=?
313.92310
z=?
315.12039
z=?
317.20267
z=1
319.19357
z=?
319.96170
z=?
321.13046
z=?
322.51526
z=?
Relative Abundance
m/z

MA

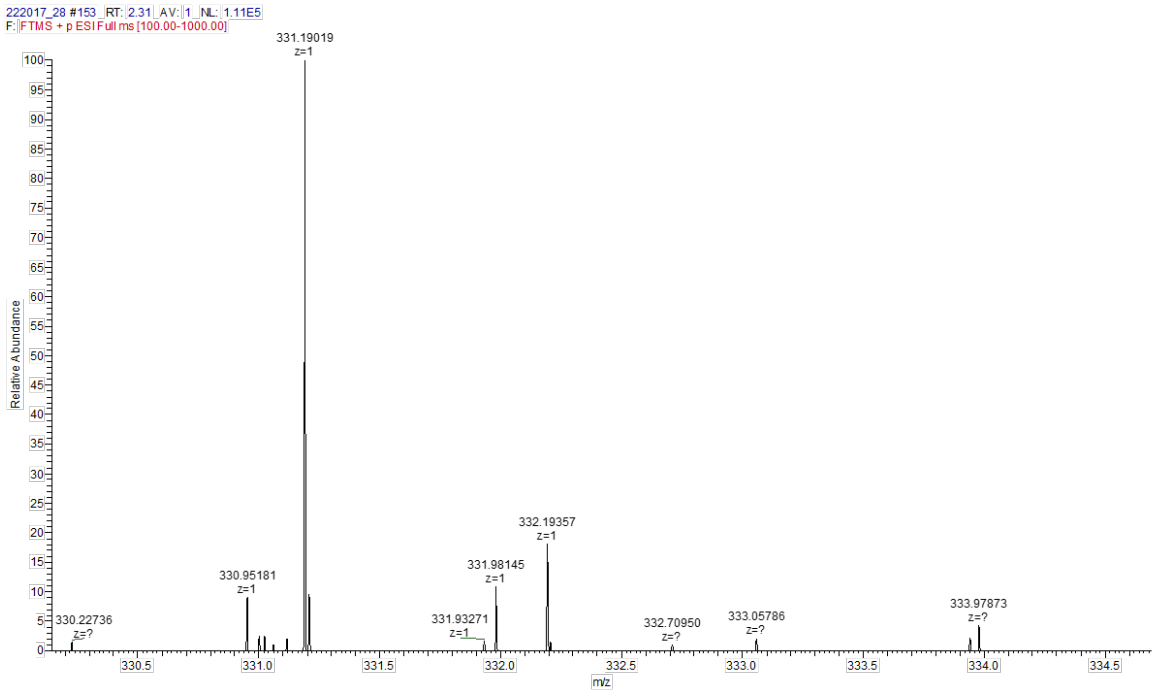
222017_28 #153 RT: 2.31 AV: 1 NL: 1.11E5
F: FTMS + p ESI Full ms [100.00-1000.00]
331.19019
z=1
332.19357
z=1
331.98145
z=1
330.95181
z=1
330.22736
z=?
331.93271
z=1
332.70950
z=?
333.05786
z=?
333.97873
z=?
Relative Abundance
m/z

MB

Figure S21. (a) Extracted ion chromatograms (EIC) and **(b)** mass spectra (MS) of momilactone A (MA) and B (MB) in gastric digested sample by ultra-performance liquid chromatography-electrospray ionization-mass spectrometry (UPLC-ESI-MS).

(a)

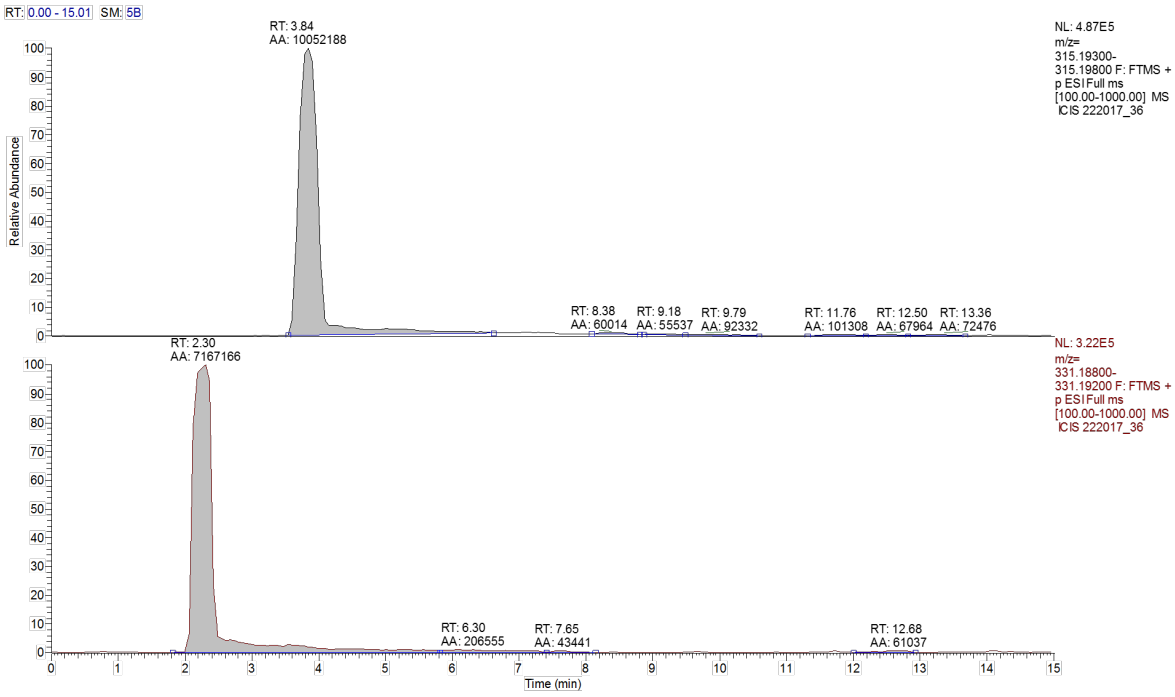

(b)

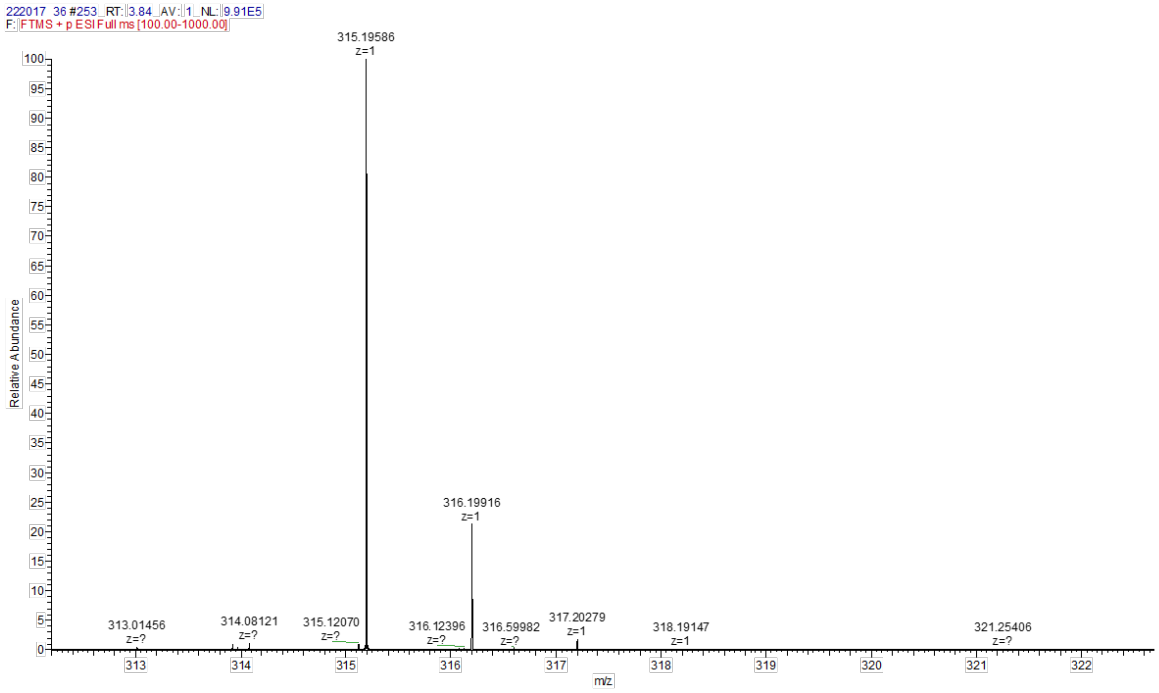

MA

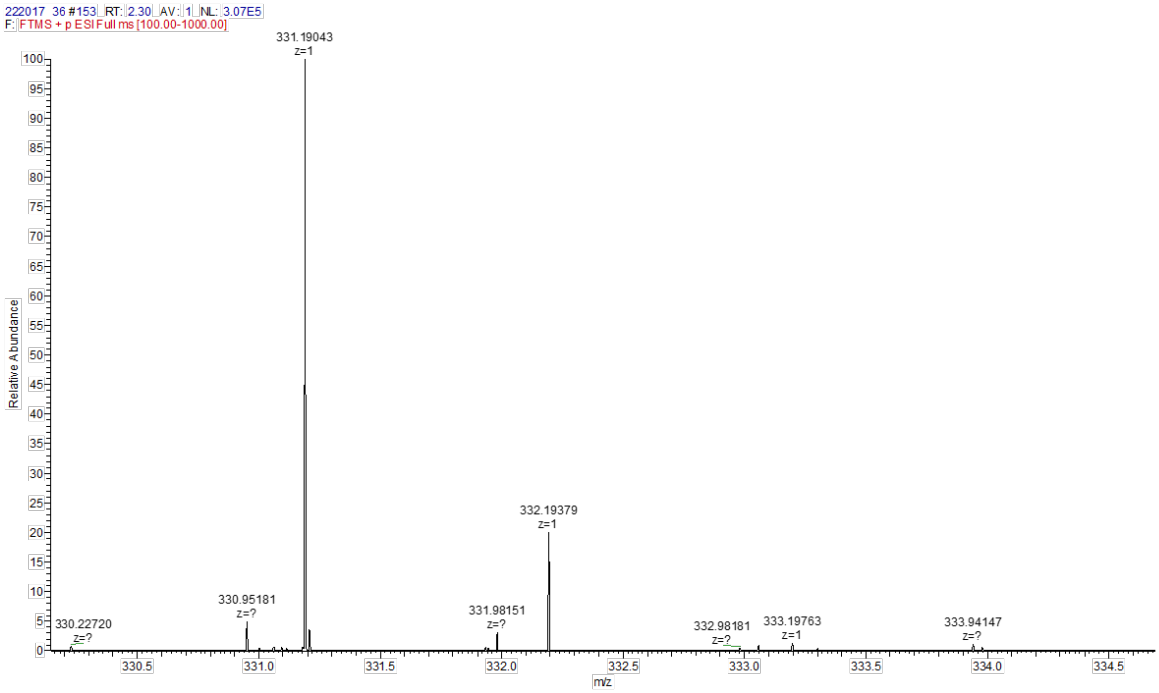

MB

Figure S22. (a) Extracted ion chromatograms (EIC) and **(b)** mass spectra (MS) of momilactone A (MA) and B (MB) in intestinal digested sample by ultra-performance liquid chromatography-electrospray ionization-mass spectrometry (UPLC-ESI-MS).

REFERENCES

Pandey, A.K.; Mishra, A.K.; Mishra, A. Antifungal and antioxidative potential of oil and extracts derived from leaves of Indian spice plant *Cinnamomum tamala*. *Cell. Mol. Biol.* **2012**, *58*, 142–147.

Abolhasani Zadeh, F.; Mardasi, M.; Rahbaran, M.; Shojaei, B.S.; Rahimi, S.; Tambrchi, P.; Razeghian, E. Genistein impairs proliferation and induces apoptosis in human leukemia MOLT-4 cells by down-regulation of anti-apoptotic proteins. *J. Cancer Res. Ther.* **2022**, *30*, 22–27. https://doi.org/10.4993/acrt.30.22.

Ajaya Kumar, R.; Sridevi, K.; Vijaya Kumar, N.; Nanduri, S.; Rajagopal, S. Anticancer and immunostimulatory compounds from *Andrographis paniculata*. *J. Ethnopharmacol.* **2004**, *92*, 291–295. https://doi.org/10.1016/j.jep.2004.03.004.

Alencar, M.V.O.B.; Islam, M.T.; Ali, E.S.; Santos, J.V.O.; Paz, M.F.C.J.; Sousa, J.M.C.; Dantas, S.M.M.M.; Mishra, S.K.; Cavalcante, A.A.C.M. Association of phytol with toxic and cytotoxic activities in an antitumoral perspective: A meta-analysis and systemic review. *Anticancer Agents Med. Chem.* **2018**, *18*, 1828–1837, doi:10.2174/1871520618666180821113830.

Al-Saeedi, A.H.; Al-Ghafri, M.T.H.; Hossain, M.A. Comparative evaluation of total phenols, flavonoids content and antioxidant potential of leaf and fruit extracts of Omani *Ziziphus jujuba* L. *Pac. Sci. Rev. A Nat. Sci. Eng.* **2016**, *18*, 78–83, doi:10.1016/j.psra.2016.09.001.

Ambade, A.; Mandrekar, P. Oxidative stress and inflammation: Essential partners in alcoholic liver disease. *Int. J. Hepatol.* **2012**, *2012*, 853175, doi:10.1155/2012/853175.

Ameade, E.P.K.; Ibrahim, M.; Ibrahim, H.-S.; Habib, R.H.; Gbedema, S.Y. Concurrent use of herbal and orthodox medicines among residents of Tamale, northern Ghana, who patronize hospitals and herbal clinics. *Evid. Based Complementary Altern. Med.* **2018**, *2018*, 1–8. https://doi.org/10.1155/2018/1289125.

Weeds of Australia – Biosecurity Queensland Edition Fact Sheet, *Andropogon virginicus.* Available online: https://keyserver.lucidcentral.org/weeds/data/media/Html/andropogon_virginicus.pdf (accessed on 20 October 2020).

European and Mediterranean Plant Protection Organization. *Andropogon virginicus* L. *Bull. OEPP/EPPO Bull.* **2019**, *49*, 61–66, doi:10.1111/epp.12526.

Anh, L.H.; Quan, N.V.; Lam, V.Q.; Iuchi, Y.; Takami, A.; Teschke, R.; Xuan, T.D. Antioxidant, anti-tyrosinase, anti-α-amylase, and cytotoxic potentials of the invasive weed *Andropogon virginicus*. *Plants* **2020**, *10*, 69. https://doi.org/10.3390/plants10010069.

Balandier, P.; Collet, C.; Miller, J.H.; Reynolds, P.E.; Zedaker, S.M. Designing forest vegetation management strategies based on the mechanisms and dynamics of crop tree competition by neighbouring vegetation. *Forestry* **2006**, *79*, 3–27, doi:10.1093/forestry/cpi056.

Biswas, S.K. Does the interdependence between oxidative stress and inflammation explain the antioxidant paradox? *Oxid. Med. Cell. Longev.* **2016**, *2016*, 5698931, doi:10.1155/2016/5698931.

Biswas, S.K.; de Faria, J.B.L. Which comes first: Renal inflammation or oxidative stress in spontaneously hypertensive rats? *Free Radic. Res.* **2007**, *41*, 216–224, doi:10.1080/10715760601059672.

Boudreau, M.W.; Peh, J.; Hergenrother, P.J. Procaspase-3 overexpression in cancer: A paradoxical observation with therapeutic potential. *ACS Chem. Biol.* **2019**, *14*, 2335–2348. https://doi.org/10.1021/acschembio.9b00338.

Cachofeiro, V.; Goicochea, M.; de Vinuesa, S.D.; Oubina, P.; Lahera, V.; Luno, J. Oxidative stress and inflammation, a link between chronic kidney disease and cardiovascular disease. *Kidney Int. Suppl.* **2008**, *111*, S4–S9, doi:10.1038/ki.2008.516.

Cartwright, D.W.; Langcake, P.; Ride, J.P. Phytoalexin production in rice and its enhancement by a dichlorocyclopropane fungicide. *Physiol. Plant Pathol.* **1980**, *17*, 259-267. https://doi.org/10.1016/S0048-4059(80)80019-1.

Cheah, C.Y.; Seymour, J.F.; Wang, M.L. Mantle cell lymphoma. *J. Clinic. Oncol.* **2016,** *34*, 1256–1269. https://doi.org/10.1200/JCO.2015.63.5904.

Choi, Y.H.; Zhang, L.; Lee, W.H.; Park, K.Y. Genistein-induced G2/M arrest is associated with the inhibition of cyclin B1 and the induction of p21 in human breast carcinoma cells. *Int. J. Oncol.* **1998**, *13*, 391–396. https://doi.org/10.3892/ijo.13.2.391.

Chung, I.M.; Ali, M.; Hahn, S.J.; Siddiqui, N.A.; Lim, Y.H.; Ahmad, A. Chemical constituents from the hulls of *Oryza sativa* with cytotoxic activity. *Chem. Nat. Compd.* **2005**, *41*, 182–189. https://doi.org/10.1007/s10600-005-0108-9.

Collins, T. Acute and chronic inflammation. In *Pathologic Basis of Disease*; Cotran, R.S., Kumar, V., Collins, T., Eds.; WB Saunders: Philadelphia, PA, USA, 1999; pp. 50–88.

de Alencar, M.V.O.B.; Islam, M.T.; de Lima, R.M.T.; Paz, M.F.C.J.; Dos Reis, A.C.; da Mata, A.M.O.F.; Filho, J.W.G.O.; Cerqueira, G.S.; Ferreira, P.M.P.; Sousa, E.J.M.C.; Mubarak, M.S.; de Carvalho Melo-Cavalcante, A.A. Phytol as an anticarcinogenic and antitumoral agent: An *in vivo* study in swiss mice with DMBA-Induced breast cancer. *IUBMB Life* **2019**, *71*, 200–212, doi:10.1002/iub.1952.

Demirseren, D.D.; Emre, S.; Akoglu, G.; Arpacı, D.; Arman, A.; Metin, A.; Cakır, B. Relationship between skin diseases and extracutaneous complications of diabetes mellitus: Clinical analysis of 750 patients. *Am. J. Clin. Dermatol.* **2014**, *15*, 65–70, doi:10.1007/s40257-013-0048-2.

Elzaawely, A.A.; Xuan, T.D.; Koyama, H.; Tawata, S. Antioxidant activity and contents of essential oil and phenolic compounds in flowers and seeds of *Alpinia zerumbet* (Pers.) B.L.

Burtt. & R.M. Sm. *Food Chem.* **2007**, *104*, 1648–1653, doi:10.1016/j.foodchem.2007.03.016.

Endrini, S.; Rahmat, A.; Ismail, P.; Taufiq-Yap, Y.H. Cytotoxic effect of γ-sitosterol from Kejibeling (Strobilanthes crispus) and its mechanism of action towards c-myc gene expression and apoptotic pathway. *Med. J. Indones.* **2014**, *23*, 203, doi:10.13181/mji.v23i4.1085.

Espinoza, J.L.; Elbadry, M.I.; Taniwaki, M.; Harada, K.; Trung, L.Q.; Nakagawa, N.; Takami, A.; Ishiyama, K.; Yamauchi, T.; Takenaka, K.; Nakao, S. The simultaneous inhibition of the mTOR and MAPK pathways with Gnetin-C induces apoptosis in acute myeloid leukemia. *Cancer Lett.* **2017**, *400*, 127–136. https://doi.org/10.1016/j.canlet.2017.04.027.

Fang, C.; Li, Y.; Li, C.; Li, B.; Ren, Y.; Zheng, H.; Zeng, X.; Shen, L.; Lin, W. Identification and comparative analysis of microRNAs in barnyardgrass (*Echinochloa crus-galli*) in response to rice allelopathy. *Plant Cell Environ.* **2015**, *38*, 1368–1381. https://doi.org/10.1111/pce.12492.

29. Ferenbach, D.A.; Bonventre, J.V. The molecular response to renal injury. In *Kidney Development, Disease, Repair and Regeneration*; Melissa, H.L., Ed.; Academic Press: Cambridge, United States, 2016; pp. 367–379. https://doi.org/10.1016/B978-0-12-800102-8.00027-8.

Jaaks, P.; Coker, E.A.; Vis, D.J.; Edwards, O.; Carpenter, E.F.; Leto, S.M.; Dwane, L.; Sassi, F.; Lightfoot, H.; Barthorpe, S.; van der Meer, D.; Yang, W.; Beck, A.; Mironenko, T.; Hall, C.; Hall, J.; Mali, I.; Richardson, L.; Tolley, C.; Morris, J.; Thomas, F.; Lleshi, E.; Aben, N.; Benes, C.H.; Bertotti, A.; Trusolino, L.; Wessels, L.; Garnett, M.J. Effective drug combinations in breast, colon and pancreatic cancer cells. *Nature* **2022**, *603*, 166–173. https://doi.org/10.1038/s41586-022-04437-2.

Ji, L., Liu, T., Liu, J., Chen, Y., & Wang, Z. Andrographolide inhibits human hepatoma-derived Hep3B cell growth through the activation of c-Jun N-erminal kinase. *Planta Medica* **2007**, *73*, 1397–1401. https://doi.org/10.1055/s-2007-990230.

Fukuta, M.; Xuan, T.D.; Deba, F.; Tawata, S.; Khanh, T.D.; Chung, I.M. Comparative efficacies *in vitro* of antibacterial, fungicidal, antioxidant, and herbicidal activities of momilatones A and B. *J. Plant Interact.* **2007**, *2*, 245–251. https://doi.org/10.1080/17429140701713811.

Global cancer observatory (GLOBOCAN). Available online: https://gco.iarc.fr (accessed on 20 October 2020).

Grgić, J.; Šelo, G.; Planinić, M.; Tišma, M.; Bucić-Kojić, A. Role of the encapsulation in bioavailability of phenolic compounds. *Antioxidants* **2020**, *9*, 923. https://doi.org/10.3390/antiox9100923.

Hanamura, I. Gain/amplification of chromosome Arm 1q21 in multiple myeloma. *Cancers* **2021**, *13*, 256. https://doi.org/10.3390/cancers13020256.

Heim, K.E.; Tagliaferro, A.R.; Bobilya, D.J. Flavonoid antioxidants: chemistry, metabolism and structure-activity relationships. *J. Nutr. Biochem.* **2002**, *13*, 572–584. https://doi.org/10.1016/S0955-2863(02)00208-5.

Hideshima, T.; Akiyama, M.; Hayashi, T.; Richardson, P.; Schlossman, R.; Chauhan, D.; Anderson, K.C. Targeting p38 MAPK inhibits multiple myeloma cell growth in the bone marrow milieu. *Blood* **2003**, *101*, 703–705. https://doi.org/10.1182/blood-2002-06-1874.

Anh, L.H.; Xuan, T.D.; Thuy, N.T.D.; Quan, N.V.; Trang, L.T. Antioxidant and α-amylase inhibitory activities and phytocompounds of *Clausena indica* Fruits. *Medicines* **2020**, *7*, 10, doi:10.3390/medicines7030010.

Hodgkinson, A.J.; Wallace, O.A.M.; Boggs, I.; Broadhurst, M.; Prosser, C.G. Gastric digestion of cow and goat milk: Impact of infant and young child in vitro digestion conditions. *Food Chem.* **2018***, 245*, 275–281. https://doi.org/10.1016/j.foodchem.2017.10.028.

Hsu, C.-Y.; Wang, P.-W.; Alalaiwe, A.; Lin, Z.-C.; Fang, J.-Y. Use of lipid nanocarriers to improve oral delivery of vitamins. *Nutrients* **2019**, *11*, 68. https://doi.org/10.3390/nu11010068.

Cancer Treatment Centers of America (CTCA). Available online: https://www.cancercenter.com/blood-cancers (accessed on 20 October 2020).

Indrayanto, G.; Putra, G.S.; Suhud, F. Validation of in-vitro bioassay methods: Application in herbal drug research. In *Profiles of Drug Substances, Excipients and Related Methodology*; Al-Majed, A.A., Ed.; Academic Press: Cambridge, United States, 2021; 46, pp. 273–307. https://doi.org/10.1016/bs.podrm.2020.07.005.

Invasive Weed; Japan Livestock Technology Association (JLTA): Tokyo, Japan, 1994; pp. 31.

Kang, D.Y.; Nipin, S.P.; Darvin, P.; Joung, Y.H.; Byun, H.J.; Do, C.H.; Park, K.; Park, M.N.; Cho, K.H.; Yang, Y.M. Momilactone B inhibits ketosis *in vitro* by regulating the ANGPTL3-LPL pathway and inhibiting HMGCS2. *Anim. Biotechnol.* **2017**, *28*, 189–197. https://doi.org/10.1080/10495398.2016.1252769.

Kato, T.; Kabuto, C.; Sasaki, N.; Tsunagawa, M.; Aizawa, H.; Fujita, K.; Kato, Y.; Kitahara, Y.; Takahashi, N. Momilactones, growth inhibitors from rice, *Oryza sativa* L. *Tetrahedron Lett.* **1973**, *14*, 3861–3864. https://doi.org/10.1016/S0040-4039(01)87058-1.

Kato-Noguchi, H. Stress-induced allelopathic activity and momilactone B in rice. *Plant Growth Regul.* **2009**, *59*, 153–158. https://doi.org/10.1007/s10725-009-9398-4.

Kato-Noguchi, H. Convergent or parallel molecular evolution of momilactone A and B: Potent allelochemicals, momilactones have been found only in rice and the moss *Hypnum plumaeforme*. *J. Plant Physiol.* **2011**, *168*, 1511–1516. https://doi.org/10.1016/j.jplph.2011.03.014,

Kato-Noguchi, H.; Hasegawa, M.; Ino, T.; Ota, K.; Kujime, H. Contribution of momilactone A and B to rice allelopathy. *J. Plant Physiol.* **2010**. https://doi.org/10.1016/j.jplph.2010.01.014.

Kato-Noguchi, H.; Ota, K.; Kujime, H.; Ogawa, M. Effects of momilactone on the protein expression in Arabidopsis germination. *Weed Biol. Manag.* **2013**, *13*, 19–23. https://doi.org/10.1111/wbm.12005.

Kato-Noguchi, H.; Peters, R.J. The role of momilactones in rice allelopathy. *J. Chem. Ecol*. **2013**. https://doi.org/10.1007/s10886-013-0236-9.

Kefayati, Z.; Motamed, S.M.; Shojaii, A.; Noori, M.; Ghods, R. Antioxidant activity and phenolic and flavonoid contents of the extract and subfractions of *Euphorbia splendida* Mobayen. *Pharmacogn. Res.* **2017**, *9*, 362–365, doi:10.4103/pr.pr_12_17.

Kim, S.-J.; Park, H.-R.; Park, E.; Lee, S.-C. Cytotoxic and antitumor activity of momilactone B from rice hulls. *J. Agric. Food Chem.* **2007**, *55*, 1702–1706. https://doi.org/10.1021/jf062020b.

Kong, F.; Singh, R.P. Disintegration of solid foods in human stomach. *J. Food Sci.* **2008a**, *73*, 67–80. https://doi.org/10.1111/j.1750-3841.2008.00766.x.

Kong, F.; Singh, R.P. A model stomach system to investigate disintegration kinetics of solid foods during gastric digestion. *J. Food Sci.* **2008b**, *73*, E202–E210. https://doi.org/10.1111/j.1750-3841.2008.00745.x.

Kopustinskiene, D.M.; Jakstas, V.; Savickas, A.; Bernatoniene, J. Flavonoids as anticancer agents. *Nutrients* **2020**, *12*, 457, doi:10.3390/nu12020457.

Krzyzanowska, J.; Czubacka, A.; Oleszek, W. Dietary phytochemicals and human health. *Adv. Exp. Med. Biol*. **2010**, *698*, 74–98. https://doi.org/10.1007/978-1-4419-7347-4_7.

Kumar, S.; Kumar, V.; Prakash, O. Enzymes inhibition and antidiabetic effect of isolated constituents from *Dillenia indica. Biomed Res. Int.* **2013**, *2013*, 382063, doi:10.1155/2013/382063.

Kumar, S.; Pandey, A.K. Chemistry and biological activities of flavonoids: An overview. *Sci. World J.* **2013**, *2013*, 162750, doi:10.1155/2013/162750.

Lam, V.Q.; Anh, L.H.; Quan, N.V.; Xuan, T.D.; Hanamura, I.; Uchino, K.; Karnan, S.; Takami, A. Cytotoxicity of *Callerya speciosa* fractions against myeloma and lymphoma cell lines. *Molecules* **2022**, *27*, 2322. https://doi.org/10.3390/molecules27072322.

Lee, C.W.; Yoneyama, K.; Takeuchi, Y.; Konnai, M.; Tamogami, S.; Kodama, O. Momilactones A and B in rice straw harvested at different growth stages. *Biosci. Biotechnol. Biochem.* **1999**, *63*, 1318–1320. https://doi.org/10.1271/bbb.63.1318.

Lee, S.C.; Chung, I.-M.; Jin, Y.J.; Song, Y.S.; Seo, S.Y.; Park, B.S.; Cho, K.H.; Yoo, K.S.; Kim, T.-H.; Yee, S.-B.; Bae, Y.-S.; Yoo, Y.H. Momilactone B, an allelochemical of rice hulls, induces apoptosis on human lymphoma cells (Jurkat) in a micromolar concentration. *Nutr. Cancer* **2008**, *60*, 542–551. https://doi.org/10.1080/01635580801927445.

Li, S.; Sun, L.; Zhou, Q.; Li, S.; Liu, X.; Xiao, J.; Xu, Y.; Wang, F.; Jiang, Y.; Zheng, C. Therapeutic effect and mechanism of Ibrutinib combined with dexamethasone on multiple myeloma. *Pharmazie* **2021**, *76*, 92–96.

Li, X.; Yin, X.; Wang, H.; Huang, J.; Yu, M.; Ma, Z.; Li, C.; Zhou, Y.; Yan, X.; Huang, S.; Jin, J. The combination effect of homoharringtonine and Ibrutinib on FLT3-ITD mutant acute myeloid leukemia. *Oncotarget* **2017**, *8*, 12764–12774. https://doi.org/10.18632/oncotarget.14463.

Libby, G.; Donnelly, L.A.; Donnan, P.T.; Alessi, D.R.; Morris, A.D.; Evans, J.M.M. New users of metformin are at low risk of incident cancer. *Diabetes Care* **2009**, *32*, 1620–1625. https://doi.org/10.2337/dc08-2175.

Lichota, A.; Gwozdzinski, K. Anticancer activity of natural compounds from plant and marine environment. *Int. J. Mol. Sci.* **2018**, *19*, 3533. https://doi.org/10.3390/ijms19113533.

Liu, G.; Franssen, E.; Fitch, M.I.; Warner, E. Patient preferences for oral versus intravenous palliative chemotherapy. *J. Clin. Oncol.* **1997**, *15*, 110–115. https://doi.org/10.1200/JCO.1997.15.1.110.

Maddocks, K.J.; Ruppert, A.S.; Lozanski, G.; Heerema, N.A.; Zhao, W.; Abruzzo, L.; Lozanski, A.; Davis, M.; Gordon, A.; Smith, L.L.; Mantel, R.; Jones, J.A.; Flynn, J.M.; Jaglowski, S.M.; Andritsos, L.A.; Awan, F.; Blum, K.A.; Grever, M.R.; Johnson, A.J.; Byrd, J.C.; Woyach, J.A. Etiology of Ibrutinib therapy discontinuation and outcomes in patients with chronic lymphocytic leukemia. *JAMA Oncol.* **2014**, *1*, 80–87. https://doi.org/10.1001/jamaoncol.2014.218.

Matthews, H.K.; Bertoli, C.; de Bruin, R.A.M. Cell cycle control in cancer. *Nat. Rev. Mol. Cell Biol.* **2022**, *23*, 74–88. https://doi.org/10.1038/s41580-021-00404-3.

Minh, T.N.; Xuan, T.D.; Ahmad, A.; Elzaawely, A.; Teschke, R.; Van, T.M. Efficacy from different extractions for chemical profile and biological activities of rice husk. *Sustainability* **2018**, *10*, 1356. https://doi.org/10.3390/su10051356.

Moen, M.D.; McKeage, K.; Plosker, G.L.; Siddiqui, M.A.A. Imatinib. *Drugs* **2007**, *67*, 299–320. https://doi.org/10.2165/00003495-200767020-00010.

Esa, M.N.; Ling, T.B. By-products of rice processing: An overview of health benefits and applications. *Rice Res.* **2016**, *4*. https://doi.org/10.4172/jrr.1000107.

National Institute for Environmental Studies (NIES). Available online: https://www.nies.go.jp/biodiversity/invasive/DB/detail/81450e.html (accessed on 20 October 2020).

NIH – National Cancer Institute. Available online: https://www.cancer.gov/publications/dictionaries/cancer-terms/def/white-blood-

cell?fbclid=IwAR1Jr1RfMklHWtlLj2eQ_HdJp9xY6-h8OQHhYkg2fnQWBeDLJbzscm9tLO8 (accessed on 20 October 2020).

Otto, T.; Sicinski, P. Cell cycle proteins as promising targets in cancer therapy. *Nat. Rev. Cancer* **2017**, *17*, 93–115. https://doi.org/10.1038/nrc.2016.138.

Park, C.; Jeong, N.Y.; Kim, G.-Y.; Han, M.H.; Chung, I.-M.; Kim, W.-J.; Yoo, Y.H.; Choi, Y.H. Momilactone B induces apoptosis and G1 arrest of the cell cycle in human monocytic leukemia U937 cells through downregulation of pRB phosphorylation and induction of the cyclin-dependent kinase inhibitor $p21^{Waf1/Cip1}$. *Oncol. Rep.* **2014**, *31*, 1653–1660. https://doi.org/10.3892/or.2014.3008.

Payne, S.A. A study of quality of life in cancer patients receiving palliative chemotherapy. *Soc. Sci. Med.* **1992**, *35*, 1505–1509. https://doi.org/10.1016/0277-9536(92)90053-S.

Pejin, B.; Kojic, V.; Bogdanovic, G. An insight into the cytotoxic activity of phytol at *in vitro* conditions. *Nat. Prod. Res.* **2014**, *28*, 2053–2056, doi:10.1080/14786419.2014.921686.

Pérez-Vicente, A.; Gil-Izquierdo, A.; García-Viguera, C. *In vitro* gastrointestinal digestion study of pomegranate juice phenolic compounds, anthocyanins, and vitamin C. *J. Agric. Food Chem.* **2002**, *50*, 2308–2312. https://doi.org/10.1021/jf0113833.

Pfeffer, C.; Singh, A. Apoptosis: A target for anticancer therapy. *Int. J. Mol. Sci.* **2018**, *19*, 448. https://doi.org/10.3390/ijms19020448.

Quan, N.V.; Anh, L.H.; Lam, V.Q.; Takami, A.; Teschke, R.; Khanh, T.D.; Xuan, T.D. Anti-diabetes, anti-gout, and anti-leukemia properties of essential oils from natural spices *Clausena indica*, *Zanthoxylum rhetsa*, and *Michelia tonkinensis*. *Molecules* **2022**, *27*, 774. https://doi.org/10.3390/molecules27030774.

Quan, N.V.; Thien, D.D.; Khanh, T.D.; Tran, H.-D.; Xuan, T.D. Momilactones A, B, and tricin in rice grain and by-products are potential skin aging inhibitors. *Foods* **2019a**, *8*, 602. https://doi.org/10.3390/foods8120602.

Quan, N.V.; Tran, H.-D.; Xuan, T.D.; Ahmad, A.; Dat, T.D.; Khanh, T.D.; Teschke, R. Momilactones A and B are α-amylase and α-glucosidase inhibitors. *Molecules* **2019b**, 24, 482. https://doi.org/10.3390/molecules24030482.

Quan, N.V.; Xuan, T.D.; Anh, L.H.; Tran, H.-D. Bio-guided isolation of prospective bioactive constituents from roots of *Clausena indica* (Dalzell) Oliv. *Molecules* **2019c**, *24*, 4442, doi:10.3390/molecules24244442.

Quan, N.V.; Xuan, T.D.; Tran, H.-D.; Ahmad, A.; Khanh, T.D.; Dat, T.D. Contribution of momilactones A and B to diabetes inhibitory potential of rice bran: Evidence from *in vitro* assays. *Saudi Pharm. J.* **2019d**, *27*, 643–649. https://doi.org/10.1016/j.jsps.2019.03.006.

Quan, N.V.; Xuan, T.D.; Tran, H.-D.; Thuy, N.T.D. Inhibitory activities of momilactones A, B, E, and 7-Ketostigmasterol isolated from rice husk on paddy and invasive weeds. *Plants* **2019e**, *8*, 159. https://doi.org/10.3390/plants8060159.

Quan, N.V.; Xuan, T.D.; Tran, H.D.; Thuy, N.T.D.; Trang, L.T.; Huong, C.T.; Yusuf, A., Tuyen, P.T. Antioxidant, α-amylase and α-glucosidase inhibitory activities and potential constituents of *Canarium tramdenum* bark. *Molecules* **2019f**, *24*, 605, doi:10.3390/molecules24030605.

Quan, N.V.; Xuan, T.D.; Teschke, R. Potential hepatotoxins found in herbal medicinal products: A systematic review. *Int. J. Mol. Sci.* **2020**, *21*, 5011. https://doi.org/10.3390/ijms21145011.

Rahaie, S.; Gharibzahedi, S.M.T.; Razavi, S.H.; Jafari, S.M. Recent developments on new formulations based on nutrient-dense ingredients for the production of healthy-functional bread: a review. *J. Food Sci. Technol.* **2014**, *51*, 2896–2906. https://doi.org/10.1007/s13197-012-0833-6.

Rajkumar, S.V. Multiple myeloma: 2022 update on diagnosis, risk stratification, and management. *Am. J. Hematol.* **2022**, *97*, 1086–1107. https://doi.org/10.1002/ajh.26590.

Richardson, P.G.; Bensinger, W.I.; Huff, C.A.; Costello, C.L.; Lendvai, N.; Berdeja, J.G.; Anderson Jr, L.D.; Siegel, D.S.; Lebovic, D.; Jagannath, S.; Laubach, J.P.; Stockerl-Goldstein, K.E.; Kwei, L.; Clow, F.; Elias, L.; Salman, Z.; Graef, T.; Bilotti, E.; Vij, R. Ibrutinib alone or with dexamethasone for relapsed or relapsed and refractory multiple myeloma: phase 2 trial results. *Br. J. Haematol.* **2018**, *180*, 821–830. https://doi.org/10.1111/bjh.15058.

Rodrigues, A.C.B.D.C.; Bomfim, L.M.; Neves, S.P.; Soares, M.B.P.; Dias, R.B.; Valverde, L.F.; Rocha, C.A.G.; Costa, E.V.; da Silva, F.M.A.; Rocha, W.C.; Koolen, H.H.F.; Bezerra, D.P. Tingenone and 22-hydroxytingenone target oxidative stress through down-regulation of thioredoxin, leading to DNA double-strand break and JNK/p38-mediated apoptosis in acute myeloid leukemia HL-60 cells. *Biomed. Pharmacother.* **2021**, *142*, 112034. https://doi.org/10.1016/j.biopha.2021.112034.

Sakthivel, R.; Sheeja, D.; Kasi, M.; Devi, P. Phytol shows anti-angiogenic activity and induces apoptosis in A549 cells bydepolarizing the mitochondrial membrane potential. *Biomed. Pharmacother.* **2018**, *105*, 742–752, doi:10.1016/j.biopha.2018.06.035.

Sanz, M.A.; Fenaux, P.; Tallman, M.S.; Estey, E.H.; Löwenberg, B.; Naoe, T.; Lengfelder, E.; Döhner, H.; Burnett, A.K.; Chen, S.J.; Mathews, V.; Iland, H.; Rego, E.; Kantarjian, H.; Adès, L.; Avvisati, G.; Montesinos, P.; Platzbecker, U.; Ravandi, F.; Russell, N.H.; Lo-Coco, F. Management of acute promyelocytic leukemia: updated recommendations from an expert panel of the European LeukemiaNet. *Blood* **2019**, *133*, 1630–1643. https://doi.org/10.1182/blood-2019-01-894980.

Sesso, H.D.; Buring, J.E.; Christen, W.G.; Kurth, T.; Belanger, C.; MacFadyen, J.; Bubes, V.; Manson, J.E.; Glynn, R.J.; Gaziano, J.M. Vitamins E and C in the prevention of cardiovascular disease in men: The physicians' health study II randomized controlled trial. *JAMA* **2008**, *300*, 2123–2133, doi:10.1001/jama.2008.600.

Sharma, N.; Dobhal, M.; Joshi, Y.; Chahar, M. Flavonoids: A versatile source of anticancer drugs. *Pharmacogn. Rev.* **2011***, 5*, 1. https://doi.org/10.4103/0973-7847.79093.

Chahar, M.K.; Sharma, N.; Dobhal, M.P.; Joshi, Y.C. Flavonoids: A versatile source of anticancer drugs. *Pharmacogn. Rev.* **2011**, *5*, 1–12, doi:10.4103/0973-7847.79093.

Simpson, M.G. Diversity and classification of flowering plants. In *Plant Systematics*; Simpson, M.G., Ed.; Elsevier, 2010; pp. 181–274. https://doi.org/10.1016/B978-0-12-374380-0.50007-52010.

Sohail, M.; Rakha, A.; Butt, M.S.; Iqbal, M.J.; Rashid, S. Rice bran nutraceutics: A comprehensive review. *Crit. Rev. Food Sci. Nutr.* **2017**, *57*, 3771–3780. https://doi.org/10.1080/10408398.2016.1164120.

Şöhretoğlua, D.; Sarib, S.; Barutc, B.; Özelc, A. Tyrosinase inhibition by some flavonoids: Inhibitory activity, mechanism by T *in vitro* and *in silico* studies. *Bioorganic Chem.* **2018**, *81*, 168–174, doi:10.1016/j.bioorg.2018.08.020.

Soobrattee, M.A.; Neergheen, V.S.; Luximon-Ramma, A.; Aruoma, O.I.; Bahorun, T. Phenolics as potential antioxidant therapeutic agents: Mechanism and actions. *Mutat. Res. Fundam. Mol. Mech. Mutagen.* **2005**, *579*, 200–213, doi:10.1016/j.mrfmmm.2005.03.023.

Su, C.H.; Lai, M.N.; Ng, L.T. Inhibitory effects of medicinal mushrooms on α-amylase and α-glucosidase enzymes related to hyperglycemia. *Food Funct.* **2013**, *4*, 644–649, doi:10.1039/c3fo30376d.

Su, C.; Hsu, C.; Huang, L. Inhibitory potential of fatty acids on key enzymes related to type 2 diabetes. *BioFactors* **2013**, *39*, 415–421, doi:10.1002/biof.1082.

Sundarraj, S.; Thangam, R.; Sreevani, V.; Kaveri, K.; Gunasekaran, P.; Achiraman, S.; Kannan, S. γ-Sitosterol from Acacia nilotica L. induces G2/M cell cycle arrest and apoptosis through c-Myc suppression in MCF-7 and A549 cells. *J. Ethnopharmacol.* **2012**, *141*, 803–809, doi:10.1016/j.jep.2012.03.014.

Sung, H.; Ferlay, J.; Siegel, R.L.; Laversanne, M.; Soerjomataram, I.; Jemal, A.; Bray, F. Global cancer statistics 2020: GLOBOCAN estimates of incidence and mortality worldwide for 36 cancers in 185 countries. *CA: Cancer J. Clin.* **2021**, *71*, 209–249. https://doi.org/10.3322/caac.21660.

Tagousop, C.N.; Tamokou, J.-d.-D.; Ekom, S.E.; Ngnokam, D.; Voutquenne-Nazabadioko, L. Antimicrobial activities of flavonoid glycosides from *Graptophyllum grandulosum* and their mechanism of antibacterial action. *BMC Complement. Altern. Med.* **2018**, *18*, 252, doi:10.1186/s12906-018-2321-7.

Tarling, C.A.; Woods, K.; Zhang, R.; Brastianos, H.C.; Brayer, G.D.; Andersen, R.J.; Withers, S.G. The search for novel human pancreatic α-amylase inhibitors: High-throughput screening of terrestrial and marine natural product extracts. *ChemBioChem* **2008**, *9*, 433–438, doi:10.1002/cbic.200700470.

Taşkın-Tok, T.; Gowder, S.J.T. Anticancer drug — friend or foe. In *Pharmacology and Therapeutics*; Gowder, S.J.T., Ed.; IntechOpen: London, UK, 2014. https://doi.org/10.5772/58552.

Teschke, T.; Eickhoff, A.; Wolff, A.; Xuan, T.D. Liver injury from herbs and "dietary supplements": Highlights of a literature review from 2015 to 2017. *Curr. Pharmacol. Rep.* **2018**, *4*, 120–131, doi:10.1007/s40495-018-0124-7.

Teschke, R.; Larrey, D.; Melchart, D.; Danan, G. Traditional Chinese medicine (TCM) and herbal hepatotoxicity: RUCAM and the role of novel diagnostic biomarkers such as microRNAs. *Medicines* **2016**, *3*, 18, doi:10.3390/medicines3030018.

Teschke, R.; Xuan, T.D. Viewpoint: A contributory role of shell ginger (*Alpinia zerumbet* (Pers.) B.L. Burtt & R.M. Sm) for human longevity in Okinawa, Japan? *Nutrients* **2018**, *10*, 166, doi:10.3390/nu10020166.

Teschke, T.; Xuan, T.D. Herbs including shell ginger, antioxidant profiles, aging, and longevity in Okinawa, Japan: A critical analysis of current concepts. In *Aging*, 2nd ed.; Preedy, V.R., Patel, V.B., Eds.; Academic Press: Cambridge, MA, USA, 2020; pp. 209–222, doi:10.1016/B978-0-12-818698-5.00021-3.

Teschke, R.; Xuan, T.D. Active nature-based ingredients for drug discovery with pivotal role of clinical efficacy: Review and prospective. *J. Mod. Med. Chem.* **2020**, *8*, 4–18, doi:10.12970/2308-8044.2020.08.02.

Testa, U.; Riccioni, R. Deregulation of apoptosis in acute myeloid leukemia. *Haematologica* **2007**, *92*, 81–94. https://doi.org/10.3324/haematol.10279.

Thavamoney, N.; Sivanadian, L.; Tee, L.H.; Khoo, H.E.; Prasad, K.N.; Kong, K.W. Extraction and recovery of phytochemical components and antioxidative properties in fruit parts of *Dacryodes rostrata* influenced by different solvents. *J. Food Sci. Technol.* **2018**, *55*, 2523–2532, doi:10.1007/s13197-018-3170-6.

Thorn, C.F.; Oshiro, C.; Marsh, S.; Hernandez-Boussard, T.; McLeod, H.; Klein, T.E.; Altman, R.B. Doxorubicin pathways: Pharmacodynamics and adverse effects. *Pharmacogenet. Genomics* **2011**, *21*, 440–446. https://doi.org/10.1097/FPC.0b013e32833ffb56.

Tropicos – Missouri Botanical Garden. Available online: https://www.tropicos.org/name/25509277 (accessed on 20 October 2020).

Tsujimoto, Y. Role of Bcl-2 family proteins in apoptosis: apoptosomes or mitochondria?. *Genes Cells* **1998**, *3*, 697–707. https://doi.org/10.1046/j.1365-2443.1998.00223.x.

Tucker, P.S.; Scanlan, A.T.; Dalbo, V.J. Chronic kidney disease influences multiple systems: Describing the relationship between oxidative stress, inflammation, kidney damage, and concomitant disease. *Oxid. Med. Cell. Longev.* **2015**, *2015*, 806358, doi:10.1155/2015/806358.

Tuyen, P.T.; Xuan, T.D.; Khang, D.T.; Ahmad, A.; Quan, N.V.; Anh, T.T.T.; Anh, L.H.; Minh, T.N. Phenolic compositions and antioxidant properties in bark, flower, inner skin, kernel and leaf extracts of *Castanea crenata* Sieb. et Zucc. *Antioxidants* **2017**, *6*, 31, doi:10.3390/antiox6020031.

Un, S.; Quan, N.V.; Anh, L.H.; Lam, V.Q.; Takami, A.; Khanh, T.D.; Xuan, T.D. Effects of *in vitro* digestion on anti-α-amylase and cytotoxic potentials of *Sargassum* spp. *Molecules* **2022**, *27*, 2307. https://doi.org/10.3390/molecules27072307.

Veeramuthu, D.; Raja, W.R.T.; Al-Dhabi, N.A.; Savarimuthu, I. Flavonoids: Anticancer properties. In *Flavonoids—From Biosynthesis to Human Health*; Justino, G.C., Ed.; IntechOpen: London, UK, 2017, doi:10.5772/68095.

Wang, T.-H.; Wang, H.-S.; Soong, Y.-K. Paclitaxel-induced cell death. *Cancer* **2000**, *88*, 2619–2628. https://doi.org/10.1002/1097-0142(20000601)88:11<2619::AID-CNCR26>3.0.CO;2-J.

Wootton-Beard, P.C.; Moran, A.; Ryan, L. Stability of the total antioxidant capacity and total polyphenol content of 23 commercially available vegetable juices before and after *in vitro* digestion measured by FRAP, DPPH, ABTS and Folin–Ciocalteu methods. *Food Res. Int.* **2011**, *44*, 217–224. https://doi.org/10.1016/j.foodres.2010.10.033.

Wu, H.; Hu, C.; Wang, A.; Weisberg, E.L.; Wang, W.; Chen, C.; Zhao, Z.; Yu, K.; Liu, J.; Wu, J.; Nonami, A.; Wang, L.; Wang, B.; Stone, R.M.; Liu, S.; Griffin, J.D.; Liu, J.; Liu, Q. Ibrutinib selectively targets FLT3-ITD in mutant FLT3-positive AML. *Leukemia* **2016**, *30*, 754–757. https://doi.org/10.1038/leu.2015.175.

Xie, J.; Wang, J.; Zhu, B. Genistein inhibits the proliferation of human multiple myeloma cells through suppression of nuclear factor-κB and upregulation of microRNA-29b. *Mol. Med. Rep.* **2016**, *13*, 1627–1632. https://doi.org/10.3892/mmr.2015.4740.

Xu, D.P.; Li, Y.; Meng, X.; Zhou, T.; Zhou, Y.; Zheng, J.; Zhang, J.J.; Li, H.B. Natural antioxidants in foods and medicinal plants: Extraction, assessment and resources. *Int. J. Mol. Sci.* **2017**, *18*, 96, doi:10.3390/ijms18010096.

Xuan, T.D.; Minh, T.N.; Anh, L.H.; Khanh, T.D. Allelopathic momilactones A and B are implied in rice drought and salinity tolerance, not weed resistance. *Agron. Sustain. Dev.* **2016**, *36*. https://doi.org/10.1007/s13593-016-0383-9.

Yip, K.W.; Reed, J.C. Bcl-2 family proteins and cancer. *Oncogene* **2008**, *27*, 6398–6406. https://doi.org/10.1038/onc.2008.307.

Zarubin, T.; Han, J. Activation and signaling of the p38 MAP kinase pathway. *Cell Res.* **2005**, *15*, 11–18. https://doi.org/10.1038/sj.cr.7290257.

Zhang, S.M.; Cook, N.R.; Albert, C.M.; Gaziano, J.M.; Buring, J.E.; Manson, J.E. Effect of combined folic acid, vitamin B_6, and vitamin B_{12} on cancer risk in women. *JAMA* **2008**, *300*, 2012. https://doi.org/10.1001/jama.2008.555.

Zhang, Z.; Wang, C.Z.; Du, G.J.; Qi, L.W.; Calway, T.; He, T.C.; Du, W.; Yuan, C.S. Genistein induces G2/M cell cycle arrest and apoptosis via ATM/p53-dependent pathway in human colon cancer cells. *Int. J. Oncol.* **2013**, *43*, 289–296. https://doi.org/10.3892/ijo.2013.1946.

Zhao, M.; Cheng, J.; Guo, B.; Duan, J.; Che, C.-T. Momilactone and related diterpenoids as potential agricultural chemicals. *J. Agric. Food Chem.* **2018**, *66*, 7859–7872. https://doi.org/10.1021/acs.jafc.8b02602.